8-1-2018

Fuel Specific Emissions Trends for In-Use Medium and Heavy-Duty Vehicle Fleets in California

Molly J. Haugen
University of Denver

Fuel Specific Emissions Trends for In-Use Medium and Heavy-Duty Vehicle Fleets in California

Abstract

New heavy-duty vehicle regulations have caused significant reductions in hazardous air pollutants, such as particulate matter (PM) and nitrogen oxides (NO_x), due to better engine management and utilization of advanced after-treatment systems. The University of Denver has collected data for gaseous and PM emission measurements from on-road heavy-duty vehicles (HDVs). The On-Road Heavy-Duty Vehicle Emissions Measurement System (OHMS) collected fuel specific emission information on individual HDVs of in-use fleets at two California locations in the spring of 2013, 2015 and 2017. These complimentary fleets, studied over multiple years, produced 7,075 measurements of gaseous and particle emission data providing the basis to quantify on-road HDV emission trends and compare a variety of factors that influence on-road emissions. The Port of Los Angeles contributes a fleet fully equipped with diesel particulate filters (DPFs) that had an observed PM increase of 30% in 2017 from 2013, but the fleet average is highly dependent on the fraction of high emitters. The second fleet measured was at the Cottonwood weigh station in Northern California, regulated at the state level and with slower fleet turn over, fleet PM emissions decrease (76% between 2013 and 2017) but at a slower rate than at the Port.

Additionally, heavy and medium-duty vehicles were measured at a second weigh station in Southern California. The Fuel Efficiency Automobile Test (FEAT) was used to collect on-road fuel specific emissions for HDVs and MDVs at the Peralta weigh station near Anaheim, CA, resulting in 2,315 measurements. The HDV's data added to measurements from 1997, 2008, 2009, 2010 and 2012 at this location. Two FEAT systems, one traditionally mounted atop scaffolding to collect emissions from HDVs with elevated exhaust stacks and a second, ground-level system were used for the first time to measure emissions from both MDVs and HDVs with ground-level exhaust. Introduction of new technologies show diminished NOx and PM emissions as HDVs saw a 55% NOx decrease since 2008 and a 33% reduction in IR %opacity. The MDV fleet was 2.1 years older than the HDV fleet and MDVs NO_x emissions show reductions approximately 2 model years (2014) earlier than HDVs.

Document Type

Dissertation

Degree Name

Ph.D.

Department

Chemistry and Biochemistry

First Advisor

Brian Majestic, Ph.D.

Second Advisor

Mark Siemens, Ph.D.

Third Advisor

Bryan Cowen

Keywords

Fuel emissions, On-road heavy-duty, Vehicle emissions measurement system, Fuel efficiency automobile

test

Fuel Specific Emissions Trends for In-Use Medium and Heavy-Duty Vehicle Fleets in California

_____

A Dissertation

Presented to

the Faculty of Natural Sciences and Mathematics

University of Denver

_____

In Partial Fulfillment

of the Requirements for the Degree

Doctor of Philosophy

_____

by

Molly J. Haugen

August 2018

Advisor: Dr. Brian Majestic

Author: Molly J. Haugen
Title: Fuel Specific Emissions Trends for In-Use Medium and Heavy-Duty Vehicle Fleets in California
Advisor: Dr. Brian Majestic
Degree Date: August 2018

Abstract

New heavy-duty vehicle regulations have caused significant reductions in hazardous air pollutants, such as particulate matter (PM) and nitrogen oxides (NO_x), due to better engine management and utilization of advanced after-treatment systems. The University of Denver has collected data for gaseous and PM emission measurements from on-road heavy-duty vehicles (HDVs). The On-Road Heavy-Duty Vehicle Emissions Measurement System (OHMS) collected fuel specific emission information on individual HDVs of in-use fleets at two California locations in the spring of 2013, 2015 and 2017. These complimentary fleets, studied over multiple years, produced 7,075 measurements of gaseous and particle emission data providing the basis to quantify on-road HDV emission trends and compare a variety of factors that influence on-road emissions. The Port of Los Angeles contributes a fleet fully equipped with diesel particulate filters (DPFs) that had an observed PM increase of 30% in 2017 from 2013, but the fleet average is highly dependent on the fraction of high emitters. The second fleet measured was at the Cottonwood weigh station in Northern California, regulated at the state level and with slower fleet turn over, fleet PM emissions decrease (76% between 2013 and 2017) but at a slower rate than at the Port.

Additionally, heavy and medium-duty vehicles were measured at a second weigh station in Southern California. The Fuel Efficiency Automobile Test (FEAT) was used to collect on-road fuel specific emissions for HDVs and MDVs at the Peralta weigh station

near Anaheim, CA, resulting in 2,315 measurements. The HDV's data added to measurements from 1997, 2008, 2009, 2010 and 2012 at this location. Two FEAT systems, one traditionally mounted atop scaffolding to collect emissions from HDVs with elevated exhaust stacks and a second, ground-level system were used for the first time to measure emissions from both MDVs and HDVs with ground-level exhaust. Introduction of new technologies show diminished NO_x and PM emissions as HDVs saw a 55% NO_x decrease since 2008 and a 33% reduction in IR %opacity. The MDV fleet was 2.1 years older than the HDV fleet and MDVs NO_x emissions show reductions approximately 2 model years (2014) earlier than HDVs.

Acknowledgements

I would like to thank California Air Resources Board and West Virginia University for the research opportunity and funding, as well as the University of Denver for providing a platform for this research. Thank you to the California Highway Patrol and Trans Pacific Container Service Corporation for site access and Sergeant Matt Boothe for helping with site logistics.

I would like to thank Ian Stedman and Lew Cohen for logistical support with various field campaigns.

I would like to thank the late Dr. Donald Stedman for his inimitable mentorship. His inventions of FEAT and OHMS have provided an irreplaceable contribution to on-road emission monitoring.

I would like to thank Dr. Gary Bishop for his patience, guidance and abundance of adventure stories.

Lastly, I would like to thank my friends and family for supporting me throughout this experience; I am extremely grateful. I have been able to achieve my goals largely due to my mom's inherent ability to find positivity in life, my dad's de-stressing advice and their unwavering support.

Table of Contents

List of Figures

Chapter 3

List of Tables

Chapter 1

Chapter 2

Chapter 3

Abbreviations

°C – Degrees Celsius

BC – Black Carbon

bhp-hr – Brake horsepower/hour

C – Carbon

CA – California

CAAP – Clean Air Action Plane

CARB – California Air Resources Board

CO – Carbon monoxide

CO_2 – Carbon dioxide

DPF – Diesel Particulate Filter

EGR – Exhaust Gas Recirculation

FEAT – Fuel Efficiency Automobile Test

FEL – Family Emission Limit

HC – Total hydrocarbons

HDV – Heavy-duty Vehicle

IL – Illinois

IR – Infrared

LA – Los Angeles

m – Meter

MDV – Medium-duty Vehicle

mph – Miles per hour

mph/s – Miles per hour per second

NH_3 – Ammonia

NGV – Natural Gas Vehicle

NO – Nitrogen oxide

NO_2 – Nitrogen dioxide

NO_x – Oxides of Nitrogen

OHMS – On-road Heavy-duty Vehicle Emission Monitory System

PM – Particulate matter

PN – Particulate number

ppm – parts per million

Q – CO/CO_2

Q’ – HC/CO_2

Q’’ – NO/CO_2

SCRs – Selective Catalytic Reduction system

SEM – Standard Error of the Mean

U.S. EPA – United States Environmental Protection Agency

UV – Ultraviolet

Chapter 1 – Introduction

The United States is the world's largest consumer of transportation energy, consuming more than 25% of the world's total in 2012.[1] Light-duty cars and trucks numerically dominate the US transportation fleet but heavy-duty vehicles (HDVs) have become the fastest growing segment. Together, these two groups consume more than 85% of all transportation fuels.[2] Combined with the consistent emission reductions experienced in light-duty fleets, HDVs only account for ~3% of the on-road fleet but are responsible for an increasing percentage of oxide of nitrogen (NO_x = NO + NO_2) and particulate matter (PM) emissions. Therefore, they continue to be a target for regulations attempting to limit or eliminate these emissions.[3-5]

Vehicles still contribute a significant source of carbon monoxide (CO), hydrocarbons (HC), NO_x and ultrafine PM despite more than 50 years of regulation.[6] HDVs mainly utilize lean-burn compression ignition engines that can elevate NO_x and PM emissions when compared to spark ignition engines due to their high combustion temperatures and unburned fuel droplet cores that can form soot particles.[7] Diesel exhaust in general has been designated as a carcinogen, as there are a variety of health problems that are induced or worsened due to PM exposure including lung damage, respiratory diseases, and premature death, as well as the black carbon (BC) component of PM being an important climate forcing agent.[8] NO_x, once emitted into the atmosphere, contributes to ozone formation and secondary PM formation.[9, 10]

The health risks and environmental deterioration associated with diesel exhaust constituents raised concern from the U. S. Environmental Protection Agency (EPA), and amendments were made to the Clean Air Act in 1990 to reduce six "criteria pollutant" including PM and NO_x from diesel vehicles, and continues to be a point of emphasis in new regulations to continually reduce these emissions.[11, 12] The EPA has recently mandated stricter emissions standards with the most recent program schedule and the history of previous standards shown in Table 1 for HDVs and medium-duty vehicles (MDVs).[13-15] MDVs are defined here as vehicles with a gross vehicle weight of 14,001 to 26,000 pounds and are subject to HDV regulations and after-treatment instillation schedules. The standards shown are specifically for PM and NO_x reductions. However, beginning in 2007 most diesel engine manufacturers opted to meet a Family Emission Limit (FEL) with the EPA allowing engine families that exceed the applicable standard introduced into the fleet prior to 2010, based on their FELs, to obtain emission credits through averaging, trading and/or banking. This has allowed for some diesel engine manufacturers to meet 2010+ model year NO_x standards with engines that above the 0.2 g/bhp-hr limit.

In 2000, the California Air Resources Board (CARB) instituted the California Diesel Risk Reduction Plan with the goal of reducing diesel PM emissions 85% statewide by 2020.[16] To achieve this goal, a variety of rules and regulations have been enacted that has encouraged the retirement of older HDVs and accelerated the penetration of lower emitting HDVs to reduce fleet average PM emissions. Additionally, the San Pedro Bay Ports Clean Air Action Plan (CAAP) banned all pre-1989 model year HDVs starting in

October 2008 at the Ports of Long Beach and Los Angeles.[17] For all of the remaining HDVs, it further required them to meet Federal 2007 emission standards by 2012. This requirement applies to all vehicles, including interstate vehicles, which move containers into the South Coast Air Basin and beyond. In California the National EPA Highway Diesel Program is a part of a number of new regulations that will continue to be implemented over the next few years.

CARB has also implemented a Drayage Truck Regulation that required all pre-1994 engines be retired or replaced by the end of 2009, as well as an 85% PM reduction for all 1994 to 2008 engines. By the end of 2013, all drayage HDVs had to meet the 2007 emission standards. This rule applied to all HDVs with a gross vehicle weight rating of 33,000 pounds or more that move through ports or intermodal rail yard properties for the purposes of loading, unloading or transporting cargo.[18] The combination of regulations has resulted in the Port of Los Angeles having a fully DPF-equipped fleet as of 2012.

In addition, CARB's Statewide Truck and Bus Regulations, an accelerated retirement rule, phased in most PM requirements for all HDVs from 2011 to 2014 and will phase in the 2010 NO_x emission standards between 2013 and 2023.[19] This will require all HDVs operating within the state of California to meet both the most recent NO_x and PM standards. It is the Truck and Bus rule that has helped to expedite heavy-duty fleet turnover across the state. With the combination of retiring older vehicles, expediting fleet turnover and newer technologies resulting from lowering emission standards, CARB anticipates a 76% reduction in ambient NO_x and a 34% reduction in ambient PM due to improvements from diesel vehicles by 2035 from 2000 levels.[20]

Table 1. United States Environmental Protection Agency MDV and HDV emission standards schedule for PM and NO_x.

Engine Model Year	NO_x (g/bhp-hr)	PM (g/bhp-hr)
Older than 1990	10.7	0.60
1990	6.0	0.60
1991-1993	5.0	0.25
1994-1997	5.0	0.1
1998-2003	4.0	0.1
2004-2006	4.0	0.1
2007 and newer	-	0.01
2007-2010[a]	0.2	-
2010 and newer[b]	0.02	-

[a] NO_x standard phased-in with 50% compliance in 2007 model years to 100% in 2010 model year vehicles for credits.

Before advanced after-treatment systems, control of NO_x and PM emissions in diesel engines were constrained to engine operations that traded-off the control of these two pollutants. This involved changing cylinder air to fuel ratios that, when enriched, would lower NO_x emissions but increase engine out PM and vice versa. Advanced control and after-treatment technologies deployed in the post-2007 timeframe for compliance with the U.S. EPA and CARB heavy-duty engine emission standards do not utilize the NO_x/PM trade-off. These advanced technologies include a combination of diesel particle filters (DPFs), selective catalytic reduction systems (SCRs), and advanced exhaust gas recirculation (EGR) control strategies, which can provide control for both species.

It is impossible to eliminate all engine-out particles from combustion engines and so the current approach has been to trap the particles before they enter the atmosphere. Therefore, DPFs, which are typically ceramic, size exclusion filters that work by physically intercepting particles from engine out exhaust and preventing them from escaping into the atmosphere, have been exclusively employed to meet the lower particle emission standards.[21] To extend service life, these devices periodically regenerate themselves with the addition of fuel to fully combust the trapped particles (active regeneration). However, DPFs have to be removed from the vehicle periodically to eliminate accumulated ash. Prior to stricter NO_x standards for model years 2010 and newer, EGR was used to reduced tailpipe NO_x for model years 2007-2009, while maintaining low PM emissions due to DPF use.[22] Because of this, engines that utilize EGR and DPFs (mainly model year 2007-2009) depend heavily on properly working DPFs in order to remove tailpipe PM emissions and require proper maintenance. If cracks or impairments from vibrations, regeneration events or improper use occur over their useful lifetime, these vehicles are subject to increased tailpipe PM emissions.

One early approach to reduce NO_x and particle emissions was to install an oxidation catalyst upstream of the DPF or catalyze the DPF itself to convert engine-out NO emissions to NO_2. NO_2 is then capable of oxidizing the trapped particles to regenerate the filter (passive regeneration), or clear the filter of particles, at lower temperatures than possible with other species. However, if the production of NO_2 is not controlled well, it can lead to an increase in NO_2 tailpipe emissions, and the unintended consequence of increased ozone and NO_2 in urban areas.[23-25] European experiences with

increasing prevalence of DPFs have shown a correlation with increases in urban NO_2 emissions.[26, 27] California has codified this concern by passing rules that limit any increases in NO_2 emissions from the uncontrolled engine baseline emissions for retrofit DPF devices.[28]

To improve NO_x reductions further and to help meet the 2010 standards, SCRs were installed downstream of a vehicle's DPF. SCRs utilize thermalized urea to produce ammonia which subsequently reduces NO_x to nitrogen (N_2) and water. The reductions have been reported between 75 and 95% for tailpipe NO_x under optimal temperature and urea dosing conditions.[29-31] An SCR system is temperature dependent for two reasons: (1) Urea requires a minimum of 200 °C for thermalization to form ammonia needed for NO_x reduction, and (2) the SCRs' catalyst is required to be above this temperature, depending on the material, to effectively reduce NO_x to N_2 due to the higher activation barrier for nitric oxide (NO).[29, 32]

Current in-use systems have been able to comply with the laboratory certification testing, but it is debated how well the standards are actually met during on-road operations to meet the anticipated reductions. Dixit et al. showed that low speed operations produce elevated NO_x emission factors, upward of 2−4 times the certification levels due to lower engine operating temperatures, and the lowest emissions factors were achieved at higher operating temperatures.[33] Similarly, Quiros et al. researched seven HDVs (five of which were diesels) and revealed that on-road HDVs, under urban driving conditions and drayage operations, tend to exceed the current NO_x standard.[34]

The robustness of these after-treatment systems in realistic everyday usage is of great importance, and the investigation of their in-use performance forms the foundation of the research presented here. One way to investigate the efficacy and reliability of vehicle emission control systems is to make repeat emission measurements of HDVs over time and document the changes observed. This approach has been used successfully for light-duty vehicles at multiple sites across the US and for HDVs at the Port of Los Angeles and the Caldecott tunnel in Oakland, CA.[35-40] Emulating these previous light-duty studies, campaigns were setup to investigate long-term trends for HDVs, creating the largest datasets for on-road HDVs in the world. It also presented an opportunity for novel MDV emission insight and comparison to other regulated vehicles.

This research collected and analyzed multi-year studies of HDV emissions and provides insights into how DPFs and SCRs age using two different on-road emission monitoring systems, the On-road Heavy-duty Measurement System (OHMS) and the Fuel Efficiency Automobile Test (FEAT). OHMS was used to measure two locations in California in 2013, 2015 and 2017: the Port of Los Angeles and the Cottonwood weigh station (17 miles south of Redding, CA). FEAT collected emission data at the Peralta weigh station located in Southern California on Eastbound Highway 91 prior to the Weir Canyon exit in 2017.

1.1 On-road Heavy-duty Vehicle Emissions Monitoring System (OHMS)

The OHMS measurement method is composed of an exhaust collection system, an exhaust measurement system and a vehicle monitoring component. The exhaust collection system consists of a modified event tent, large enough for HDV to drive under, which acts as a containment vessel for exhaust from vehicles with elevated exhaust stacks. The tent used in this study is shown in Figure 1 and was 50 ft. long, 15 ft. wide and 18 ft. high at its peak. The vehicle's passenger side of the tent has a ¾ length side wall to help trap the exhaust, as HDVs typically have at least one elevated exhaust stack behind the passenger side of the cabin. The driver's side tent wall was left open so the driver would not have an obstructed view of traffic. The completely open side wall also helped to reduce the tent's wind profile. The tent's legs were secured to the ground with either water barrels or cement weights.

Anchored underneath the roof of the tent, along the passenger side of the vehicle, is the exhaust air intake pipe (Figure 2). It consists of a 50-foot long piece of 4" diameter light-weight, thin wall polyethylene irrigation pipe secured with rope to the underneath side of the tent roof with air intake holes drilled every foot for a total of 50 holes. The holes' diameters gradually decrease in size from ~1 inch at the entrance of the tent to ¼ inch at the exit and were generally angled toward the roadway. At the tent exit, the pipe was attached to a short section of pipe with two 90º elbows that move the air flow to the outside wall of the tent and point it toward the ground where, after an additional 5 feet of pipe, it was connected to an inline fan (Fantech FG 4XL, 135 cfm). One final piece of

pipe, ~2 feet long, was added after the fan through which the analyzer sampling lines are inserted into the exhaust air stream.

Figure 1. A photograph of the OHMS setup at the Cottonwood weigh station in northern California. The exhaust intake pipe is in the upper left part of the tent and two of the water barrels are visible next to the right front tent leg. The orange road barrel just to the right of the mobile laboratory contains the camera used to take the picture of each vehicles license plate.

As a HDV with elevated exhaust drives through the tent, the exhaust contained in the tent is drawn through the holes throughout the length of the tent. When the vehicle speed matches the pipe's air speed, exhaust sampled from a previous hole is accumulated with new exhaust at each successive hole. The air intake pipe has an estimated residence time of approximately 8 seconds, and the vehicle emissions are rapidly diluted in the process by an approximate factor of 1000. In this way, the perforated tube integrates the

vehicle's exhaust over any drive cycle occurring under the tent. The design goal was a typical on-road acceleration cycle that a HDV might use while driving in any urban area.

Figure 2. Photograph showing a closer view of the exhaust sampling pipe anchored to the roof of the tent. The inline fan is the metal oval between the two sections of pipe.

The emission analyzers were housed in the University's mobile lab parked next to the tent exit (shown in Figure 1) and consisted of a Horiba AIA-240 CO and CO_2 analyzer, two Horiba FCA-240 THC/NO analyzers for the gaseous pollutants and for particle measurements, a Dekati Mass Monitor (DMM 230-A), a Droplet Measurement Technologies Photoacoustic Extinctiometer (PAX) and a TSI fast mobility particle sizer

(FMPS) were used. The Horiba AIA-240 measured CO and CO_2 using non-dispersive infrared absorption. The determination of total hydrocarbons (THC) is made with one of the Horiba FCA-240 instruments using a flame ionization detector (FID). This analyzer was also used to measure NO using the ozone chemiluminescent reaction. The second Horiba FCA-240 was only used for a second NO measurement and is configured to measure total NO_x (NO + NO_2). This is accomplished with the addition of a reaction chamber and a catalyst supplied by the manufacturer in the analyzer that converts all nitrogen dioxide (NO_2) to NO which is then measured using ozone chemiluminescence.

The Dekati DMM was used to measure total particle mass (PM) and particle number concentration ([PN]) measurements and contains an inertial 6-stage cascade impactor with a mobility channel for aerodynamic size and a corona charger with an online particle density measurement for particle mobility size information. These two components combined with the assumption that the particles measured are spherical and there is a lognormal particle size distribution enable density calculations of the particles required for conversion from measured impactor current values to report total PM in $\mu g/m^3$ and [PN]. The DMM sampled over a particle size range from 0 to 1.2 μm and particles larger than 1.2 μm are not measured.

The PAX measured light scattering for all particles with a reciprocal nephelometer and a photoacoustic cell for absorption measurements of only black particles to determine BC mass concentration. A modulated diode laser simultaneously measured the scattering and absorption of particles. The standard 870 nm wavelength is highly specific for BC particles with little absorption from other gases or aerosols. As the

laser beam is directed through the aerosol stream, absorbing particles heat up and transfer energy to the surrounding air producing pressure waves detected by a microphone in the photoacoustic cell.

The FMPS elucidated particle distributions by size (5.6-560 nm) with electrometers. This instrument was used for specific vehicle analysis on a case by case basis, as all data from this instrument required post-data collection time alignment and calculations. All analyzers sampled continuously at 1Hz, but only the PM, [PN] and BC data are continuously recorded and saved.

Figure 3 is a schematic diagram (not drawn to scale) of the exhaust sampling system, vehicle monitoring components and data collection computers.[41] The gaseous analyzers were fed by a twin piston pump (KNF NeuBerger) which delivered 55 L/min of exhaust via ¼ inch Teflon tubing. The compressed sample was routed through a water condensation trap to dry the sample before it passed through the analyzers. The particulate instruments had individual sampling pumps and were fed by separate ¼ inch copper tubes.

Additional information collected on each vehicle measured included a front license plate picture, speed and acceleration rates, external exhaust pipe thermographs and a digital picture of the driver's side of the vehicle. The license plate of each vehicle is captured using a camera positioned in front of the tent inside a road barrel. The camera, when triggered by a vehicle, captures an image of the front of each vehicle. The images are stored digitally and the transcribed plates were incorporated into the emissions database. The license plates were matched against a number of state registration records

as availability dictated and non-personal vehicle information was retrieved and added to the emissions database.

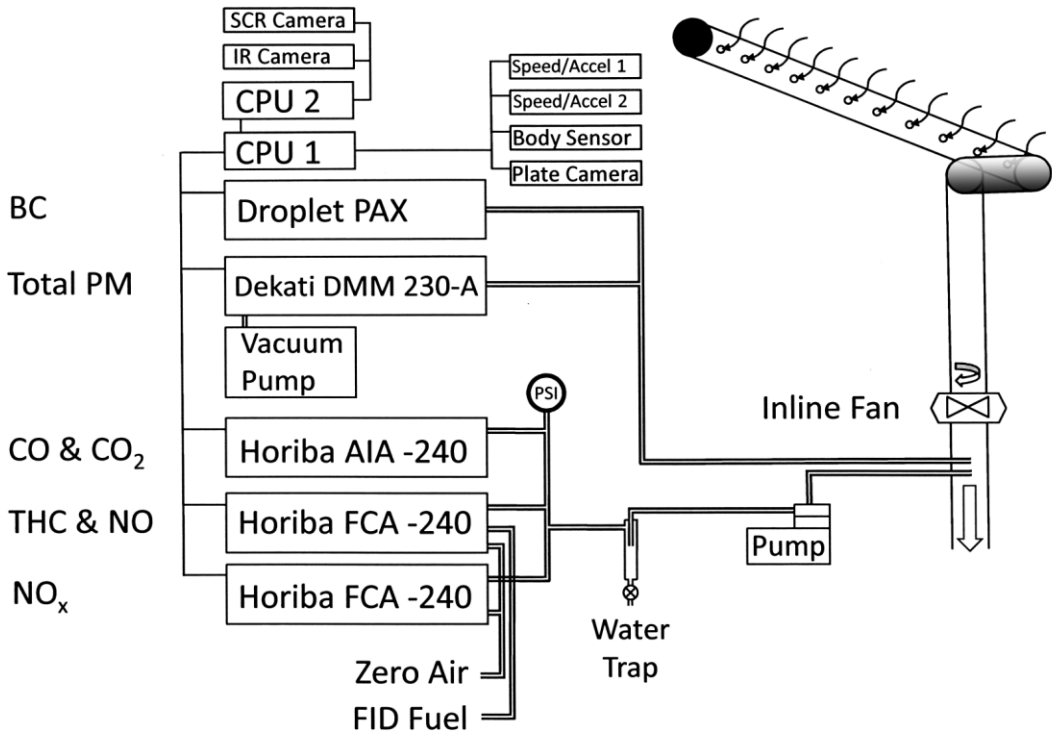

Figure 3. Schematic drawing (not to scale) of the OHMS exhaust sampling, analysis and vehicle emissions data collection systems.

Speed and acceleration were measured on each vehicle at the entrance and exit to the tent. Speed sensing bars (Banner Industries) consisted of a pair of infrared beams passing across the road, 6 feet apart and approximately four feet above the roadway. OHMS set-up utilized two pairs of speed sensing bars (entrance and exit) reporting two sets of speeds and accelerations. Vehicle speeds are reported in units of mph and were calculated at each location from the average of the two reported times collected when the front cab of the tractor blocks the first and second beam, and when the rear of the cab

unblocks each beam. The acceleration at the entrance and exit are reported in units of mph/s.

An infrared camera (Thermovision A20, FLIR Imaging) was used to capture IR thermographs, an example is shown in Figure 4, of elevated exhaust pipes to qualitatively record vehicle operating temperature. An additional computer system and software were installed to store the captured thermographs from the infrared camera on the passenger side of each HDV. The thermographs were initially compared to a laboratory calibration using a stainless-steel exhaust pipe and temperatures were estimated for the individual exhaust.[37]

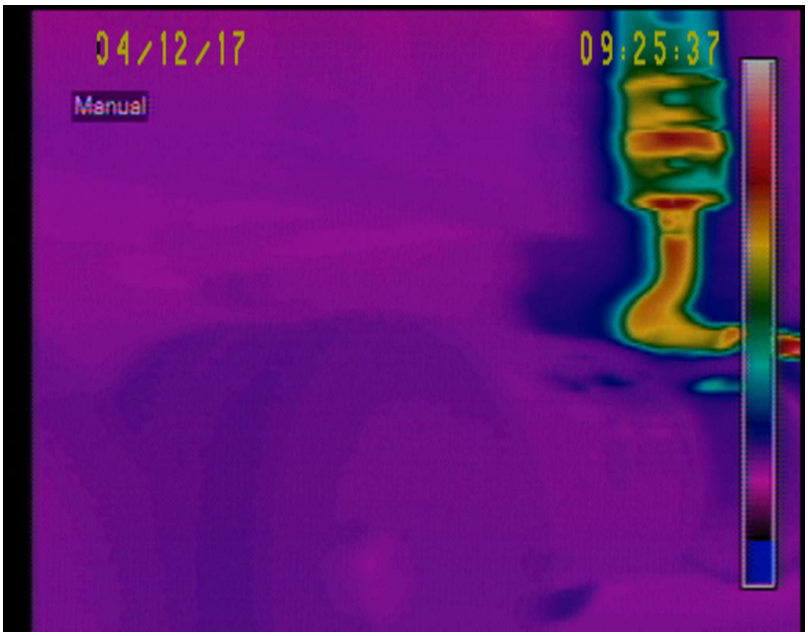

Figure 4. IR thermographic image of the exhaust pipe taken at the Cottonwood location of a truck leaving the scales. The relative scale ranges from approximately ~50°C for blue to ~160°C for bright red.

To convert infrared emission images to an absolute temperature involves knowing the emissivity of the material being imaged. HDV exhaust systems are primarily stainless

steel, thus the choice for the laboratory calibration, however small alterations in its formulation and finish can result in large (in some cases up to a factor of 10) changes to the steel's emissivity.[42] Because of these uncertainties in emissivity, the infrared camera was calibrated with on-road HDV's exhaust pipes in December of 2014, and exhaust pipe temperatures were recorded with a thermocouple between 50°C to 150°C for individual vehicles in combination with IR thermographs. Appendix A details the temperature measurements on 226 HDVs which resulted in a significant reduction in the temperature scale range than was originally used to assign temperatures to the IR thermographs.

A second, consumer grade, digital camera (Canon SX100) was used to collect images of the driver side of the vehicles measured in the OHMS setup. DMV registration information does not provide any information regarding the emission control devices that might be installed on HDVs limiting data analysis to using chassis model year as the defining emissions classification. Since the NO_x emission standard was phased in beginning with 2010 engines and was not fully phased in until after 2016 engines, many vehicles in that age range do not have SCR systems. These pictures are an attempt to locate vehicles with visible urea tanks, often with distinguishable blue tank caps visible on the driver's side of the truck, as shown in Figure 5. These images were visually inspected and HDVs found to have a urea tank were marked as such in the database. The visibility of these blue caps has declined over the years as they have been covered in newer model years as manufacturers are making SCR equipped vehicles more esthetically pleasing and more aerodynamic. The data acquired with this camera is merely for qualitative support and was more useful in the beginning years of this work.

Figure 5. Driver side image of a truck leaving the port location with the urea tank (blue cap) clearly visible.

OHMS directly measures HDVs fuel specific emissions of CO, THC, NO, NO_x, PM and BC as ratios to CO_2, which yields molar ratios that are often constant for a given exhaust plume. The tent is long enough to allow the possibility of multiple operating modes to be observed and introduces the possibility of measuring differing emission ratios. This means that some of the fuel specific emissions that are reported are averages of those multiple operating modes.

For field calibration, the CO_2 analyzer was spanned at each site with a certified mixture of 3.5% CO_2 in nitrogen (Air Liquide). The CO, HC, NO and total NO_x analyzers are adjusted to have a positive offset when sampling background air to preclude any negative readings. Daily calibrations of CO, HC, NO and the total NO_x analyzers are made with multiple injections of a BAR-97 certified low-range calibration gas (0.5% CO, 6% CO_2, 200ppm propane and 300ppm NO in nitrogen) using a large Delrin syringe and injecting into the gas sampling pump intake tube above the inline fan and averaging the measured CO/CO_2, HC/CO_2, NO/CO_2 and NO_x/CO_2 ratios and then dividing by the

cylinder's certified ratios. The results are used to scale all measured vehicle emission ratios. The Dekati DMM-230A was factory calibrated and calibration of the PAX was performed in-lab prior to field measurements following the manufacturer's instructions. Both particle instruments were zero-corrected daily as needed.

Data collection is initiated when the IR body sensor at the tent exit is blocked, signaling the presence of a vehicle. Digital images are recorded from the plate camera, the IR camera and the SCR camera and emissions voltage data are collected at 1Hz from the five analyzers. The length of the sampling can be tailored, depending on the frequency of the HDV traffic. Initially, 20 seconds of data was collected for each HDV at the Port and 15 seconds of data at the Cottonwood weigh station in 2013. In 2015 and 2017 only 15 seconds of data was collected at both sites to prevent interferences from HDVs following each other too closely. The voltage data are converted into concentrations, either ppm or $\mu g/m^3$, depending on the analyzer, using the instrument response equations. Figures 6 and 7 are the reported second by second emission concentrations for a 2003 Freightliner measured at the Cottonwood weigh station. The raw data as shown have not yet been time aligned, which is apparent comparing the CO_2 trace with the NO_x measurements.

Time lags, by instrument, are determined during OHMS's setup and used to correct for the difference in response times. Although this is not always perfect and occasionally needs adjusting throughout a campaign, it allows for each emission species to be correlated to CO_2. With this correlation, a least squares line is fit to the data with the slope of the line equal to the species fuel specific emissions ratio.

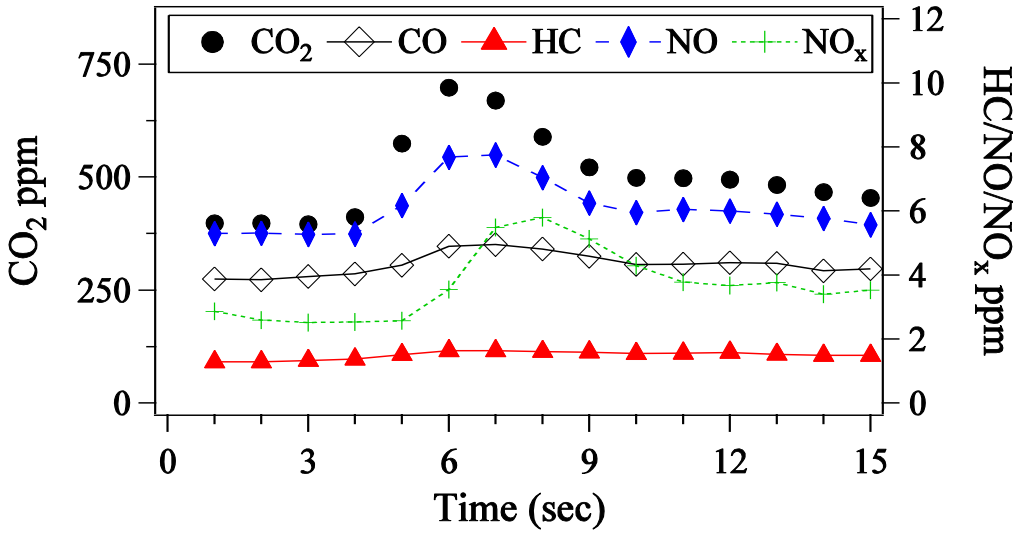

Figure 6. Concentration time series for the gaseous species from a 2003 Freightliner measured at the Cottonwood site. CO_2 data (circles) are plotted on the left axis while the CO (open diamonds), HC (triangles), NO (filled diamonds) and NO_x (pluses) are plotted on the right axis. Data has not been time aligned.

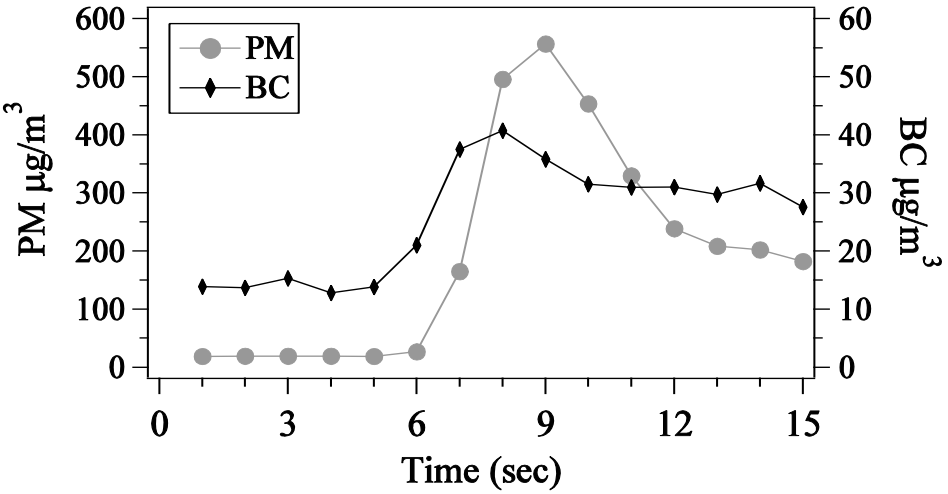

Figure 7. Concentration time series for the particulate emissions from a 2003 Freightliner measured at the Cottonwood scales. Total PM mass (circles) data are plotted on the left axis and the BC mass (diamonds) are plotted on the right axis. Data are not time aligned.

Figures 8 and 9 show the emission correlation results for this specific 2003 Freightliner vehicle. The y-axis offsets are merely to show the relationship clearer. The

measured pollutant ratios can be reported as the final measurement but in this research they are directly converted into grams of pollutant per kilogram of fuel burned by carbon balance. The molar ratios are converted to moles of pollutant per mole of carbon in the exhaust with the following equation:

$$\frac{\text{moles pollutant}}{\text{moles C}} = \frac{\text{pollutant}}{CO + CO_2 + HC} = \frac{\left(\frac{\text{pollutant}}{CO_2}\right)}{\left(\frac{CO}{CO_2}\right) + 1 + \left(\frac{HC}{CO_2}\right)} = \frac{Q, Q', Q''}{Q + 1 + Q'}$$

OHMS directly measures the ratios of $Q = \frac{CO}{CO_2}$, $Q' = \frac{HC}{CO_2}$, $Q'' = \frac{NO}{CO_2}$, etc. that are often constant for a given exhaust plume. Moles of pollutant are converted to grams by multiplying by molecular weight, such that if CO is the gas measured, then 28gCO/mole is used, and the moles of carbon in the exhaust are converted to kilograms by multiplying the result by 0.014 kg of fuel per mole of carbon in fuel (~860 gCarbon/kg of fuel), assuming the fuel is stoichiometrically CH_2. Grams per brake-horsepower hour emissions (HDV Federal certification units) can be estimated from grams per kg of fuel burned by assuming an engine fuel usage rate. An estimate for constant fuel usage rate of 0.15 kg/bhp-hr has previously been used, based on an average assumption of 470g CO_2/bhp-hr.[43] This assumption will be used for comparing our data to standards that are in g/bhp-hr.

Emission measurements were collected at two locations in California in the spring of 2013, 2015 and 2017, one at the Port of Los Angeles and the other at the California Highway Patrol's Cottonwood weigh station. Figure 10 is a map showing the two sites relative location to each other. The Port of Los Angeles site in Wilmington, CA has been used since 2008 for four additional measurement campaigns of HDV conducted by the

University of Denver using the FEAT system.[36, 37] Measurements were made at the exit gate from TraPac's container berths just west of the intersection of West Water Street and South Fries Avenue. The Cottonwood weigh station is located on North I-5 outside of Cottonwood, CA (17 miles South of Redding, CA) and measurements were collected on the inside lane as the vehicles exited the facility.

OHMS measurement quality assurance parameters are detailed in Appendix B.

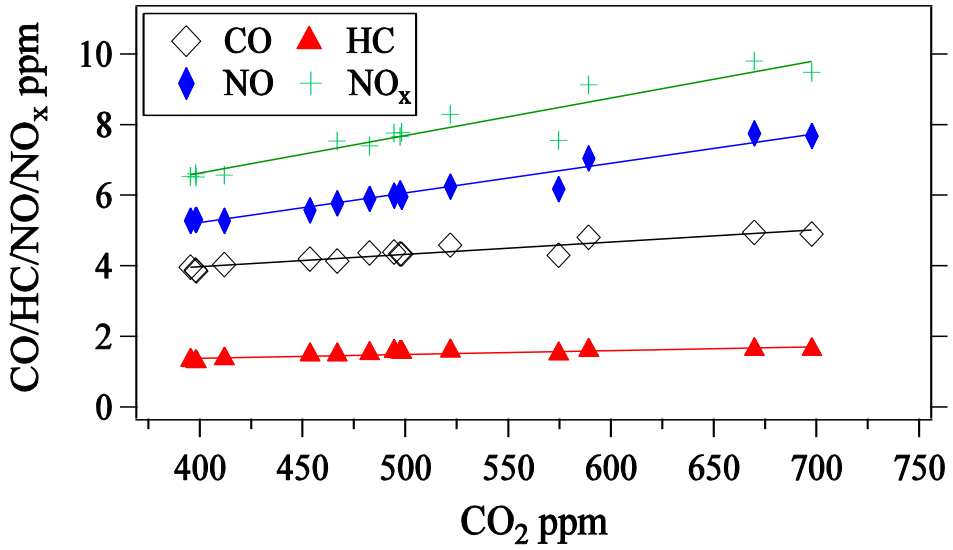

Figure 8. Correlation plots for each of the gaseous species against CO_2 for the 2003 Freightliner measured at the Cottonwood weigh station. The NO_x concentration data have been offset from their true values to clearly show the data points.

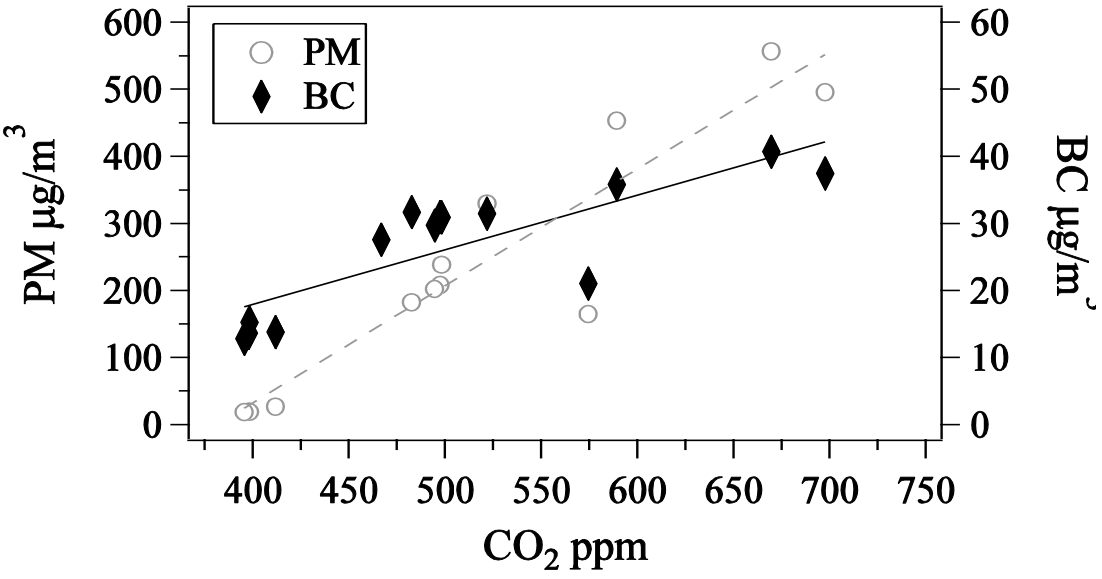

Figure 9. Correlation plots for fuel specific PM (left axis) and BC (right axis) against CO_2 for the 2003 Freightliner measured at the Cottonwood weigh station.

Figure 10. Map showing relative locations of the two California sampling sites. *California map from geology.com

1.2 Fuel Efficiency Automobile Test (FEAT)

The FEAT remote sensors used in this study were developed at the University of Denver for measuring the pollutants in motor vehicle exhaust, and have previously been described in the literature.[44-46] The instrument consists of a non-dispersive infrared component for detecting CO, CO_2, HC, and Infrared (IR) percent opacity, and two dispersive ultraviolet (UV) spectrometers for measuring nitric oxide (NO), nitrogen dioxide (NO_2), sulfur dioxide (SO_2), and NH_3 with NO_x determined by the addition of NO and NO_2. The source and detector units are positioned on opposite sides of the road

in a bi-static arrangement. Collinear beams of IR and UV light are passed across the roadway into the IR detection unit, and are then focused onto a dichroic beam splitter, which serves to separate the beams into their IR and UV components. The IR light is then passed onto a spinning polygon mirror, which spreads the light across the four IR detectors: CO, CO_2, HC, and reference (opacity is determined by plotting reference vs. CO_2). The UV light is reflected off the surface of the beam splitter and is focused onto the end of a quartz fiber-optic cable, which transmits the light to dual UV spectrometers. The UV spectrometers are capable of quantifying NO, SO_2, NH_3 and NO_2 by measuring absorbance bands in the regions of 200 - 226 nm and 429 - 446 nm respectively, in the UV spectrum and comparing them to calibration spectra in the same regions.

The exhaust plume path length and density of the observed plume are highly variable from vehicle to vehicle, and are dependent upon, among other things, the height of the vehicle's exhaust pipe, exhaust volume, wind, and turbulence behind the vehicle. For these reasons, the remote sensor directly measures only molar ratios of CO, HC, NO, NO_2, NH_3, SO_2 to CO_2. Appendix C provides a list of the criteria for valid/invalid data. These measured ratios can be converted directly into grams of pollutant per kilogram of fuel. This conversion is achieved by first converting the pollutant ratio readings to the moles of pollutant per mole of carbon in the exhaust from the following equation:

$$\frac{\text{moles pollutant}}{\text{moles C}} = \frac{\text{pollutant}}{CO + CO_2 + 3HC} = \frac{(\text{pollutant}/CO_2)}{(CO/CO_2) + 1 + 6(HC/CO_2)} = \frac{(Q,2Q',Q'')}{Q+1+2*3Q'}$$

Q represents the CO/CO_2 ratio, Q' represents the HC/CO_2 ratio and Q" represents the NO/CO_2 ratio. Next, moles of pollutant are converted to grams by multiplying by molecular weight (e.g., 44 g/mole for HC since propane is measured), and the moles of

carbon in the exhaust are converted to kilograms by multiplying (the denominator) by 0.014 kg of fuel per mole of carbon in fuel, assuming the fuel is stoichiometrically CH_2. The HC/CO_2 ratio includes a factor of two (Singer factor) times the reported HC because the equation depends upon carbon mass balance and the NDIR HC reading is about half a total carbon FID reading.[47] For natural gas vehicles the appropriate factors for CH_4 are used along with a Singer factor of 3.13. Grams per kg fuel can be approximately converted to g/bhp-hr by multiplying by a factor of 0.15 based on an average assumption of 470 gCO_2/bhp-hr as previously discussed.[48]

The FEAT detectors were calibrated, as external conditions warranted, from certified gas cylinders containing known ratios of the species that were tested. This ensures accurate data by correcting for ambient temperature, instrument drift, etc. with each calibration. Because of the reactivity of NO_2 with NO and NH_3 with CO_2, three separate calibration cylinders were needed: 1) 6% CO, 6% CO_2, 0.6% propane (HC), 0.3% NO and N_2 balance; 2) 0.05% NO_2, 15% CO_2 and air balance; 3) 0.1% NH_3, 0.6% propane and balance N_2. Since fuel sulfur has been nearly eliminated in US fuels, SO_2 emissions are generally below detection limits, and although SO_2 measurements are routinely collected and archived for each data campaign, since 2012 SO_2 has not been calibrated for and is not included in the discussion of the results.

For the first time, two FEAT instruments were used concurrently in the Peralta weigh station campaign in 2017. One was 14’3” above the ground to capture elevated exhaust plumes (High FEAT), while a second FEAT instrument was placed on the pavement to collect emission data for low exhaust vehicles (Low FEAT). These two

FEAT devices had different triggers for data collection. The High FEAT was triggered when a vehicle passed through an IR body sensor which started 1 second of 100 Hz data collection. The Low FEAT was triggered conventionally when a vehicle's tire passed through the Low FEAT IR beam, causing the reference signal to be blocked, and half a second of data was collected for each Low FEAT measurement. The Low FEAT uses a shorter sampling time in order to complete the sampling before the rear trailer wheels interrupt the measurements.

The FEAT remote sensors were accompanied by a video system that recorded a freeze-frame image of the license plate of each vehicle measured. The emissions information for the vehicle, as well as a time and date stamp, is recorded for each video image. The images are stored digitally, so that license plate information may be incorporated into the emissions database during post-processing. A device to measure the speed and acceleration of vehicles driving past each remote sensor was also used in this study. The system consisted of a pair of infrared emitters and detectors (Banner Industries) which generate a pair of infrared beams passing across the road, six feet apart and approximately four feet above the surface. Vehicle speed is calculated from the average of two times collected when the front of the tractor's cab blocks the first and the second beam and the rear of the cab unblocks each beam. From these two speeds, and the time difference between the two speed measurements, acceleration is calculated, and reported in mph/s.

A satellite photo showing the weigh station grounds and the approximate location of the scaffolding and FEAT instruments are shown in Figure 11. High FEAT was setup

for all measurement days, whereas Low FEAT was operational for the last three days. The High FEAT detectors were positioned on clamped wooden boards atop aluminum scaffolding at an elevation of 13’3”, making the IR/UV beams and detectors at an elevation of 14’3” (see Figure 12). The scaffolding was stabilized with three wires arranged in a Y shape. A second set of scaffolding was set up directly across the road on top of which the IR/UV light source was positioned. The Low FEAT unit was setup on the ground just to the east of the scaffolding towers. Behind the detector scaffolding was the University of Denver’s mobile lab housing the auxiliary instrumentation (computers, calibration gas cylinders and generator). Speed bar detectors were attached to each scaffolding unit which reported truck speed and acceleration for the High FEAT and on tripods just after the Low FEAT. Three video cameras were placed down the road from the scaffolding, taking pictures of license plates, urea tanks and an IR image of exhaust pipes when triggered.

Exhaust thermographs were taken with an infrared camera (Thermovision A20, FLIR Systems) for qualitatively estimating the exhaust temperatures of HDVs with elevated exhaust pipes leaving the weigh station and remote controlled digital pictures of the vehicle’s driver side for investigating the presence of urea tanks. Both video systems were successfully operated with the IR camera system capable of imaging the exhaust systems for a majority of the HDVs that had elevated exhaust systems, and a field-calibration of this IR camera allows for these images to be converted into temperatures as previously mentioned. MDVs’ IR thermographs were not captured as most were low exhaust. In addition, a consumer grade Canon digital camera was set up and could be

remotely triggered by a computer controlled garage door opener to take pictures of the driver side of the truck chassis to help identify urea tanks, indicative of SCR systems, on individual HDVs.

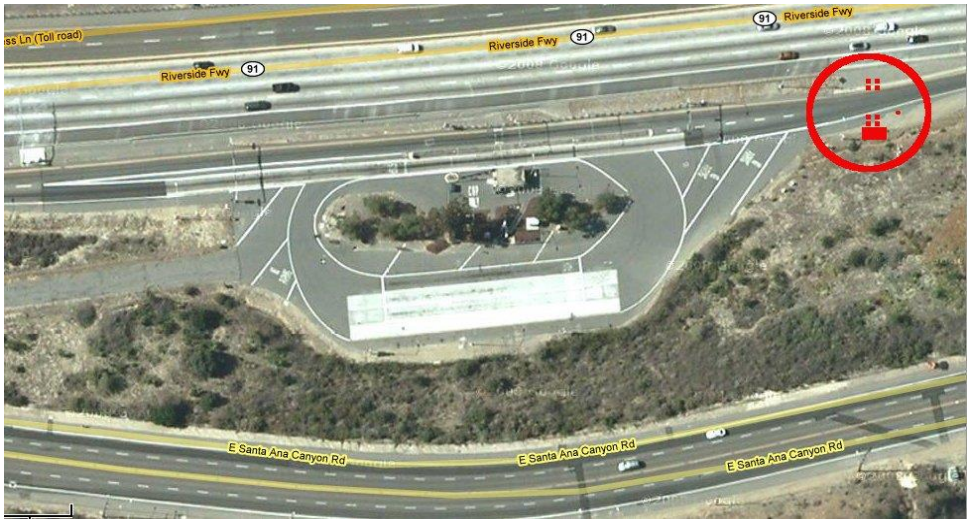

Figure 11. A satellite photo of the Peralta weigh station located on the Riverside Freeway (State Route 91). The scales are located on the inside lane next to the building in the top center and the outside lane is for unloaded HDVs. The measurement location is circled at the upper right with approximate locations of the scaffolding, support vehicle and camera.

Figure 12. Photograph at the Peralta Weigh Station of the High and Low FEAT setup used to detect exhaust emissions from heavy and medium-duty vehicles.

Measurements on HDVs were first collected in 1997 at this location and with the current measurements reported on in this thesis will form one of the longest emissions measurement records (20 years) for HDVs in the US. There are now six completed campaigns to date: 1997, 2008, 2009, 2010, 2012 and 2017.[36] The 2017 data were collected similarly to the previous measurements, but with the addition of the Low FEAT. In 2017, data was collected over four days in March (20-23) from 8:00 to 14:00 on the lane reentering Highway 91 eastbound (SR-91 E) after the vehicles had been weighed. Sampling took place in the exact location used for all of the previous campaigns on the single lane at the end of the station where vehicles were reentering the highway. Most vehicles were traveling between 10 and 20 mph in an acceleration mode to regain speed for the upcoming highway merger. This weigh station is just west of the Weir Canyon Road exit (Exit 39).

The new data collected in the spring of 2017 allows for the continuing evaluation of emission trends for HDVs, and for the first time a detailed study of MDV emissions both of which are subject to the current California standards.

Chapter 2 – OHMS

The three campaigns using the OHMS technology have resulted in the collection of a total of 7,073 HDV emission measurements and vehicle information being compiled for study. This comprises one of the largest in-use emissions data set collected to date on HDVs. Data at both locations were filtered of measurements with unmatched license plates or invalid CO_2 detection. These databases, as well as any previous data our group has obtained for HDVs can be found at www.feat.biochem.du.edu. Summary for each year is provided, followed by a discussion of the combined data sets.

2.1 2013 Measurement Summary

The Port sampling collection was conducted between Monday April 22 and Friday April 26, 2013 from approximately 8:00 to 17:00 just beyond the checkout exit kiosk at the Port of Los Angeles. Three lanes led to the exit, lane one was used for the OHMS set-up and data collection and the remaining two lanes were used by Trapac for overflow and bobtails. The set-up is just west of the intersection of West Water Street and South Fries Avenue approximately 30 feet beyond the blue exit kiosk. A picture of the 2013 OHMS set-up at the port is shown in Figure 13. The vehicles would come to a halt at the exit kiosk and then accelerate through the OHMS set-up. As seen in previous campaigns at the Port, the majority of vehicles at this location are California registered

vehicles with only 37 vehicles registered outside of the state in 2013. License plates were match for the California and Oregon registered HDVs.

Figure 13. Photograph at the Port of Los Angeles of the OHMS setup in 2013 used to detect exhaust emissions from heavy-duty vehicles. The perforated exhaust sampling and integration tube is again visible on the left side of the tent.

The Cottonwood weigh station is located on the northbound side of I-5 in Tehama County 17 miles south of Redding, CA. Sampling collection from 8:00 to 17:00 occurred on Monday May 6th to Friday May 10th, 2013. Three lanes pass through the weigh station with the OHMS equipment occupying the east lane.

The five days of data collection at the Cottonwood weigh station resulted in 2,316 readable license plates with a valid CO_2 plume detection. With the weigh station on a major north-south trade route the number of vehicles registered outside of California

increased significantly. License plates in 2013 were matched for California, Oklahoma, Oregon, Washington State and British Columbia Canada.

Because the vehicle emissions data is not normally distributed, using the standard error of the mean calculated from the average of the individual measurements would result in an unrealistically small uncertainty. However, the distributions of the daily averages are normally distributed and therefore calculating the standard error of the mean from the daily average distribution and then applying that fractional uncertainty to the overall mean can be used to provide a useful standard error of the mean (SEM) for mean emission factors. An example of SEM calculation is detailed in Appendix D. This methodology is used for all subsequent uncertainty analyses at all locations for both OHMS and FEAT measurement techniques.[49]

Table 2 provides a data summary of all the measurements that were collected with OHMS at the two sites in 2013. The measured mean ratios to CO_2 are reported along with the g/kg of fuel emissions with SEM calculated using the daily measurements at each site. The Port fleet is much younger than the weigh station fleet as a result of the San Pedro Bay Ports Clean Air Action Plan (CAAP) having been fully implemented.[17, 50] Since the CAAP requires all of the class 7 and class 8 vehicles to be DPF equipped the fleet means for PM and BC are significantly lower at the Port location.

Table 2. OHMS 2013 Data Summary.

Study Site	Port of Los Angeles	Cottonwood Weigh Station
Mean CO/CO_2 (g/kg of fuel ± SEM)	0.0012 (2.3 ± 0.4)	0.0026 (5.1 ± 0.2)
Median gCO/kg	0.74	3.0
Mean HC/CO_2 (g/kg of fuel ± SEM)	0.0002 (0.20 ± 0.03)	0.00025 (0.25 ± 0.04)
Median gHC/kg	0.086	0.11
Mean NO/CO_2 (g/kg of fuel ± SEM)[a]	0.0058 (12.4 ± 0.3)	0.005 (10.6 ± 0.4)
Median gNO/kg[a]	11.2	10.1
Mean gNO_x/CO_2 (g/kg of fuel ± SEM)[b]	0.0063 (20.7 ± 0.8)	0.0062 (20.3 ± 0.7)
Median gNO_x/kg[b]	19.5	19.3
Mean NO_2/CO_2 (g/kg of fuel ± SEM)	0.00069 (2.3 ± 0.3)	0.0011 (3.5 ± 0.1)
Median gNO_2/kg	1.1	3.1
Mean Mass NO_2/NO_x	0.11	0.17
Mean gPM/kg ± SEM	0.031 ± 0.007	0.65 ± 0.11
Median gPM/kg	0.003	0.21
Mean gBC/kg ± SEM	0.020 ± 0.003	0.23 ± 0.03
Median gBC/kg	0.002	0.074
Mean PN/kg ± SEM	$1.5 \times 10^{14} \pm 2.5 \times 10^{13}$	$2.1 \times 10^{15} \pm 6.0 \times 10^{13}$
Median PN/kg	2.8×10^{12}	5.8×10^{14}
Mean Model Year	2009.1	2005.6
Mean IR Estimated Exhaust Temp. (°C) ± SEM	86 ± 1	98 ± 5
Mean Entrance Speed (mph)	4.8	9.8
Mean Exit Speed (mph)	5.8	10.5
Mean Entrance Accel. (mph/s)	0.24	0.68
Mean Exit Accel (mph/s)	0.34	0.55
Slope (degrees)	0°	(-0.5)°

[a]grams of NO

[b]grams of NO_2

The measured exhaust pipe temperatures at the Port are lower than measured at Cottonwood (86 ± 1 and 98 ± 5, respectively) due in large part to the stop and go nature of Port vehicles driving before our measurement site.[37] Mean NO and NO_x emissions are similar to the means observed at Cottonwood, due to only a small percentage of vehicles that are model year 2011 or newer (11% at the Port and 18% at Cottonwood) that could even potentially be equipped with SCRs. Figure 14 is a bar chart showing the IR estimated exhaust temperature distributions for each site. Note these temperatures observed on the external exhaust pipes are likely a lower limit since the external pipes are not necessarily adjacent to the exhaust after-treatment equipment, meaning it is a qualitative examination of how hot a specific HDV's engine is. There is a higher percentage of lower exhaust pipe temperature HDVs at the Port compared to Cottonwood, which is consistent with other researchers who have identified that short-haul activities, such as those at a Port location, will have lower temperatures than vehicles under long-haul operations, characteristic of the Cottonwood fleet.[33, 34] This temperature difference is not as important for the 2013 measurement year, as vehicles without SCRs comprise the majority of the vehicles measured at these locations.

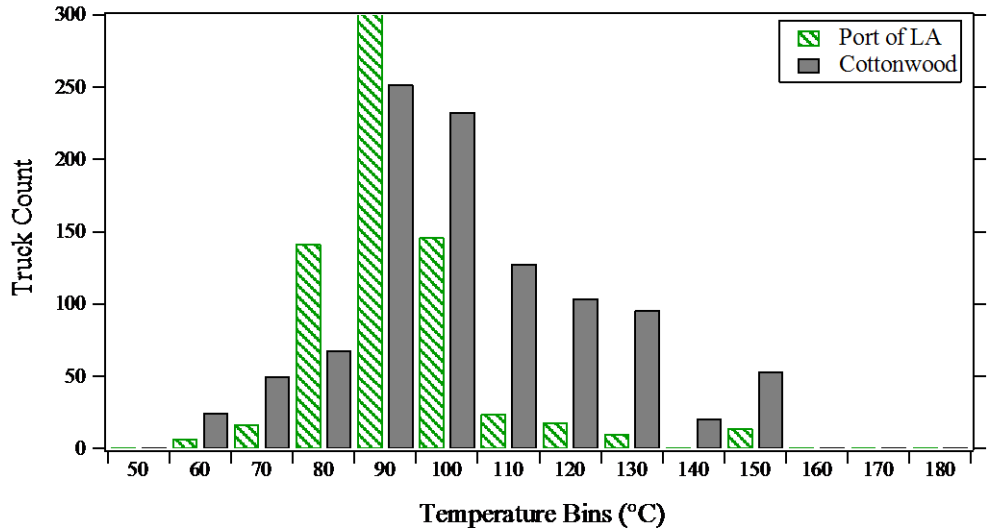

Figure 14. Distribution of infrared estimated exhaust temperatures for HDV at the two measurement locations in 2013. These data use the 2015 field calibration of the infrared camera (see Appendix A).

The majority of the Cottonwood fleet (61%) was older than 2008 models when newly manufactured vehicles were equipped with DPFs. If the 2008 and newer HDV models are compared between the Port and Cottonwood, the mean gPM/kg of fuel values are 0.03 and 0.17 gPM/kg of fuel, respectively. The factor of 5.7 differences in the means is largely accounted for by one extreme 2009 outlier (74 gPM/kg of fuel), a white smoker with no significant BC emissions, which if excluded from the Cottonwood average reduces the mean to 0.07 ± 0.01 gPM/kg of fuel. Except for this HDV, there are no other measurements that exceed ~20 gPM/kg of fuel. The Dekati DMM has an internal particle size cutoff at 1.2µm which likely helps to establish this ceiling without there being an extreme level of smaller particles as seems to be the case with the 2009 vehicle. Diesel particulate emissions generally do not even approach the 1.2µm size limit in the Dekati instrument but there have been suggestions that soot accumulating on cylinder walls can be dislodged in larger aggregates of material that could possibly explain this result.[51]

2.2 Comparison with the Most Recent Port of Oakland Measurements

In addition to our measurements at the Port of Los Angeles, measurements have also been collected in 2011 and 2013 and reported from the Port of Oakland by a University of California Berkeley group.[39, 52] The Berkeley group collects fuel specific emission measurements from HDVs using an aluminum duct suspended from an overpass as vehicles pass underneath. The 2013 Oakland BC and PN measurements included a significant number of DPF equipped vehicles and mean gBC/kg of fuel emissions for the 2013 fleet was 0.28 ± 0.05 and PN/kg of fuel was $2.47 \times 10^{15} \pm 0.48 \times 10.^{15}$ These values are significantly larger than the values measured with the OHMS system at the Port of Los Angeles of 0.020 ± 0.003 and $1.5 \times 10^{14} \pm 2.5 \times 10^{13}$ for fuel specific BC and PN respectively.

The 2013 Oakland measurements include engine model year enabling a direct comparison with our 2013 Port of Los Angeles measurements with the OHMS system. Figure 15 includes a plot of fuel specific 15a) BC and 15b) PN versus chassis model year (one year was added to the reported Oakland engine model to convert to chassis model year). The Port of Los Angeles data collected using the OHMS system (squares) is plotted against the left axis while the Port of Oakland data (circles) is plotted against the right axis. Uncertainties for the Port of Los Angeles data are SEM calculated using the daily means. If, for a moment, one ignores the absolute values for the fuel specific BC measurements, the trends and emission comparison looks quite similar. However, the y-axis scaling is exactly a factor of 10 lower for the OHMS measurements. A similar comparison is made for PN in Figure 15b, and while the trends are not as good as they

are for the BC measurements, if scaling is ignored, there is a large drop in PN for the newer model year vehicles in both datasets.

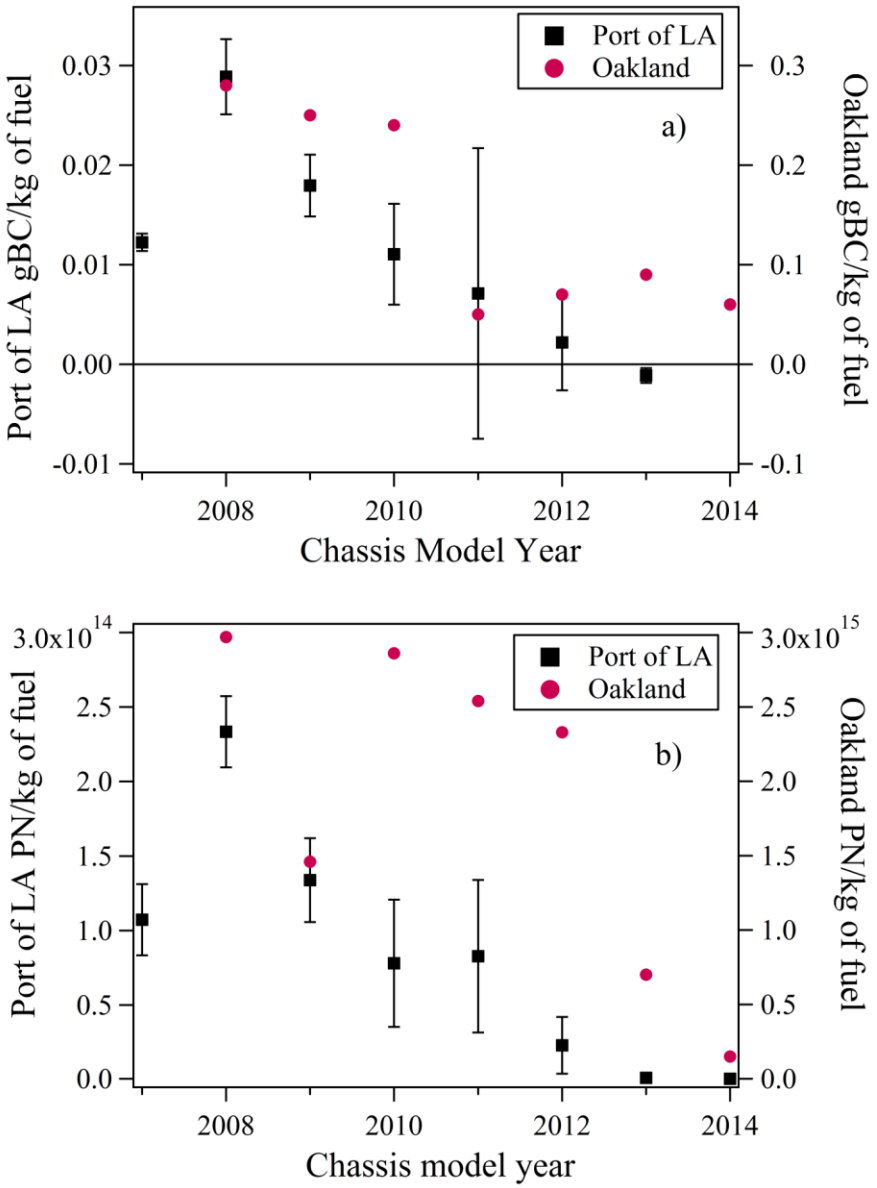

Figure 15. Fuel specific a) BC and b) PN emissions by model year collected at the Port of Los Angeles (left axis) in 2015 and data collected at the Port of Oakland (right axis) in 2013. Uncertainties for the Port of Los Angeles data are SEM calculated using the daily means.

There are a myriad of differences between the LA and Oakland studies that includes BC instruments, photoacoustic versus an aethalometer, integrated emission samples versus a single inlet sample, different fleets, and different operating modes with the Oakland data being collected at higher speeds. However, despite all these differences the fuel specific NO_x emission measurements were much closer with the Port of Los Angeles means of 20.7 ± 0.8 gNO_x/kg of fuel versus 15.4 ± 0.9 gNO_x/kg of fuel for the Oakland measurements. One possible explanation for the difference is that particle losses in the OHMS sampling plumbing could lead to underreporting of emissions which would be consistent with the direction of the differences in Figure 15.

To evaluate this possibility, a series of particle challenges with the OHMS sampling lines setup was performed in the lab. The 50-foot long pipe used in OHMS was secured to the ceiling on the first floor of the University of Denver Chemistry building and sampling lines for the gaseous and particulate instruments mirrored the set-up used for field testing with OHMS. Soot particles were generated using an oxygen starved propane torch and extinguishing the tip of the flame with a wire mesh for roughly five minutes and capturing the particles in a large plastic bag. A large diameter syringe was then used to extract particles from this bag; half of the syringe was filled with air from the particle bag and the rest was filled with 3.5% CO_2 (General Air, Denver). This establishes a fixed ratio of particles to CO_2 for each syringe. However, the mixing is inexact and the particle to CO_2 ratio did change from syringe to syringe. The syringe was large enough for multiple injections of the mock-exhaust at various positions along the

pipe. Any changes in the particle to CO_2 ratio within a given trial would indicate there are potential particle losses due to the sampling system since there should be no CO_2 losses.

Figures 16 and 17 details the tests conducted investigating whether there are any significant particle losses induced because of the presence of the 90° elbow for PM and BC, respectively. The mock exhaust was injected before and after the 90° elbow in the polyethylene pipe used in OHMS. Three injections were given for each trial, repeating the first injection a second time to reveal any changes that might occur in the syringe with time that are independent of the elbow. Trial 1 is comprised of only two injections, one of which was invalid for BC, but both had valid PM readings. Trials 2 and 3 consisted of the three injections, and all measurements were valid. Trial 3 in Figure 16 has PM/CO_2 ratios that increased with time indicating an unexplained increase in particle concentration within the syringe but are not consistent with the elbow causing particle losses. The final injection below the elbow showed additional particle losses which could not be the result of the elbow. There was no reason to suspect that any of these features would negatively impact the CO_2 measurements and therefore any large changes in the measured ratios would indicate the loss of particles.

Figure 18 shows the measured PM to CO_2 ratio from an individual syringe versus where the mock-exhaust was injected along the polyethylene pipe. “Long” indicates injections from the far end of the pipe, meaning the particles were required to travel the entire length of the pipe, injections coming from the middle of the pipe are reported as “middle” and “short” is representative of injections from the close end of the pipe, just prior to the 90° bend. While there are some issues for repeatability, on average, this

analysis shows that there was no dependence on where the exhaust started in the sampling system. The ratio for injections inserted at the long end of the pipe to injections from the short end of the pipe was 1.02, and the ratio for injections made from the long end to the middle of the pipe was 0.97. Figure 19 shows the results for the companion BC to CO_2 measurements. These figures again show that there was no significant dependence on where the first injection was along the pipe indicating no particle losses due to the sampling tube.

An experiment was conducted to determine if there was particle loss due to the inline fan in the OHMS setup, shown in Figures 20 and 21 for PM and PN, respectively. The inlet for the particle instruments was moved to sample before (triangles) and after (diamonds) the fan. Separate injections of mock exhaust were used for each trial, and with each extraction from the garbage bag of particles, the concentration within the bag was diluted. This explains why the concentration decreases for sequential trials, regardless of where the sample was introduced into the sampling line. The total particle mass and particle number was determined for each injection by integrating the area under the respective peaks from the Dekati Mass Monitor to give micrograms of particle mass per cubic centimeter and particle number per cubic centimeter. Aside from particle depletion from the artificial exhaust source, the placement of the inlet in relation to the OHMS fan also does not appear to influence the PM and PN measured.

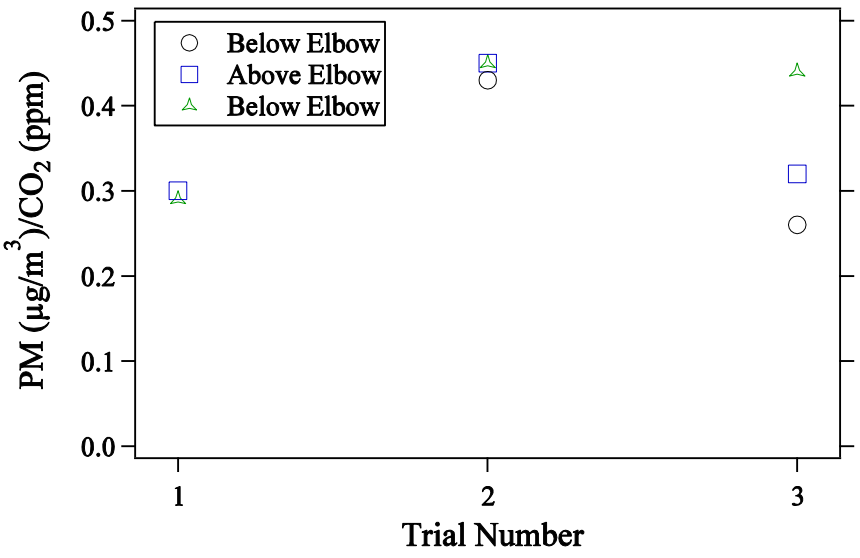

Figure 16. PM to CO_2 measured ratio for mock exhaust injected below and above the 90° elbow in the OHMS set-up. The first injection is below the elbow (circles), the second injection is above the elbow (squares) and the third trial is injected below the elbow (triangles) to empty the syringe. Trial 1 is comprised of only two injections, whereas trials 2 and 3 each have 3 injections.

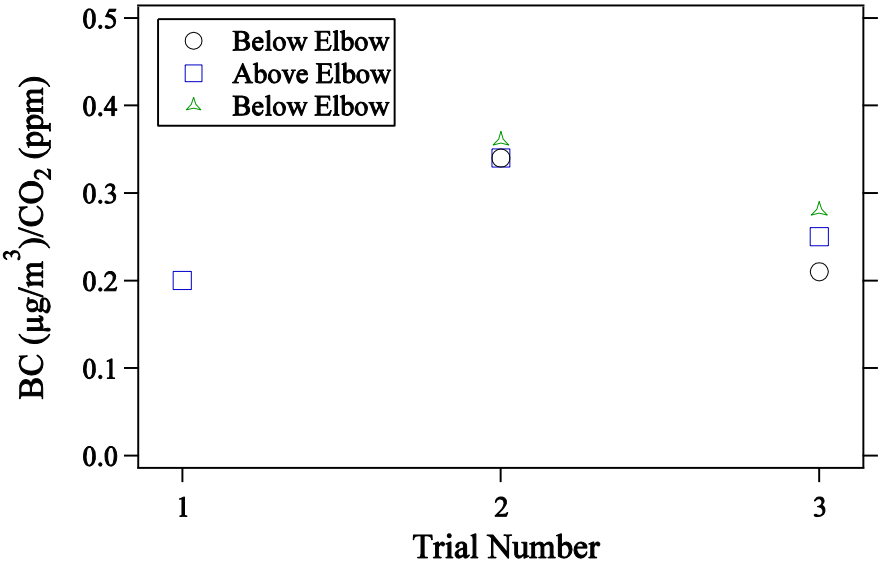

Figure 17. BC to CO_2 measured ratio for mock exhaust injected below and above the 90° elbow in the OHMS set-up. The first injection is below the elbow (circles), the second injection is above the elbow (squares) and the third trial is injected below the elbow (triangles) to empty the syringe. Trial 1 is comprised of only two injections, one of which was invalid for BC, and trial 2 and 3 each have 3 injections.

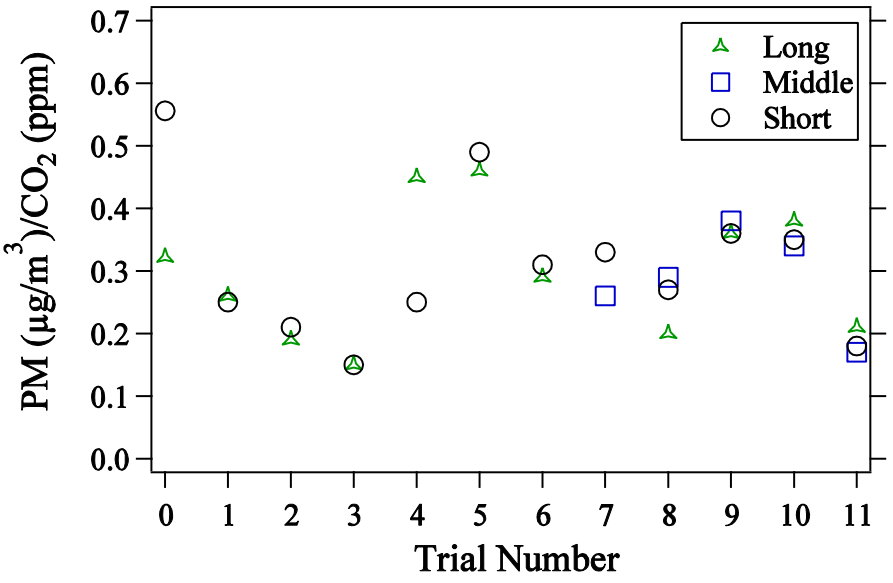

Figure 18. PM to CO_2 ratio shown for mock exhaust inserted at the long (green triangles), middle (blue squares) and short (black circles) end of the polyethylene pipe. Each trial is one syringe of mock exhausted divided between the number of positions.

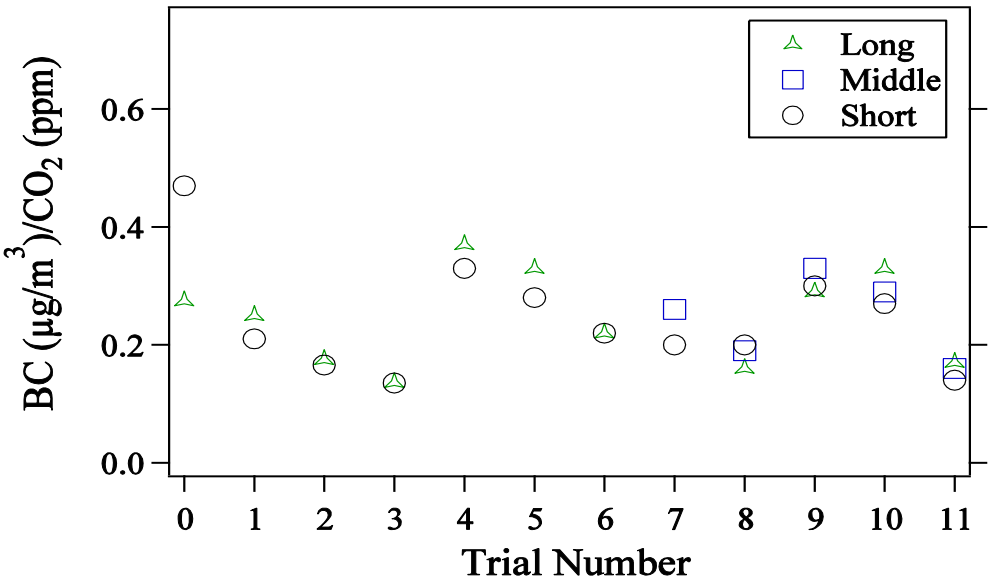

Figure 19. BC to CO_2 ratio shown for mock exhaust inserted at the long (green triangles), middle (blue squares) and short (black circles) end of the polyethylene pipe. Each trial is one syringe of mock exhausted divided between the number of positions.

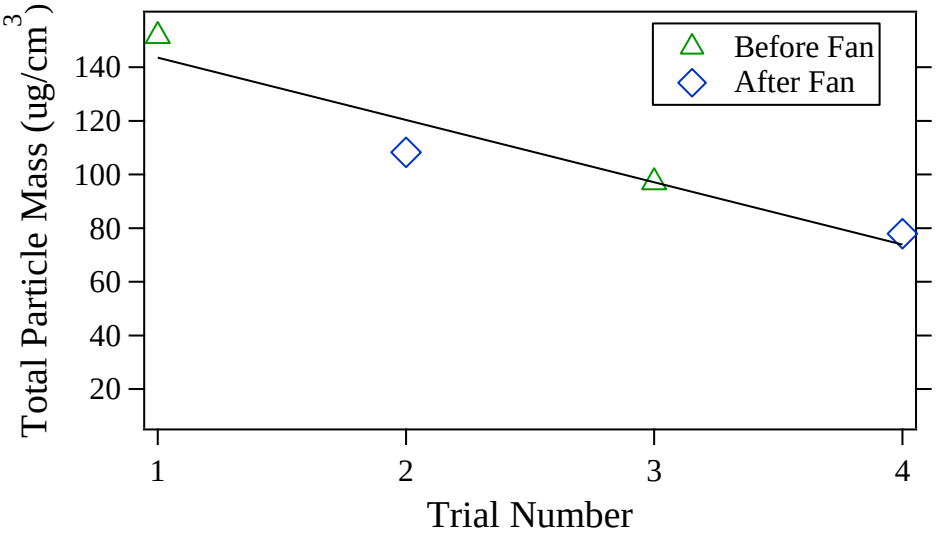

Figure 20. Total particle mass concentration for samples collected before the exhaust fan (triangles) and after the fan (diamonds). Each trial is a separate syringe injection.

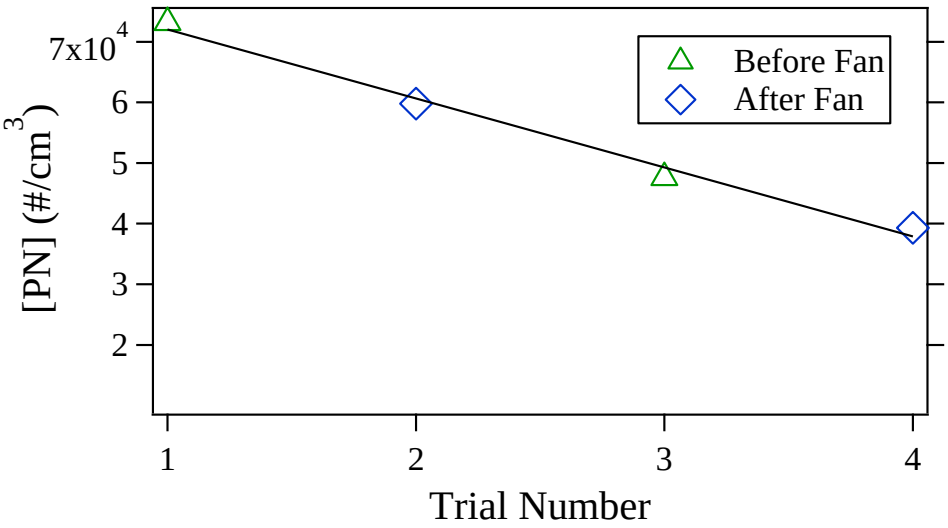

Figure 21. Total particle number concentration for sample intake before the fan (triangles) and after the fan (diamonds). Each trial is a separate syringe injection.

From these experiments, an order of magnitude reduction in particles due to the OHMS sampling setup was ruled out and begs the question as to which group's BC and PN measurements are accurate. The Federal particle standard for HDV is 0.01g/bhp-hr

which translates to approximately 0.07 gPM/kg of fuel assuming the average fuel consumption rate of 0.15 kg of fuel/bhp-hr. In the 2013 OHMS measurements for 2008 and newer chassis model year vehicles equipped with DPFs approximately 12% of the measurements at the Port of Los Angeles and 16% of the Cottonwood weigh station measurements exceed the Federal standard. Therefore, based on the OHMS measurements, a large majority of the HDVs have particle emissions within the certification limits, which is expected, and are consistent with other values reported in the literature, suggesting that the OHMS measurements are likely correct [23, 53, 54]. The exact reasons is unknown for the observed differences in the two data sets but it is not likely coincidental that the values appear to be off by exactly an order of magnitude, suggesting a possible calculation error as the source for the difference.

2.3 2015 Measurement Summary

The University of Denver continued the HDV emissions research in California at the Port of Los Angeles and Cottonwood weigh station sites in 2015 with a total of eight days of sampling. Sampling took place at the Port of Los Angeles between Monday, March 23 and Friday, March 27. The measurements were made from approximately 8:00 to 17:00, with 1,456 total successful measurements made during the week. The location of the sample collection was moved slightly from the 2013 measurements due to TraPac reconstructing their entrance and exit into the port. In 2015 there were two new automated exit lanes and OHMS was setup on the eastern most lane. The majority of the HDV passed through the lane that OHMS was set-up over, but the other lane was used for overflow when the exit became congested and for bobtails. The new exits were more

automated than in the past and while many of the HDV did stop before exiting, thus encouraging acceleration under the OHMS tent, not all of the HDV were required to as in the past. This combined with the OHMS tent having to be situated about 15 feet further away from the exit gate than in 2013 allowed for an increase in average vehicle speeds. Figure 22 is a photograph of the OHMS system installed at the new exit from the Trapac facility in 2015. On average, the speeds at the new exit were higher in 2015, with similar entrance accelerations. The exit accelerations for the 2015 measurements had to be disregarded due to an unfound error in the data collection program.

Figure 22. Photograph at the new Trapac Port of Los Angeles exit with the OHMS setup used to detect exhaust emissions from heavy-duty vehicles in the foreground. The nearest blue roofed canopy at the rear of the tent indicates one of the new exit check points.

Sampling was conducted at the Cottonwood weigh station on I-5 near Redding CA from Wednesday, April 8th to Friday, April 10th. High winds prohibited measurements from being made on Monday and Tuesday of that week, April 6th and 7th. During the three days of work we collected emission measurements on a total of 694 HDV.

The licenses for both locations measurements were read for the HDVs that had CO_2 emissions levels exceeding the minimum plume criteria. At the Port, out of state plates were matched against the drayage truck registry for make and model year and a few additional vehicles from Colorado, Georgia, Illinois, New Jersey, Ohio, Texas and Utah were included, but the vast majority of the HDVs came from California, Oregon and Washington. Vehicles with valid CO_2 emissions and a matched license plate had their emissions measurement reviewed one final time to exclude any measurements that indicate the presence of more than one vehicle in the tent during the data sampling period. If the presence of a second vehicle plume is found the vehicle is eliminated from the final data set.

A detailed summary of the measurements for both sites made in 2015 are provided in Table 3 with SEM calculated using the daily means shown as well. The measured mean ratios to CO_2 are reported along with the g/kg of fuel values for all gaseous, particulate and number emissions. In addition to the exhaust species measured, the mean model year, infrared temperatures, speed and accelerations were also obtained. The accelerations reported by the second speed unit (exit location) at the Port are not reported because of a software error that invalidated those measurements. In 2015 the

fleet measured at our Port location remained younger than the fleet measured at Cottonwood (mean model year of 2009.3 compared to 2008.1). However, the fleet ages were found to be moving in opposite directions with the Cottonwood fleet getting younger (~ 0.5 model years younger since 2013) while the Port fleet got older (~ 1.8 model years older since 2013). Accompanying the age changes in the two fleets are changes in the measured emissions as well. At the Port particulate emissions increased from previously very low values while large reductions in particulate emissions occurred at the weigh station. These year-to-year changes will be discussed in detail later.

IR images captured at each location allowed for analysis of external exhaust pipe temperatures. Pictures that had a clear IR image of an elevated exhaust pipe were assigned a temperature based on the field calibration previously mentioned. The histograms for these temperatures at both locations in 2015 are shown in Figure 23. The Port location had an average temperature of 91 ºC and at Cottonwood the average exhaust pipe temperature was hotter at 105 ºC. Although the average temperature is only slightly higher at Cottonwood, it is important to note that Cottonwood had a higher percentage of HDVs with exhaust pipe temperatures above 120 ºC degrees than at the Port (20% compared to 3%).

Table 3. OHMS 2015 Data Summary.

Study Site	Port of Los Angeles	Cottonwood Weigh Station
Mean CO/CO_2 (g/kg of fuel ± SEM)	0.0016 3.0 ± 0.4	0.0015 3.0 ± 0.2
Median gCO/kg	0.27	0.65
Mean HC/CO_2 (g/kg of fuel ± SEM)	0.00039 1.2 ± 0.4	0.00020 0.66 ± 0.05
Median gHC/kg	0.20	0.27
Mean NO/CO_2 (g/kg of fuel ± SEM)[a]	0.0060 12.8 ± 0.5	0.0056 11.9 ± 0.2
Median gNO/kg[a]	11.1	10.8
Mean gNO_x/CO_2 (g/kg of fuel ± SEM)[b]	0.0066 21.6 ± 2.1	0.0068 22.1 ± 0.7
Median gNO_x/kg[b]	19.5	19.6
Mean NO_2/CO_2 (g/kg of fuel ± SEM)	0.00071 2.3 ± 1.0	0.0012 4.1 ± 0.5
Median gNO_2/kg	1.3	3.4
Mean Mass NO_2/NO_x	0.11	0.18
Mean gPM/kg ± SEM	0.11 ± 0.01	0.22 ± 0.04
Median gPM/kg	0.0042	0.002
Mean gBC/kg ± SEM	0.08 ± 0.01	0.08 ± 0.002
Median gBC/kg	0.0039	0.011
Mean PN/kg ± SEM	$2.8 \times 10^{14} \pm 2.8 \times 10^{13}$	$1.7 \times 10^{15} \pm 1.4 \times 10^{13}$
Median PN/kg	7.6×10^{12}	1.2×10^{13}
Mean Model Year	2009.3	2008.1
Mean IR Estimated Exhaust Temperature (ºC) ± SEM	91 ± 2	105 ± 1
Mean Entrance Speed (mph)	7.0	9.0
Mean Exit Speed (mph)	7.8	9.3
Mean Entrance Accel (mph/s)	0.2	0.38
Mean Exit Accel (mph/s)	N/A	0.32
Slope (degrees)	0º	-0.5º

[a]grams of NO

[b]grams of NO_2

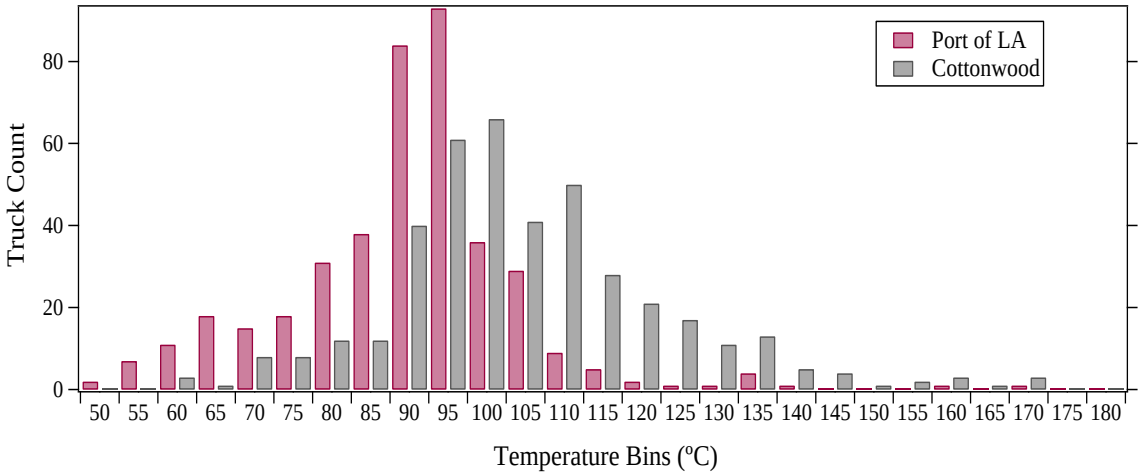

Figure 23. Infrared temperature distributions for the two locations in 2015.

Comparing particle emissions from Table 2 and Table 3, there was an increase in mean PM from 2013 to 2015. Due to the San Pedro Clean Port initiative completely turning over the fleet in 2010 with DPF engines, the Port's fleet consisted of an abundance of 2008 and 2009 chassis model year vehicles, which were 5 to 6 years old in 2015. Because of their disproportionate share of the fleet, the increases in PM are dominated by these model years. However, there was one vehicle with exceedingly high PM levels measured multiple times during the 2015 campaign that was responsible for the majority of the changes.

This particular 2009 vehicle at the Port was measured six times during the 2015 campaign and exhibited an apparent time dependence in its particle emissions. Table 4 summarizes the six emission measurements collected over the course of 4 days in chronological order with measurements made before noon (AM, highlighted) differentiated from those collected after noon (PM). Exit accelerations were invalid for all measurements due to an equipment problem; all other measurements that exceeded

measurement confidence limits are denoted by a dash in Table 4. Noticeably, the DPF in this HDV is not in perfect working order, as most of the gPM/kg of fuel emissions are significantly higher than the average for any model year at the Port and often resembles pre-DPF HDV emission levels.[41] However, the two morning measurements on March 26th and 27th (2.0 and 0.14 gPM/kg of fuel) were much lower and the measurement on the morning of the 27th is close to the Port's fleet mean of 0.11 ± 0.01.

Table 4. 2015 measurement summary for a 2009 model year repeat HDV at the Port of Los Angeles showing the date, AM (highlighted) or PM measurement time, fuel specific emissions, speed and acceleration, IR exhaust temperatures (°C), roadside opacity percentage and pass or fail of the roadside Test.

Date/AM/PM	**gCO/kg**	**gNO_x/kg**	**gPM/kg**	**gBC/kg**	**gPN/kg**	**Entrance/Exit**		**Exh. Temp (°C)**	**Roadside Test % Opacity (P/F)**
						Speed[a]	**Accel**[b]		
3/23/2015 / PM	-	2.1	21.3	19.2	2.7 E+16	14.2 / 18.2	1.2 / -	90	-
3/24/2015 / PM	220	-	13.4	9.4	1.5E+16	13.8/ 15.8	1.2 / -	70	-
3/26/2015 / AM	-	2.4	2.0	0.9	6.0E+15	- / 12.8	- / -	80	-
3/26/2015 / PM	324	1.5	18.7	14.6	2.0E+16	12 / 14.1	1.2 / -	65	95.5% (F)
3/27/2015 / AM	0	30.0	0.1	0.1	4.0E+14	14.6 / -	1.6 / -	95	10.8% (P)
3/27/2015 / PM	-	24.6	12.3	7.2	7.6E+15	14.4 / 15.2	1.2 / -	130	-

[a] kilometers per hour [b] kilometers per hour/sec

Concurrent with the OHMS measurements, the State of California conducted random roadside opacity inspections using a snap-acceleration test which reports an average tailpipe opacity reading for three rapid acceleration events.[55, 56] The 2009 HDV discussed in Table 4 was tested by the inspection team on the afternoon of the 26th and the morning of the 27th immediately after passing through the OHMS tent. The inspection results mirror the OHMS results with the vehicle having afternoon average tailpipe opacity of 95.5% and failing the test (OHMS 18.7 gPM/kg of fuel) followed the next morning with a passing opacity test of only 10.8% (OHMS 0.1 gPM/kg of fuel). If repairs were attempted on the vehicle overnight, they were not lasting as the measurements from this vehicle in the afternoon of the 27th would again far exceed certification limits.

It is difficult to fully explain the extreme variability of the particle emissions from this vehicle, verified by two different testing methods (OHMS and snap-acceleration). One possibility is that this vehicle's DPF has been tampered with or removed leaving tailpipe particle emissions strictly a function of engine operation. Fuel specific CO emissions correlate (see Table 4) with the fuel specific PM and BC emissions indicating fuel enrichment for the high PM events. Figure 24 shows FMPS fuel specific particle size distribution data collected in the morning (solid line) and afternoon (dashed line) of March 26th for this HDV post processed with TSI's soot inversion matrix. PM increases in the afternoon result in a shift in the peak particle size from ~70nm to >150nm. This shift in peak particle size is also seen between the morning and afternoon measurements, collected on March 27th, and this distribution is consistant with a number of other high emitting HDVs measured at the Port of Los Angeles in 2015. The shift in the particle

distribution is consistent with the use of large amounts of exhaust gas recirculation (EGR) in combustion, which would lower NO_x emissions by enrichening the cylinder air to fuel ratio, and has been observed by other researchers.[57, 58] Increased EGR in the afternoon could be a consequence of increased ambient temperature and/or may reflect this vehicles particular work cycle.

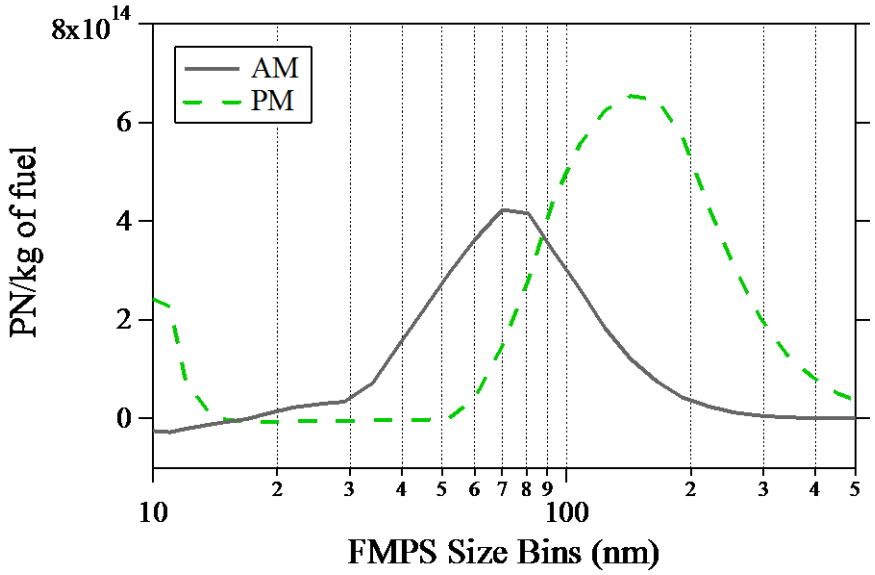

Figure 24. Repeat FMPS fuel specific particle size distribution data collected in the morning (solid line) and afternoon (dashed line) of March 26th from a 2009 HDV measured at the Port of Los Angeles, and processed with TSI's soot inversion matrix.

A second potential explanation has to include the possiblity that the DPF remains in the vehicle but only functions sporatically. It has been shown that cracks due to thermal expansion or vibrations over time will reduce filter surface area in a DPF, as well as cause filter "leakages" which may increase as the day progresses.[21, 59] In addition, the presence of a soot-cake significantly increases the filter efficiency of the DPF, thus it is also within the realm of possibilities that some of the emissions variability is related to its

regeneration frequency with lower PM emissions prior to a regeneration event when the soot-cake is present.[60]

To date there has been no research that has looked at how and why DPFs fail, which could shed light on the previously investigated high emitting HDV. Although this example was drastic, there are other high emitting vehicles within both the Cottonwood and the Port fleets. The Port measurements show that the largest increase in emissions are from the 2008 – 2010 model year vehicles which were initally designed to have higher engine out PM emissions, to limit NO_x emissions as there is no NO_x after-treatment system on these vehicles.[61] DPFs in these vehicles will therefore require more frequent active regeneration events, where fuel is introduced into the filter to combust the accumulated soot and restore exhaust flow rates. The increased thermal stress coupled with the likely need to manually remove accumulated ash more often may increase the chances for defects to be introduced into these early generation filters. Many of these issues have been addressed in the later model vehicles (2011 and newer) as engines are now designed to limit PM emissions reducing the demand on DPFs. However, ensuring the long term integrity of installed DPFs is paramount to maintaining the particle emissions reductions achieved to date.

In 2015 the Port of Los Angeles had 271 vehicles with multiple successful measurements (repeat vehicles) and the Cottonwood weigh station had 70 vehicles. These repeat measurements can be used to show that high emitting vehicles have increasing variable emissions, whereas low emitting vehicles, with properly working DPFs maintain low exhaust PM levels, Figures 25 and 26 show the repeat HDV measurements at the

Port and at Cottonwood for gPM/kg of fuel in 2015. The HDVs are rank ordered by their average fuel specific PM emissions and then each sequentially plotted along the x-axis with each HDV's repeat measurements. Note both axes are split for the Port of Los Angeles data (Figure 25). As the average emissions increase, so does the variability of the repeat emissions measured. This is not due to variations in the testing method, as low emitting vehicles have high repeatability, but a result of variability in the exhaust emissions of the vehicle. This is identical to behavior previously seen from light-duty vehicles.[62]

Particle emissions variability involves an additional factor that is not found in variable exhaust gas emissions. Two steps are required for an elevated particle emission measurement (1) the HDVs engine must generate particles and (2) those particles have to escape the DPF. If either of these steps is not completed, OHMS will report a low measurement reading. This serves to potentially increase particle measurement variability in vehicles with a compromised DPF as not all engine operations generate significant particles. However, even a single high particle emissions measurement requires that the particle filter is not operating as designed. Conversely, HDVs with properly working DPFs should never have elevated particle measurement, as the filters are able to trap particles regardless of the driving mode. This can be seen in the low measurement to measurement emissions variability in the large majority of repeat vehicles.

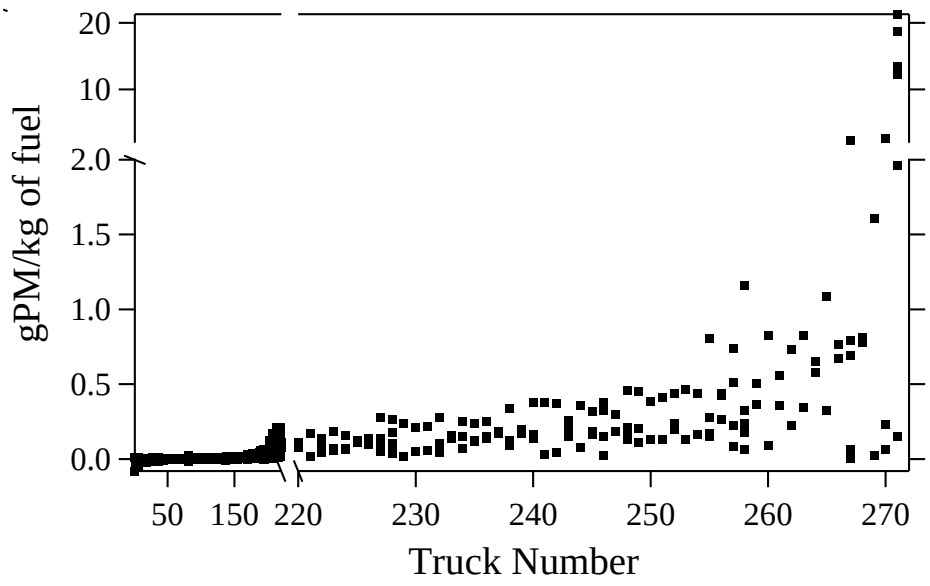

Figure 25. Repeat HDV measurements at the Port of Los Angeles in 2015 for gPM/kg of fuel. Vehicles have been rank ordered by mean gPM/kg of fuel emissions and plotted sequentially on the x-axis. Note that both the x- and y-axis are split.

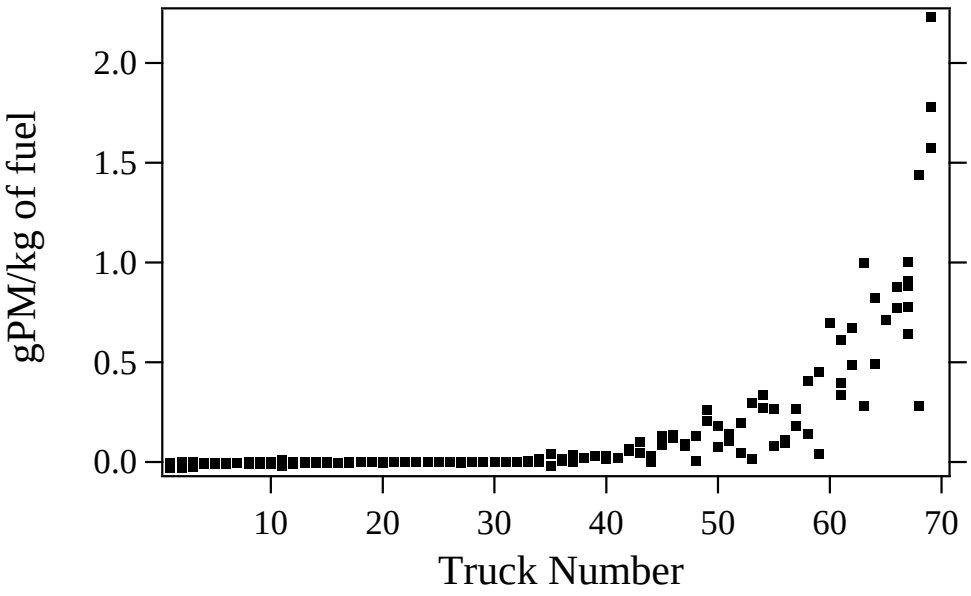

Figure 26. Repeat HDV measurements at the Cottonwood weigh station in 2015 for gPM/kg of fuel. Vehicles have been rank ordered by mean gPM/kg of fuel emissions and plotted sequentially on the x-axis.

At Cottonwood, there are an increasing number of new vehicles in the 2015 fleet and as correspondingly older vehicles are being eliminated from this fleet. Because newer vehicles generally have lower emissions, the fleet turnover has proven beneficial for overall emission averages at this weigh station. The California Truck and Bus rule has helped to expedite fleet turnover at Cottonwood weigh station as well as encourages HDV owners to install DPFs on their existing vehicles. This process is known as retrofitting and the DPFs for these vehicles are known as retrofit DPFs. It was proven with 2015 data that HDVs with retrofit DPFs have similar particle emissions to vehicles that have been manufactured with DPFs. The State of California has a Truck and Bus Rule Reporting System that records retrofit activity for Californian vehicles based on information provided by the owner. This system provided information on 109 out of the 142 pre-2008 chassis model year HDVs registered in California, 24 of which had reported installing retrofit DPFs.[63] Figure 27 shows that retrofit vehicles (blue diamonds) compared to non-retrofit vehicles (gray triangles) experienced a significant reduction in PM emissions for all model years. The mean and SEM for fuel specific PM and BC emissions of those 24 HDVs were 0.06 ± 0.07 and 0.03 ± 0.04 respectively and are comparable to newer DPF-equipped HDV emission levels that have consistently low PM measurements. The remaining 85 non-retrofit HDVs had mean fuel specific PM and BC emissions of 0.66 ± 0.16 and 0.21 ± 0.001 respectively, which are an order of magnitude greater.

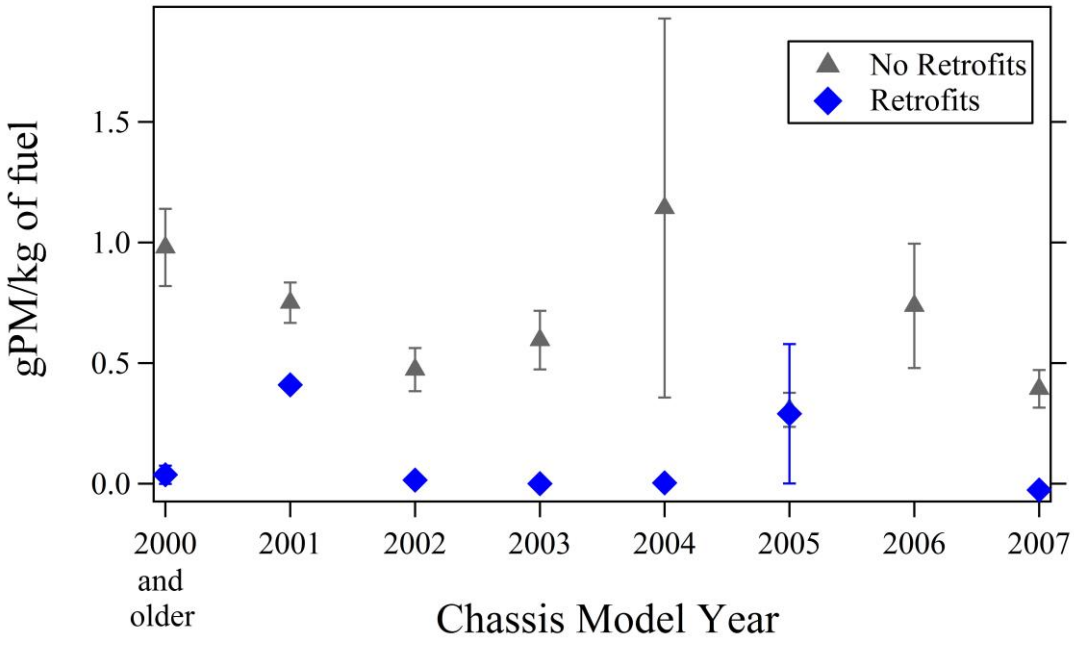

Figure 27. Cottonwood weigh station gPM/kg of fuel emissions versus chassis model year for HDV older than 2008 models. Three vehicle groups are graphed HDV identified as having a retrofitted DPF (diamonds) and vehicles with no indication of a retrofit DPF (triangles). The uncertainties plotted are SEM calculated using the daily means.

2.4 2017 Measurement Summary

The 2017 campaign continued the study of fleets from the Port of Los Angeles, CA and Cottonwood weigh station in northern California. The 2017 OHMS setup duplicated the 2015 setup at the Port of Los Angeles except for a permanent speed bump added across all of the exit lanes that was located at the very end of the OHMS tent (Figure 28). This unavoidable change to the location caused a significant change in the observed driving pattern with vehicles decelerating at the tent exit when reaching the speed bump, diminishing the volume of exhaust emitted from the vehicles. This was particularly problematic for HDVs that were leaving the Port with empty containers and or unloaded trailers as many did not meet the minimum required threshold of CO_2 for a

valid measurement (a 75 ppm rise in CO_2 above background levels). This resulted in fewer HDVs measured at the Port of Los Angeles location in 2017 than in previous years.

Figure 28. Photograph at the Port of Los Angeles of the OHMS setup in 2017 used to detect exhaust emissions from heavy-duty diesel vehicles. The perforated exhaust sampling and integration tube is again visible on the left side of the tent and the new speed bump is located at the nearest end of the tent.

Sampling took place at the Port of Los Angeles between Monday, April 3 and Friday, April 7. The measurements were made from approximately 8:00 to 17:00, with 795 total successful measurements made during the week. There were fewer successful measurements in 2017 from previous campaigns due to several factors. In addition to the instillation of a speed bump previously mentioned, the added automated exit gate that was installed in 2015 was in full use in 2017. This often allowed HDV drivers the choice of going through the OHMS tent, or going out of the exit adjacent to the tent. Depending

on the congestion and the officers working, the latter option was used frequently, avoiding the OHMS setup. Additional downstream measurements and snap idle testing by the Air Resources Board further complicated the exit process leading to traffic slow-downs (lower HDV CO_2 emissions) and the presence of the California Highway Patrol on the OHMS exit lane the first day increased the number of vehicles bypassing the OHMS exit lane for the remainder of the week and further lowered our measurement opportunities.

Sampling was also conducted at the Cottonwood weigh station from Monday, April 10th to Friday, April 14th. During the five days of work we collected emission measurements on a total of 1,043 HDV. The setup at this location was recreated from previous years, and was ongoing with CARB's roadside opacity testing.

The licenses for measurements collected at both locations were read for the HDVs with CO_2 emissions levels that exceeded our minimum plume criterial. Measurement validity requirements, previously mentioned, are detailed in Appendix B. Readable license plates were matched against registration records as previously described and measurements were graphically inspected to exclude any measurements that indicate the presence of more than one vehicle through the tent during data collection.

On-road fuel specific emission factors were collected at the Port of Los Angeles (795 measurements) and Cottonwood Weigh Station (1,043 measurements) in the spring of 2017 adding to the 2013 and 2015 data sets. Although 2017 had a lower number of unique measurements at the Port of Los Angeles, there was a higher percentage of HDVs that were measured more than once compared to the other campaign years. Table 5 shows

the 2017 data summary for both the Port of Los Angeles and Cottonwood weigh station with mean CO, HC, NO, NO_2, NO_x, PM, BC and PN as a ratio over CO_2 and as fuel specific values as grams of pollutant per kg of fuel burned. Fuel specific medians for these pollutants are also shown. Average model year, exhaust pipe temperature, entrance and exit speed, entrance and exit acceleration, and roadway slope at each location are also included. The uncertainties are SEM calculated using the daily averages.

Table 5. OHMS 2017 Data Summary.

Study Site	Port of Los Angeles	Cottonwood Weigh Station
Mean CO/CO_2 (g/kg of fuel ± SEM)	0.0010 (1.74 ± 0.3)	0.0014 (2.8 ± 0.4)
Median gCO/kg	0.61	0.35
Mean HC/CO_2 (g/kg of fuel ± SEM)	0.00013 (0.41 ± 0.08)	0.0001 (0.28 ± 0.04)
Median gHC/kg	0.22	0.11
Mean NO/CO_2 (g/kg of fuel ± SEM)[a]	0.0068 (14.6 ± 0.2)	0.004 (9.6 ± 0.7)
Median gNO/kg[a]	12.7	6.6
Mean NO_x/CO_2 (g/kg of fuel ± SEM)[b]	0.0084 (27.6 ± 0.4)	0.0057 (18.6 ± 1.2)
Median gNO_x/kg[b]	25.3	12.3
Mean NO_2/CO_2 (g/kg of fuel ± SEM)	0.0011 (3.7 ± 0.3)	0.001 (2.94 ± 0.1)
Median gNO_2/kg	2.3	1.7
Mean Mass NO_2/NO_x	0.14	0.16
Mean gPM/kg ± SEM	0.04 ± 0.01	0.09 ± 0.005
Median gPM/kg	0.0003	0.0003
Mean gBC/kg ± SEM	0.03 ± 0.01	0.06 ± 0.003
Median gBC/kg	0.007	0.004
Mean PN/kg ± SEM	$2.2 \times 10^{14} \pm 2.6 \times 10^{13}$	$7.7 \times 10^{14} \pm 9.5 \times 10^{13}$
Median PN/kg	9.7×10^{12}	3.2×10^{12}
Mean Model Year	2009.8	2011.3
Mean IR Estimated Exhaust Temperature (°C) ± SEM	86 ± 3	108 ± 3
Mean Entrance Speed (mph)	5.3	7.0
Mean Exit Speed (mph)	4.5	7.4
Mean Entrance Accel (mph/s)	0.19	0.14
Mean Exit Accel (mph/s)	-0.42	0.10
Slope (degrees)	0°	(-0.5)°

[a]grams of NO

[b]grams of NO_2

Overall, fleet average fuel specific NO_x emissions at Cottonwood were 33% lower than at the Port. Figure 29 graphs the 2017 fuel specific NO_x emissions as a function of model year for the Port of Los Angeles (gray) and Cottonwood (red) data. NO is displayed as grams of NO_2 (solid and hatched bars) along with NO_2 (open bars) so the height of the bar is total gNO_x/kg of fuel by model year. Uncertainties are SEM calculated using the daily means. A third of this difference is due to the fact that the newest model years shown in Figure 29 at Cottonwood have lower fuel specific NO_x emissions. The Port data is noisier due to a smaller number of 2011 and newer vehicles in the fleet but does not show the same systematic NO_x reductions with model year as observed at Cottonwood. To emphasize this point, average NO_x emissions for model years 2011 and newer at the Port of Los Angeles were 20.1 ± 0.9 gNO_x/kg of fuel, compared to 10.6 ± 1.2 gNO_x/kg of fuel at Cottonwood. Even after age adjusting the Port of Los Angeles 2011 and newer fleet to match that of Cottonwood, the mean fuel specific NO_x emissions of the Port fleet changed little (20.1 to 19.6 gNO_x/kg of fuel) again demonstrating the lack of a NO_x model year dependence at the Port. The remaining NO_x difference is simply due to a higher percentage of 2011 and newer HDVs at Cottonwood.

Proper SCR function relies on temperatures hot enough to thermalize urea (typically a minimum of 200 ºC prior to the catalyst) in addition to a catalyst temperature that lowers the activation barrier to successfully reduce NO_x. As reported by others, HDVs subject to drayage driving modes have been found to have lower average engine temperatures, problematic for current SCR systems.[34, 64] Table 5 shows that the average IR exhaust pipe temperature observed at Cottonwood which is significantly higher than at

the Port of Los Angeles. If the comparison is restricted to only vehicles model year 2011 and newer, the difference increases to 110 ºC and 79 ºC (t-test, greater than 99% confidence). This temperature difference is likely the major factor in the difference in observed NO_x emissions for the newest model year HDVs at each location. The lack of any meaningful decrease in NO_x, especially NO_2 emissions, for the newer model years at the Port of Los Angeles supports other reports that the activity cycle for a majority of the HDVs at the Port is insufficient to consistently support active SCR systems which are required to lower NO_x emissions.[34, 65]

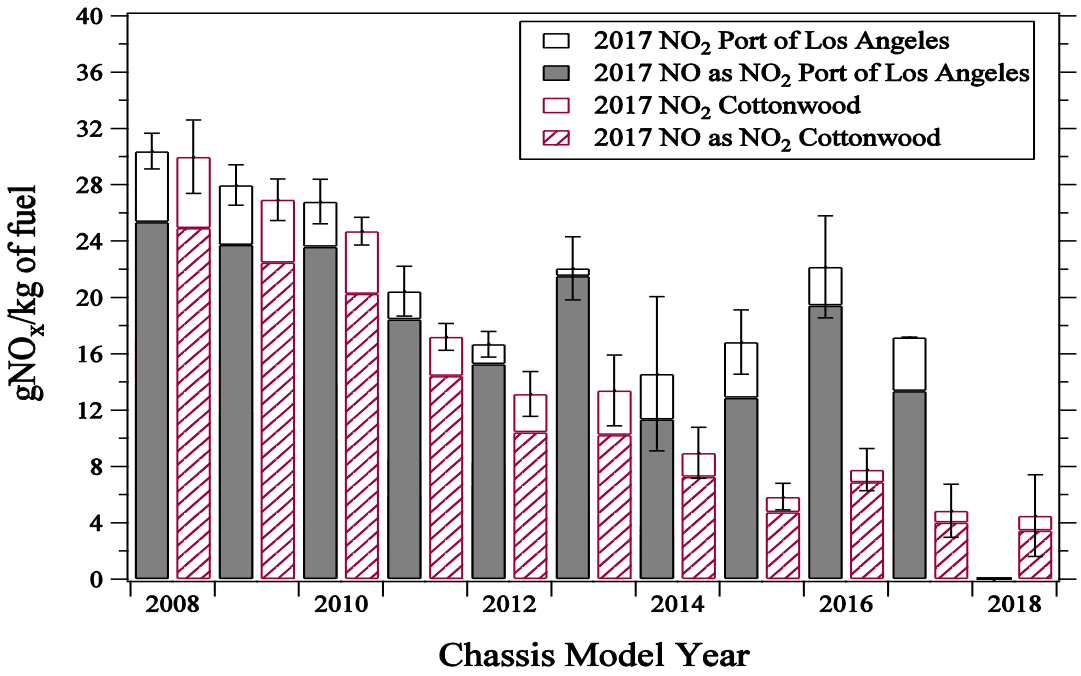

Figure 29. gNO_x/kg of fuel for 2017 data for the Port of Los Angeles (gray-left bars) and Cottonwood (red-right bars). Filled/hatched portions are gNO/kg of fuel as NO_2 and open portions are gNO_2/kg of fuel. Uncertainties are SEM for the total gNO_x/kg of fuel calculated using the daily measurements.

The reduction observed at Cottonwood is a result of a newer fleet having an increasing percentage of low emitting NO_x HDVs than at the Port, indicating the SCRs at Cottonwood are more effective likely due to elevated operating temperatures. As the California Truck and Bus rule forces the early retirement of pre-SCR HDVs, there is an expectation that the NO_x emissions will continue to decrease in the Cottonwood fleet. Using the 2017 and newer model year average emissions (~4.7 gNO_x/kg of fuel), a factor of 4 further reduction is possible from the current fleet average. While HDV SCR systems are not expected to perform at optimum levels in a weigh station, the observations at both locations strongly suggest that current on-road HDV NO_x emissions are higher than the certification standards.

2.5 Discussion of OHMS Emission Trends

By compiling the 2013, 2015 and 2017 OHMS datasets at Cottonwood and the Port of Los Angeles, comprehensive analyses can show average on-road emissions for in-use vehicles. The discussion of these campaigns elucidates how fleet turnover, implementation of new after-treatment systems, and how they age, influence emissions over the course of 5 years.

In 2017 the measured fleet at the Port of Los Angeles had an average model year of 2009.8, which is only half a year newer than it was in 2015 and only 0.7 years newer than in 2013 indicating that the age of the Port fleet has been steadily increasing (+3.3 years older) since measurements began in 2013. This slow turnover is a result of the Port's forced retirement program, which resulted in operators purchasing vehicles in 2008 – 2010 coupled with the fact that HDVs generally have long useful lives. One can expect

this fleet to continue to change little until the California Truck and Bus rule requires HDVs to have 2010 compliant engines by the end of 2022. Contrary to the fleet at the Port of Los Angeles, the Cottonwood fleet has experienced significant turnover with a 2017 mean model year of 2011.3 (1.8 years newer than the 2015 fleet and 5.7 years newer than the 2013 fleet). 2011 and newer vehicles make up 59% of the 2017 measurements, an increase of 70% from the 2013 measurements (18%) at Cottonwood.

Figure 30 shows the five-year emission trends at both locations for all gaseous emissions. 2013 (gray), 2015 (green) and 2017 (red) are shown for CO (solid), HC (triangles), NO (moles of NO, open), NO_2 (striped) and NO_x (moles of NO_2, hatched) at the Port of Los Angeles and Cottonwood. A 26% increase at the Port and a 16% decrease at Cottonwood in fleet average NO_x emissions, mainly NO, from 2015 to 2017 data were the only gaseous emission with a statistically significant change (validated with a null hypothesis test at the 95% confidence level). The NO_x fleet average in 2017 (27.6 gNO_x/kg of fuel) at the Port of Los Angeles is a significant increase from the means observed in 2013 and 2015 (20.7 and 21.6 gNO_x/kg of fuel respectively).

The Port and Cottonwood have similar 2008-2010 model year average NO_x emissions (30.0 ± 0.5 and 27.4 ± 1.0 respectively). The common NO_x reduction strategy for these model years is EGR, meaning it is likely that EGR effectiveness is similar, and that there are a comparable percentage of vehicles utilizing EGR, at both Cottonwood and the Port of Los Angeles.

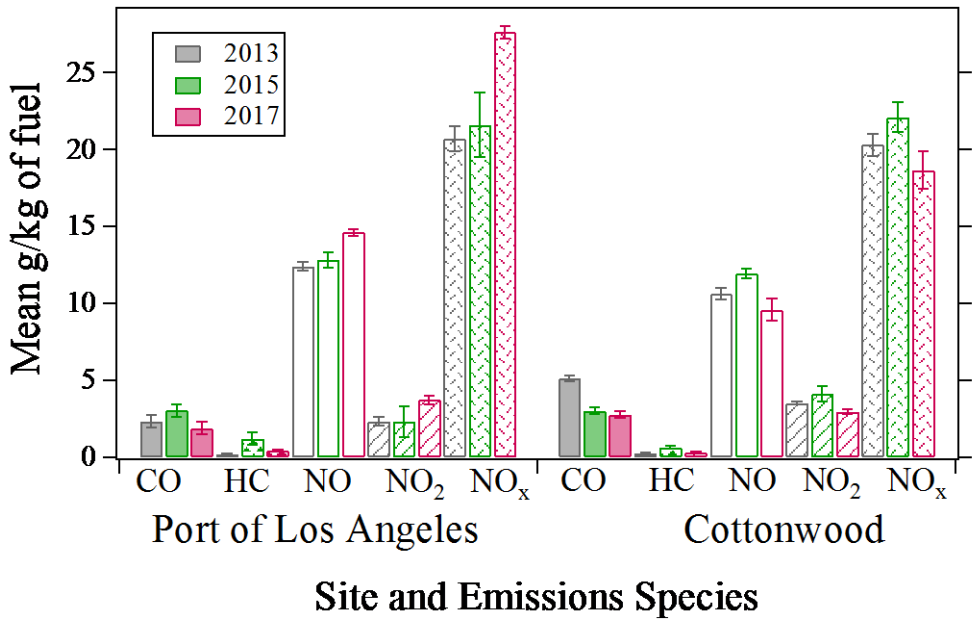

Figure 30. 2013 (gray left bars), 2015 (green middle bars) and 2017 (red right bars) data from the Port of Los Angeles (left) and Cottonwood (right) for CO (solid), HC (triangles), NO (open), NO_2 (striped) and NO_x (hatched) gases. Uncertainties are SEM calculated using the daily means.

The PM reduction story parallels other observations of dramatic reductions in diesel PM with the introduction of DPFs, where PM emissions have been measured to be more than 90% lower from pre-DPF levels filtering out all but the smallest of nanoparticles. [23, 36, 52, 66] Overall fleet average emissions for the Port of Los Angeles (left) and Cottonwood (right) for 2013 (gray), 2015 (green) and 2017 (red) measurement years are displayed in Figure 31. Fuel specific PM (solid bars) and BC (hatched bars) are plotted against the left axis and fuel specific PN (open bars) are shown against the right axis. Uncertainties are SEM calculated using the daily means. The averages from the Port of Los Angeles have been consistently lower than the Cottonwood fleet, a result stemming from all vehicles at the Port having DPFs installed since 2010.

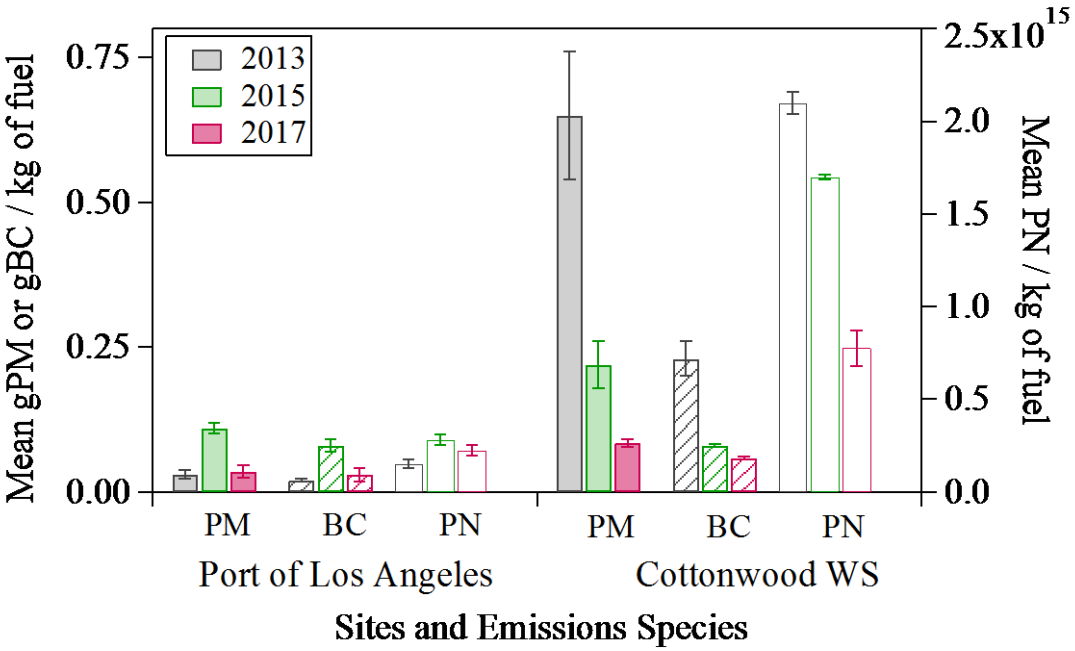

Figure 31. Fuel specific mean emissions for PM (solid), BC (diagonal) and PN (open) at the Port of Los Angeles and Cottonwood Weigh Station for 2013 (gray-left bar), 2015 (green-middle bar), 2017 (red-right bar) HDV fleets. Uncertainties are SEM calculated using the daily means.

In 2015 there were significant increases at the Port for all three particle species, as there was an increase in the fraction of higher emitting HDVs, and in particular one very high emitting vehicle previously discussed. The 2015 fleet PM, BC and PN increased from the 2013 data by +266%, +300% and +87% respectively. Figure 32 shows 2013 (circles), 2015 (diamonds) and 2017 (squares) data for 32a) PM, 32b) BC and 32c) PN at the Port of LA. Uncertainties are SEMs calculated using the daily means. Newer model years have consistently low particle emissions across all measurement years. High emitting HDVs were found in model years 2008-2010 and were responsible for this increase. These model years possess engines that trade higher engine out PM emissions for NO_x control and therefore rely heavily on the functionality of a properly working

DPFs in order to limit tailpipe PM emissions, as previously mentioned.[61] In 2017 the removal and or repair of these vehicles accounts for the decrease in particle emissions and a return to near 2013 levels (63% reduction from 2015 PM and BC levels). In particular, a single 2009 vehicle measured in 2015 was responsible for over 40% of the cumulative PM and 47% of BC. When measured again in 2017 it was found to be low emitting and accounts for a majority of the reductions observed. Another possible source of PM reduction seen in 2017 is that the Air Resources Board increased roadside compliance testing and issuance of statewide citations since 2015 have increased significantly which may have encouraged corrective maintenance or relocation for some of the high emitting vehicles observed in 2015.[67]

Figure 33 shows the percentage of the fleet that is responsible for the fraction of total PM emissions for the 2013 (black dotted line), 2015 (green dashed line) and 2017 (red solid line) fleets at the Port of LA. Greater deviation from the 1:1 line indicates increasing skewness where the fleet's total emissions are dependent on fewer vehicles. The emissions distribution in 2017 is still more skewed than observed in 2013, indicating the remaining presence of HDVs with improperly working DPFs, though less so than observed in 2015.

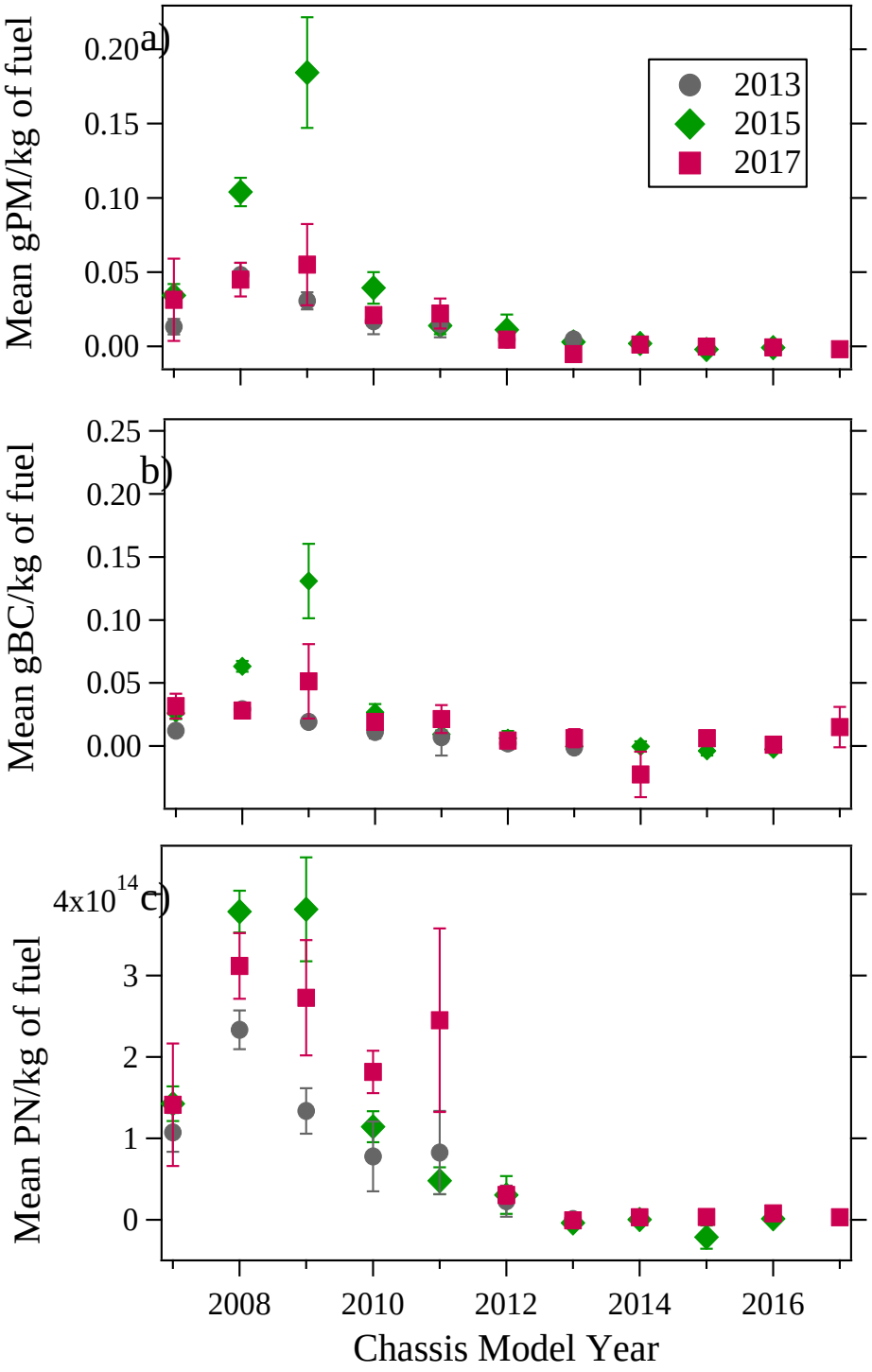

Figure 32. Mean a) gPM, b) gBC and c) PN/kg of fuel emissions by model year at the Port of Los Angeles for measurement years 2013 (circles), 2015 (diamonds) and 2017 (squares). Uncertainties plotted are SEM calculated using the daily means.

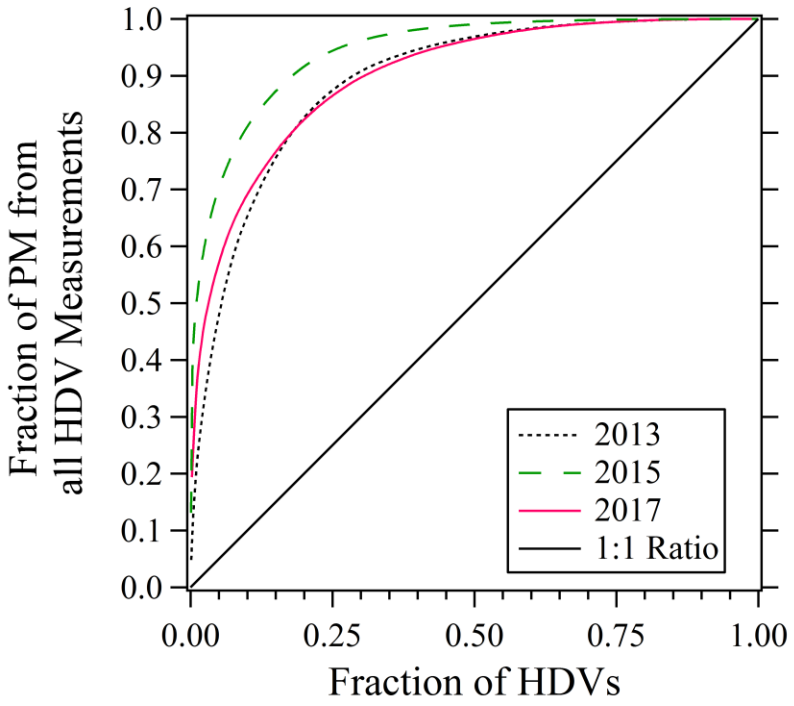

Figure 33. Fraction of HDVs responsible for the fraction of fuel specific PM from all HDV measurements at the Port shown for 2013 (dotted black line), 2015 (dashed green line) and 2017 (solid red line). The solid black line represents the 1:1 ratio.

The 2013 fuel specific particle emission averages at Cottonwood were significantly higher than at the Port (Figure 31) due to it being an older, less regulated fleet with more pre-DPF engines (pre-2008 chassis model year vehicles). In 2015 the measurements showed decreases from the 2013 data (PM -66%, BC -65% and PN -19%) in response to newer vehicles being added to the fleet and older vehicles being retrofit with DPFs due to the California Truck and Bus rule, decommissioned or relocated.[68] Previous behaviors continued to lower emissions in the 2017 fleet leading to an additional PM, BC and PN decreases of -60%, -25% and -55% respectively from 2015 data. The PM and BC levels at Cottonwood are now comparable to the levels found with the fully DPF equipped fleet at the Port of Los Angeles. The overall reduction of 87% of

PM from 2013 to 2017 for the Cottonwood fleet is three years ahead of the goal set in the Diesel Risk Reduction Plan by the California Air Resources Board that strived for an 85% reduction of diesel PM by 2020.[16]

Cottonwood's particle emissions have been positively impacted through the shift to newer model year vehicles and retrofit activity among remaining older model year vehicles. Contributions from each model year at Cottonwood are shown in Figure 34 for 34a) mean fuel specific BC by model year, 34b) fleet percentage by model year and 34c) the percent contribution for each model year, assuming equal vehicle fuel consumption, to the total BC emissions for 2013 (black) and 2017 (red) measurements. Uncertainties are SEM calculated using the daily means, and vehicles model year 2000 and older have been combined. All particle emissions in the remaining older model year vehicles have undergone significant BC decreases as retrofits have been installed.[68] The large decrease between model year 2007 and 2008 coincides with the introduction of vehicles originally manufactured with DPFs.

Vehicles model year 2007 and older comprised 61% of the Cottonwood fleet measured in 2013 (Figure 34b), but only 13% of the 2017 fleet; the highest individual fleet percentage in 2013 came from vehicles that were older than model year 2001 (more than 20%). These vehicles also dominated the BC total percent contribution (Figure 34c) while model year 2010 and newer were a minor contribution to the overall total in 2013. HDVs with retrofits are evident in Figure 34a, as the remaining older model year vehicles have reduced gBC/kg of fuel average in 2017 compared to 2013. In 2017 the newest model year vehicles are now responsible for the majority of the overall BC emissions but

those percentage contributions are for a fleet total which has undergone a factor of 7 reduction in the total between 2013 and 2017. The five year reductions observed at Cottonwood illustrate the effectiveness of the new technology and how the California Truck and Bus Rule helping lower the on-road PM emissions inventory in California.

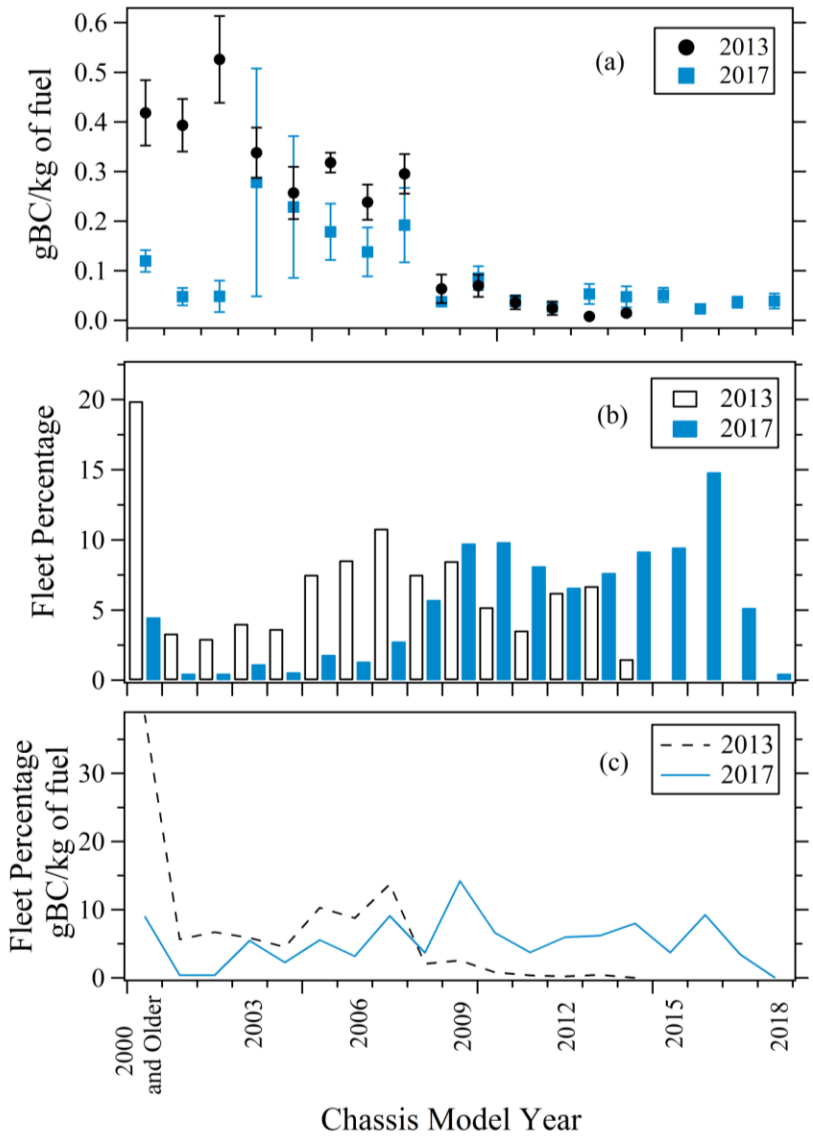

Figure 34. Cottonwood 2013 and 2017 a) mean fuel specific black carbon emissions, b) fleet percentages and c) fleet percent contribution, assuming equal vehicle fuel consumption, all versus model year. Uncertainties are SEM calculated using the daily means.

As the particle emissions at Cottonwood have steadily decreased, the fleet averages are now dominated by a few high emitting vehicles. Figure 35 shows the fuel specific PM distribution versus fleet fraction at the Cottonwood weigh station for 2013 (black dotted line), 2015 (blue dashed line) and 2017 (red solid line) data. The 1:1 line would be representative of each HDV in the fleet contributing equally to the overall fleet averages, and deviation from this ratio indicates a more skewed emissions distribution. In 2013, half of the PM emissions were from 12% of the measurements, and in 2017 half of the PM emissions were from 5.5% of the measurements. This is the result of not just newer HDVs being added to the fleet but a majority of the older vehicles that remain in the Cottonwood fleet having lower emissions both contributing to improved fleet emissions over the years.

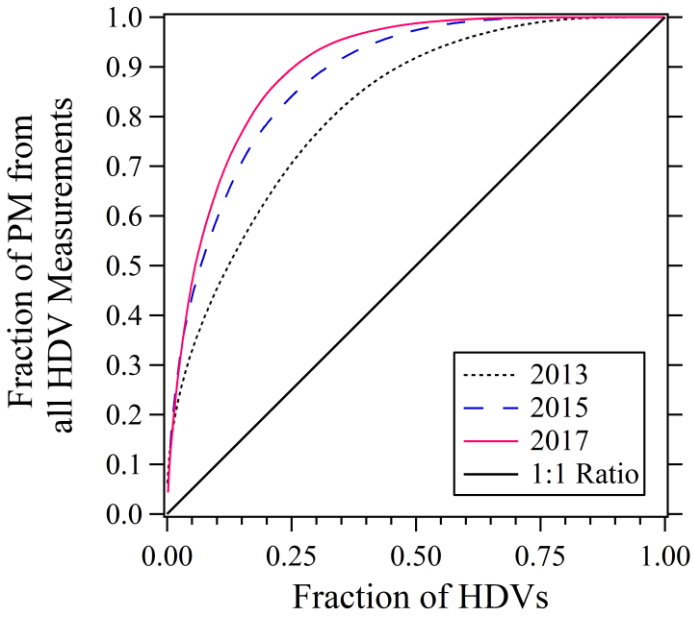

Figure 35. Fraction of HDVs responsible for the fraction of fuel specific PM from all HDV measurements at Cottonwood shown for 2013 (dotted black line), 2015 (dashed blue line) and 2017 (solid red line). The solid black line represents the 1:1 ratio.

In general, particle emissions, shown in Figure 36 a) PM, b) BC and c) PN, at Cottonwood for 2013 (circles), 2015 (diamonds) and 2017 (squares) data has not changed significantly for model years 2008 and newer throughout the three campaigns. Uncertainties are the SEM calculated using the daily measurements. The one exception is for the 2013 measurements for model year 2009 where a single white smoker accounts for all of the PM emission's difference and the increased uncertainty shown in Figure 36a. The large uncertainties in older model years are in part the result of the low number of vehicles measured for those model years. HDVs that were not manufactured with DPFs (chassis model year 2007 and older) have maintained their low PM emissions from measurement year 2015. Pre-DPF models have continued to show decreases in fuel specific PM and BC emissions in 2017 from the previous measurements which has been attributed to retrofit DPF installations first observed in 2015.

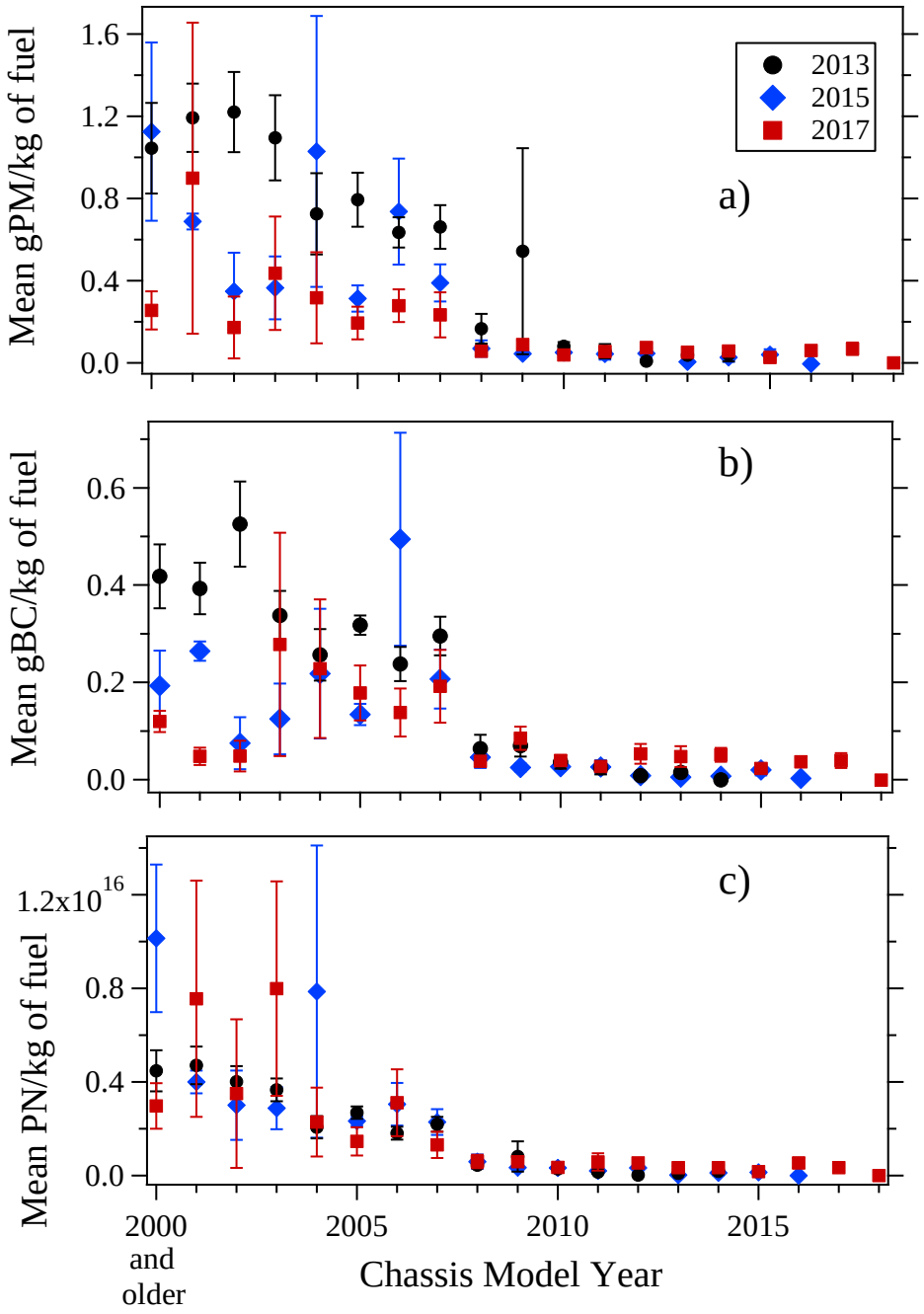

Figure 36. Mean a) gPM, b) gBC and c) PN/kg of fuel emissions by model year at Cottonwood weigh station for measurement years 2013 (circles), 2015 (diamonds) and 2017 (squares). Uncertainties are SEM calculated using the daily means.

The impact of high emitting vehicles on model year averages is easier to see in a box and whisker plot. Figure 37 is a box and whisker plot for fuel specific a) PM, b) BC and c) PN showing all measurements taken at the Port of Los Angeles with the y-axis split. The mean is represented by a filled square and a horizontal line indicates the median for the model year. The box denotes the 25^{th} to the 75^{th} percentile and the whiskers are the 10^{th} to the 90^{th} percentiles. All other measurements outside the 10^{th} to 90^{th} percentiles are signified with symbols. The interquartile ranges for model years 2008 and 2009 decreased in 2017, highlighting that the Port of Los Angeles had fewer high emitting vehicles than in the previous measurement year. The range for particle emissions at the Port though are relatively similar for all years with the exception of a single 2009 HDV measured in 2015 that is responsible for the four highest measurements of PM and BC. This of course is one gigantic exception, as those 4 readings (12.3, 13.4, 18.7 and 21.3 gPM/kg of fuel and 7.2, 9.4, 24.6 and 19.2 gBC/kg of fuel) accounted for 41% of the total PM emitted and 47% of the total BC emitted from all of the measurements in 2015.

The BC trends mirror the PM trends, however there were 13 HDVs in 2017 above 0.21 gBC/kg of fuel (a high emitter threshold chosen arbitrarily as its three times the approximate fuel specific certification standard of 0.07 g/kg of fuel), whereas 24 HDVs had gPM/kg of fuel above the same threshold. The differences are likely the result that some HDVs are not solely emitting black carbon, or soot. There are also a higher number of HDVs, specifically model years 2009-2011, in which PN measurements deviate from PM and BC measurements in 2017.

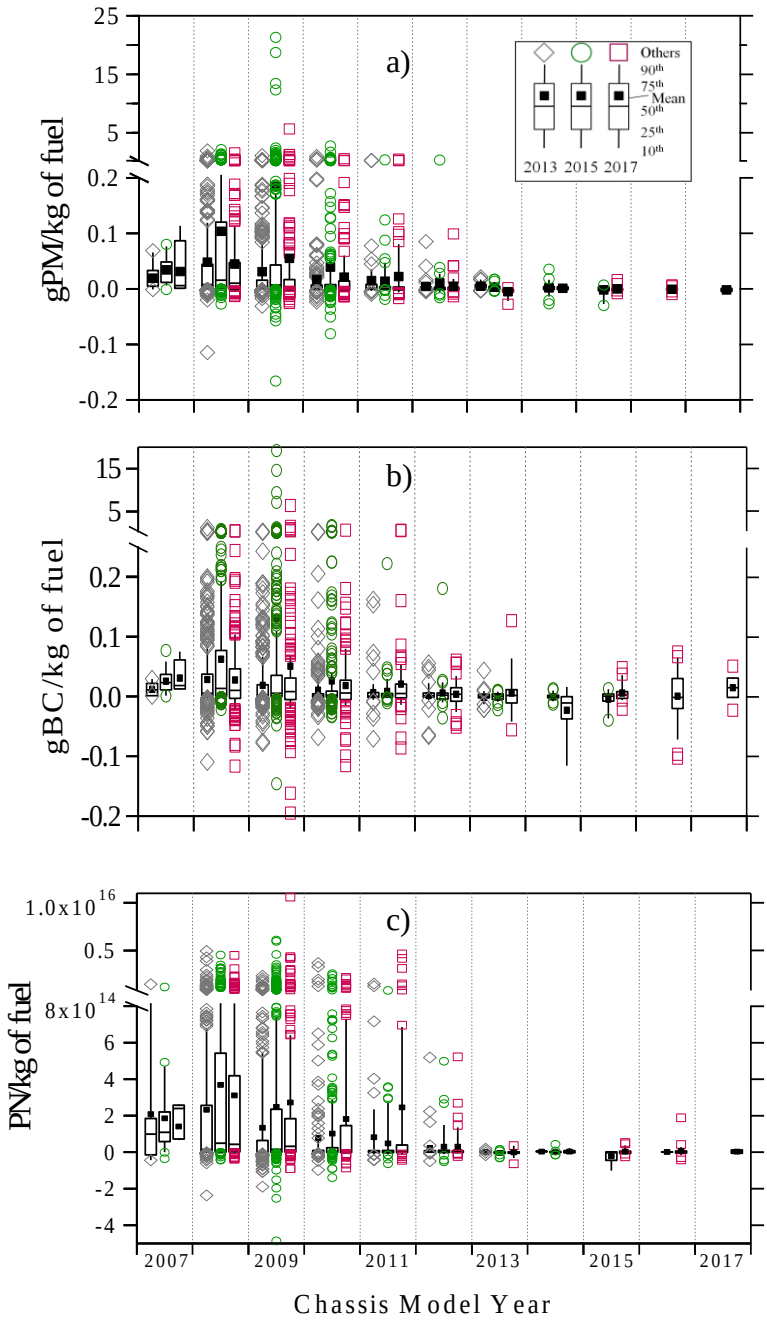

Figure 37. Box and whisker plot for a) gPM, b) gBC and c) PN/kg of fuel for 2013 (left, diamonds), 2015 (middle, circles) and 2017 (right, squares) at the Port of Los Angeles with a split y-axis. Black squares represent the model year mean, horizontal lines denote the median, the box encloses the 25th to the 75th percentiles, the vertical lines represent the 10th to the 90th percentile with symbols representing the other individual measurements.

The model year averages at the Port of Los Angeles are dependent on the high emitting vehicles, as shown with the mean and median deviation, especially for the most abundant model year vehicles (2008-2010). The measured fleet in 2017 reduced the number of the high emitting vehicles, and therefore the averages, as mentioned previously. Newer model year vehicles, 2013 and newer, have a very compact, unchanging interquartile range throughout the measurement years, indicating that these model year vehicles are more consistent at eliminating engine out PM.

Figure 38 shows individual a) PM, b) BC and c) PN measurements at Cottonwood in a box and whisker plot for 2013 (left, diamond), 2015 (middle, circles) and 2017 (right, squares) data. The y-axis has been split. The filled square represents the mean for the model year, the horizontal line indicates the median, the open box signifies the 25^{th} to the 75^{th} percentiles, the whiskers encompass the 10^{th} to the 90^{th} percentile and the symbols are the remaining measurements. Model years are grouped inclusively.

As with the mean emissions, overall the 2017 measurements have a downward trend for all species when compared to the emission distribution observed in the 2015 measurements. The inter-quartile range has contracted significantly for the oldest HDVs as DPFs have been retrofit and this coupled with the shift from older to newer models is responsible for the reductions in the fleet means. One apparent increase in emissions is for model years 2012 – 2014. There are slight increases, especially in the extent of the range of values observed, in both PM and BC emissions; however, the number of vehicles observed in these model years has more than doubled since 2015. Increases in

the mean particle emissions are not observed for these groups because of the large number of low emitters contained below the 90th percentile.

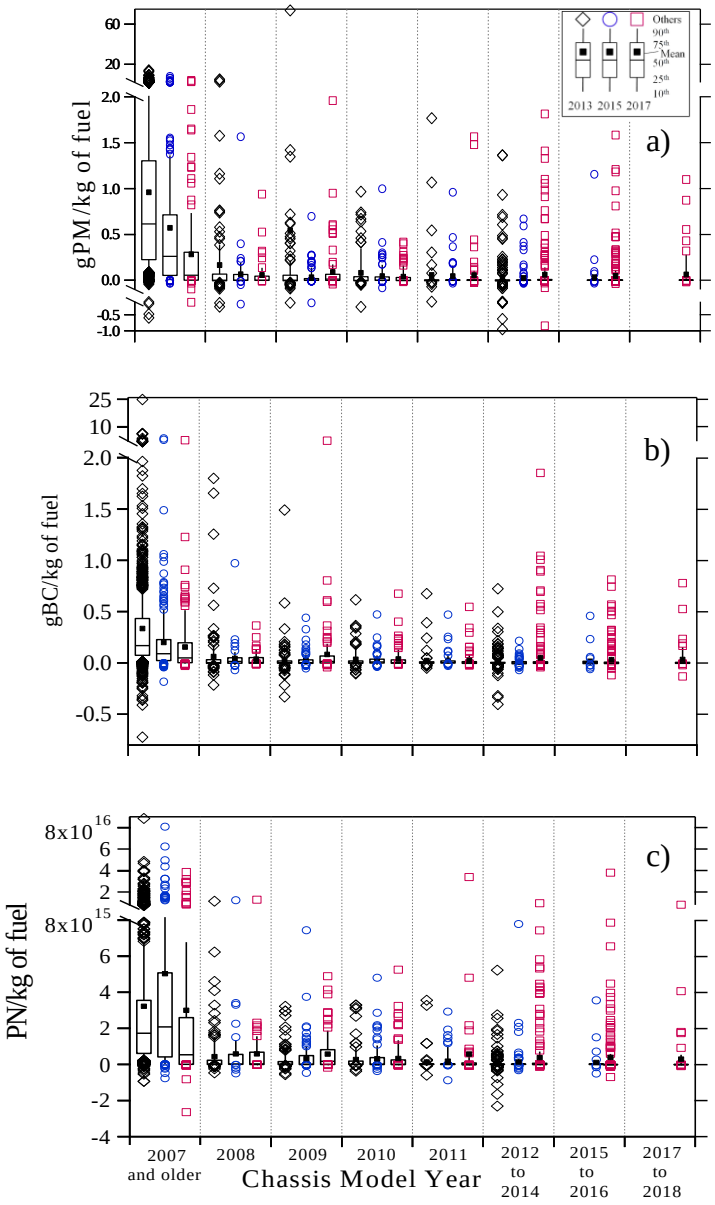

Figure 38. Box and whisker plot for a) gPM, b) gBC and c) PN/kg of fuel for 2013 (left, diamonds), 2015 (middle, circles) and 2017 (right, squares) at the Cottonwood scales with a split y-axis. Black squares are the model year means, horizontal lines denote the median, the box encloses the 25th to the 75th percentiles, the whiskers extend to the 10th and 90th percentiles with symbols representing the other individual measurements.

The OHMS research has shown that DPFs have proven to be very successful at reducing tailpipe PM emissions in compliance with engine standards. However, the phased-in NO_x standards are still a work-in-progress for on-road emissions. Total fuel NO_x ($NO + NO_2$) is displayed in Figure 39 and 40 for the Port and Cottonwood fleets by model year for 2013 (solid-left bar), 2015 (diagonal-middle bar) and 2017 (hatched-right bar) data sets with the uncertainties as the SEM calculated using the daily means. The open bars for each model year represent the amount of NO_2 and the filled or hatched portion represent the amount of NO reported as NO_2 equivalents so the total height of each bar is equal to the total gNO_x/kg of fuel measured. For Figure 40, model years 2000 and older have been combined. At the Port there is no discernable emissions reduction with model year as would be expected with models newer than 2010. As discussed previously, the majority of vehicles at the Port are 2010 and older chassis model years due to the forced early retirement program. Newer HDV model year vehicles are filtering into the fleet, as 2012 and newer HDV comprised 6.9% of the 2015 measurements and make up 15.1% of the 2017 measurements. However, operating temperatures of these vehicles are low, which works against a fully functioning SCR system. The mean gNO_x/kg of fuel for the Port fleet of 27.6 ± 0.4 is still approximately 40% less than the pre-control fleet measured by remote sensing in 2008 (45.4 ± 1.2).[36] Though some deterioration in fuel specific NO_x emissions has occurred since the 2012 remote sensing measurements of 20.6 ± 0.6 gNO_x/kg of fuel, which were nearly identical to the OHMS 2013 mean of 20.7 ± 0.8 measured at the original Trapac exit.[37] Cottonwood's fuel

specific nitric oxide emissions show a steady decline in total NO_x emissions for the newer model years in all campaign years, indicating better SCR performance.

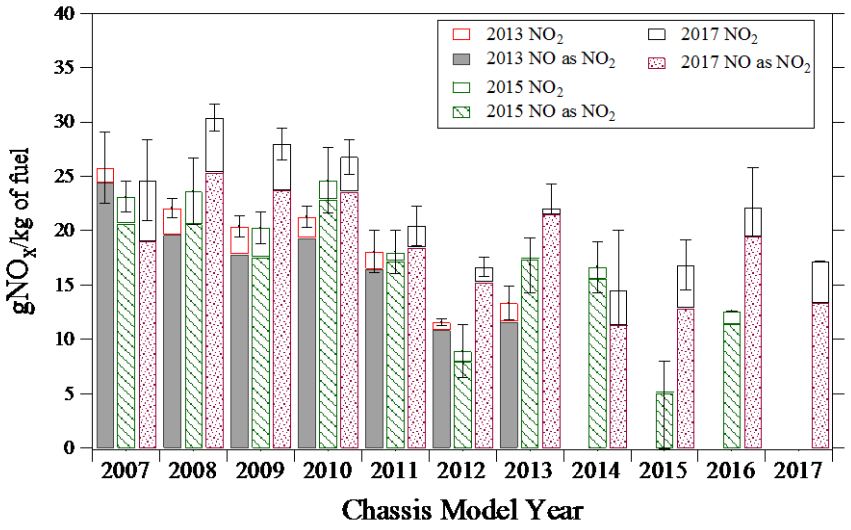

Figure 39. Fuel specific nitric oxides by model year at the Port of Los Angeles for measurement years 2013 (left bars), 2015 (middle bars) and 2017 (right bars). Open portion represents gNO_2/kg of fuel, filled or hatched portion represent the amount of NO expressed as NO_2, and the height of each bar represents total gNO_x/kg of fuel. Uncertainties are SEM determined using daily means of total NO_x.

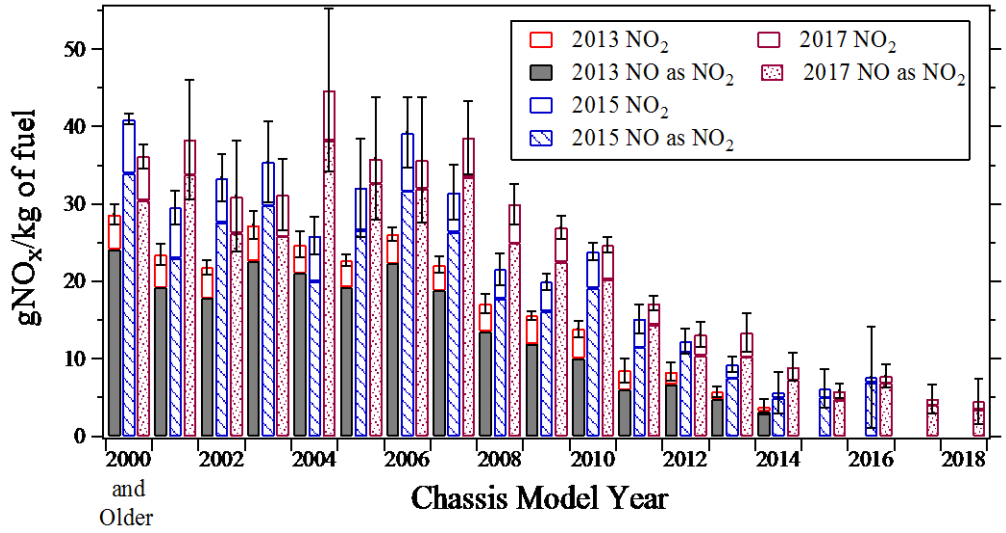

Figure 40. Fuel specific nitric oxides by model year at Cottonwood weigh station for measurement years 2013 (left bars), 2015 (middle bars) and 2017 (right bars). Open portion represent gNO_2/kg of fuel, filled portion represent the amount of NO expressed as NO_2, and the height of each bar represents total gNO_x/kg of fuel. Uncertainties are SEM calculated using the daily means of total NO_x.

2.6 Reoccurring Heavy-duty Vehicles

The site operations influence the number of repeat vehicles measured (HDVs measured more than once in a given measurement year). Table 6 shows the number of times HDVs were measured at each location for each measurement year. There are significantly more repeat vehicles at the Port of Los Angeles, as these vehicles are merely transfer agents picking up containers at the Port, delivering them locally and then repeating the process. Because these vehicles are staying in the area, as shown by a higher percentage of repeat measurements, it is much easier to assess the change in individual HDV's emissions from year to year for vehicles at the Port of Los Angeles.

Particle emissions variability were explored in detail with the 2015 measurements (see Figures 25 and 26) and trends similar to those previously presented were found with the reoccurring HDVs (measured in more than one measurement year). To limit some of the repetitiveness, this discussion is limited to PM for HDVs that were measured in 2015 and 2017, and if any of these vehicles were measured in 2013, their 2013 measurements were also included. Figure 41 graphs the fuel specific PM measurements for Port vehicles with valid measurements measured in 2015 (circles) and 2017 (squares) displayed with a split y-axis. The vehicles were rank ordered and plotted along the x-axis using the 2017 average gPM/kg of fuel. As with the previously discussed analysis from 2015, as vehicle average gPM/kg of fuel emissions increases so does the variability of repeat measurements. It is very noticeable that there are more 2015 (circles) measurements that are above the general 2017 emissions trend than there are elevated 2017 measurements

which follows the observed increase in mean fuel specific PM emissions in 2015 and the subsequent reduction in 2017.

Table 6. Number of measurements by site and year.

Times Measured	Port of Los Angeles			Cottonwood		
	2013 Number (%)	2015 Number (%)	2017 Number (%)	2013 Number (%)	2015 Number (%)	2017 Number (%)
1	711 (78%)	654 (70.7%)	511 (64.3%)	1578 (92.3%)	557 (88.8%)	912 (87.4%)
2	134 (14.7%)	149 (16.1%)	82 (20.6%)	110 (6.4%)	64 (10.2%)	48 (9.2%)
3	43 (4.7%)	58 (6.3%)	23 (8.7%)	16 (1.0%)	3 (0.5%)	6 (1.7%)
4	14 (1.5%)	27 (2.9%)	9 (4.5%)	5 (0.3%)	0	0
5	7 (0.8%)	19 (2.1%)	3 (1.9%)	0	0	1 (0.5%)
6	2 (0.2%)	11 (1.2%)	0	0	3 (0.5%)	2 (1.2%)
7	0	3 (0.3%)	0	0	0	0
8	1 (0.1%)	1 (0.1%)	0	0	0	0
9	0	0	0	0	0	0
10	0	2 (0.2%)	0	0	0	0
11	0	0	0	0	0	0
12	0	1 (0.1%)	0	0	0	0

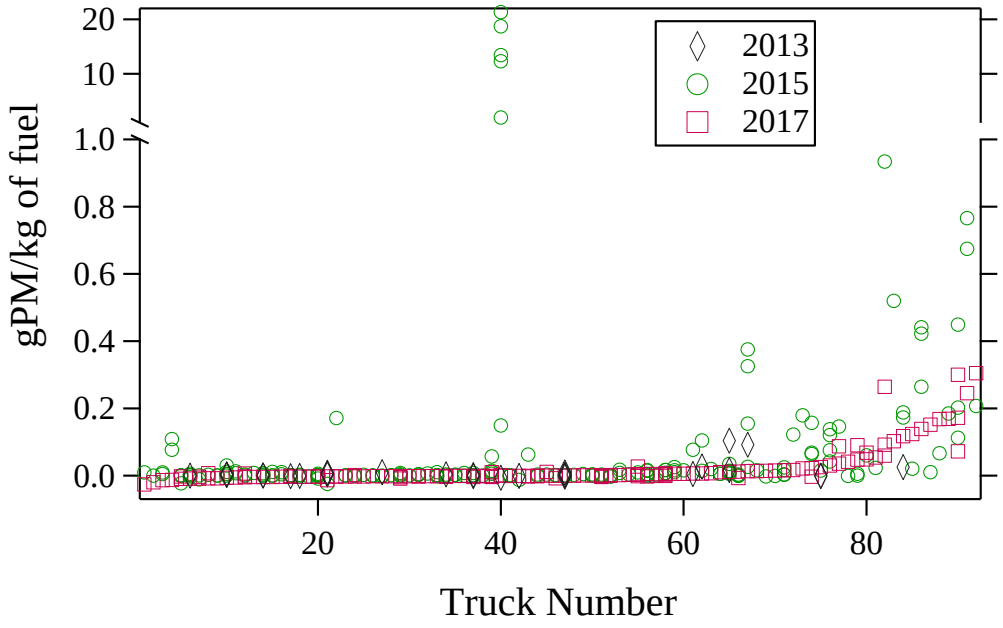

Figure 41. Fuel specific PM emissions for reoccurring HDVs measured in 2015 (circles) and 2017 (squares) at the Port of Los Angeles with a split y-axis. A few vehicles were also measured in 2013 (diamonds). Vehicles are rank ordered using the 2017 average gPM/kg of fuel.

Figure 42 is the same analysis performed using the multi-year measurements collected at the Cottonwood weigh station for PM. Reoccurring HDVs measured in 2015 (circles) and 2017 (squares) data is shown along with any measurement data collected on the same vehicle in 2013 (diamonds). Truck number is calculated from the measured 2017 gPM/kg of fuel average. There are far fewer reoccurring HDVs measured at Cottonwood and the HDVs at Cottonwood include older model years that were not originally equipped with DPFs. Truck numbers 34 and greater have increasing PM emissions from 2015 to 2017. These vehicles, with exception of truck number 36 and 37, are 2008 to 2010 HDVs and all are from the same chassis manufacturer. A number of the

observed large decreases in 2017 are from older vehicles believed to have installed retrofit DPFs to comply with the California Truck and Bus rule.

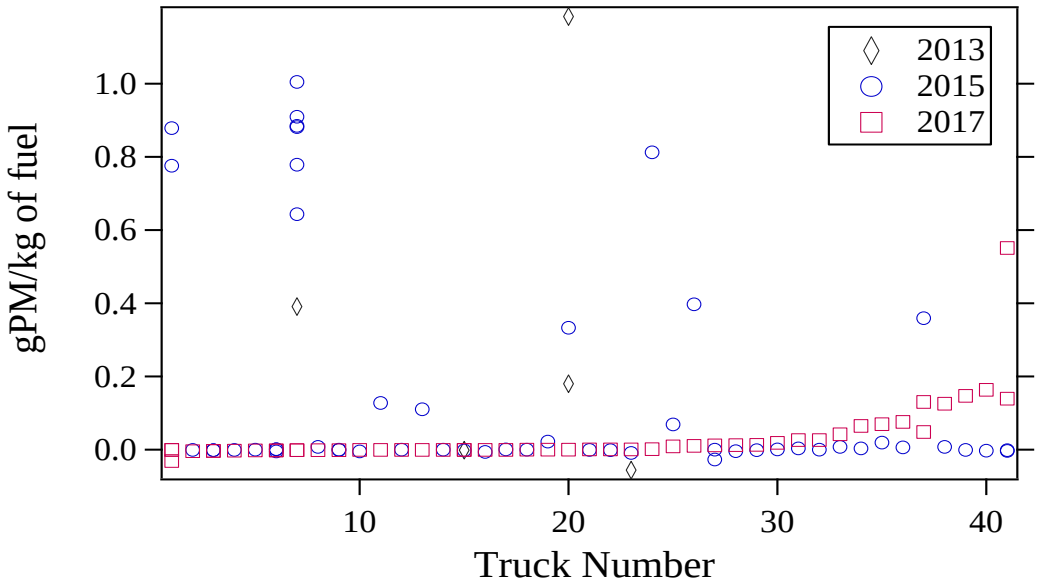

Figure 42. Reoccurring HDVs measured in 2015 (circles) and 2017 (squares) at the Cottonwood weigh station for gPM/kg of fuel. A few vehicles were also measured in 2013 (diamonds). Truck number is calculated using the average gPM/kg of fuel for the 2017 measurements.

Chapter 3 – FEAT Measurements

The 2017 Peralta weigh station campaign resulted in 2,315 measurements from HDVs (1,844) and MDVs (471). The two vehicle classifications have been separated by gross vehicle weight > 26,001 lbs for HDVs and 14,001-26,000 lbs for MDVs. Table 7 provides a summary of fleet emission averages for the High and Low FEATs as well as the entire HDV and MDV fleets. The mean emission ratios to CO_2 are shown as well as mean and median g/kg of fuel emissions for CO, HC, NO, NO_2, NO_x, NH_3, IR %opacity, average chassis model year, speed (mph), acceleration (mph/s), and the road slope (degrees).

3.1 FEAT Heavy-duty Vehicles

There were 1,368 HDVs measured with the High FEAT over four days and 476 HDVs measured with the Low FEAT over the course of 3 days. Approximately 30% of the HDVs measured over the last three days had low exhaust. The mean emission ratios to CO_2 are shown in Table 8 for solely HDVs in 2017 for High and Low FEAT as well as mean and median g/kg of fuel emissions for CO, HC, NO, NO_2, NO_x, NH_3, IR %opacity, and average model year, speed (mph), acceleration (mph/s), and the road slope (degrees). The Low FEAT's NO_x average is 12% lower than the High FEAT, a result of the newer HDVs measured with SCR systems. Although the opacity measurements are not as reliable as other gases measured, 60% of the Low FEAT measurements had valid opacity readings and High FEAT had 88% of the measurements with valid opacity readings.

Interestingly, the opacity for Low FEAT was 2.25 times the average opacity of the High FEAT. This is likely biased high not because of BC emissions but because Low FEAT was on the roadway where dirt and other roadway debris likely interfered with the measurements. Figure 43 shows the differences in the HDV fleet emissions between those measured with the High (blue filled bars) and Low (open black bars) FEAT setups.

Since California registered vehicles are known to be under more stringent regulations for vehicles operating within the state; Table 9 compares California HDVs with out-of-state HDVs for CO, HC, NO, NO_2, NO_x, NH_3, IR %opacity and model year differences. Noticeably, the out-of-state vehicles, albeit much fewer, are 3.5 model years newer than the California HDVs measured, which corresponds with a 46% decrease in NO_x emissions. The newer non-California registered vehicles are more likely to have an SCR installed meaning urea is being used, which could also explain the out-of-state HDVs having higher (186%) average fuel specific NH_3 emissions due to ammonia slip, characteristic of HDVs with SCRs.[69]

The 2017 overall fleet averages (gray bars) for HDVs at Peralta are shown in Figure 44 for fuel specific CO, HC, NO, NO_x (all on the left axis), NO_2, NH_3 and IR %opacity (all on right axis). NO means are plotted as moles of NO while NO_2 and NO_x means are plotted as moles of NO_2. The fleet has also been segregated to compare the natural gas vehicle (NGV) emissions (open blue bars) to the diesel fleet (red striped bars). Uncertainties are SEM calculated using the daily means. The NGV averages are elevated, especially for CO, HC (methane) and NH_3 (a consequence of stoichiometric combustion and 3-way catalytic converters with available hydrogen for reducing NO emissions);

however, there were only a small number of NG vehicles in the entire fleet (21 out of 1844 HDVs) which accounts for the larger uncertainties. Unless noted, the entire fleet, including NGV vehicles, will be used in the subsequent analyses when discussing the HDV fleet.

Table 7. Peralta weigh station data summary for 2017.

FEAT Number of Measurements	High 1408	Low 907	All HDV 1844	All MDV 471
Mean CO/CO_2 (g/kg of fuel)	0.003 (5.5)	0.006 (10.0)	0.003 (5.9)	0.006 (11.0)
Median gCO/kg	2.7	6.9	3.0	7.6
Mean HC/CO_2 (g/kg of fuel)	0.0004 (2.1)	0.0003 (1.9)	0.0004 (2.2)	0.0002 (1.03)
Median gHC/kg	1.3	0.8	1.3	0.6
Mean NO/CO_2 (g/kg of fuel)	0.004 (7.8)	0.004 (7.6)	0.004 (7.4)	0.004 (8.8)
Median gNO/kg	4.2	3.2	3.7	5.9
Mean NH_3/CO_2 (g/kg of fuel)	0.00007 (0.08)	0.0005 (0.06)	0.00008 (0.09)	0.000003 (0.002)
Median gNH_3/kg	0.01	0.02	0.01	0.01
Mean NO_2/CO_2 (g/kg of fuel)	0.0003 (1.1)	0.0003 (1.0)	0.0003 (1.1)	0.0003 (1.1)
Median gNO_2/kg	0.5	0.4	0.5	0.5
Mean gNO_x/kg Median gNO_x/kg	13.0 7.3	12.5 5.4	12.4 6.5	14.5 10.0
Mean IR %Opacity Median IR %Opacity	0.4 0.3	0.9 0.8	0.5 0.3	0.9 0.7
Mean Model Year	2010.7	2010.7	2011.0	2009.6
Mean Speed (mph)	14.0	15.2	14.0	15.8
Mean Acceleration (mph/s)	0.7	0.2	0.7	0.2
Slope (degrees)	1.6°	1.6°	1.6°	1.6°

Table 8. Peralta weigh station data summary for HDVs in 2017.

FEAT Number of Vehicles	High 1,368	Low 476
Mean CO/CO_2 (g/kg of fuel)	0.003 (5.2)	0.003 (7.7)
Median gCO/kg	2.7	5.9
Mean HC/CO_2 (g/kg of fuel)	0.0004 (2.2)	0.0004 (2.5)
Median gHC/kg	1.3	1.0
Mean NO/CO_2 (g/kg of fuel)	0.004 (7.6)	0.003 (6.8)
Median gNO/kg	1.3	2.2
Mean NH_3/CO_2 (g/kg of fuel)	0.00007 (0.08)	0.0001 (0.1)
Median gNH_3/kg	0.01	0.02
Mean NO_2/CO_2 (g/kg of fuel)	0.0003 (1.1)	0.0003 (1.0)
Median gNO_2/kg	0.5	0.4
Mean / Median gNO_x/kg	12.8/ 7.2	11.3/ 3.9
Mean/ Median IR %opacity	0.4/ 0.3	0.9/ 0.9
Mean Model Year	2010.7	2011.9
Mean Speed (mph)	14.0	14.0
Mean Acceleration (mph/s)	0.8	0.1
Slope (degrees)	1.6°	1.6°

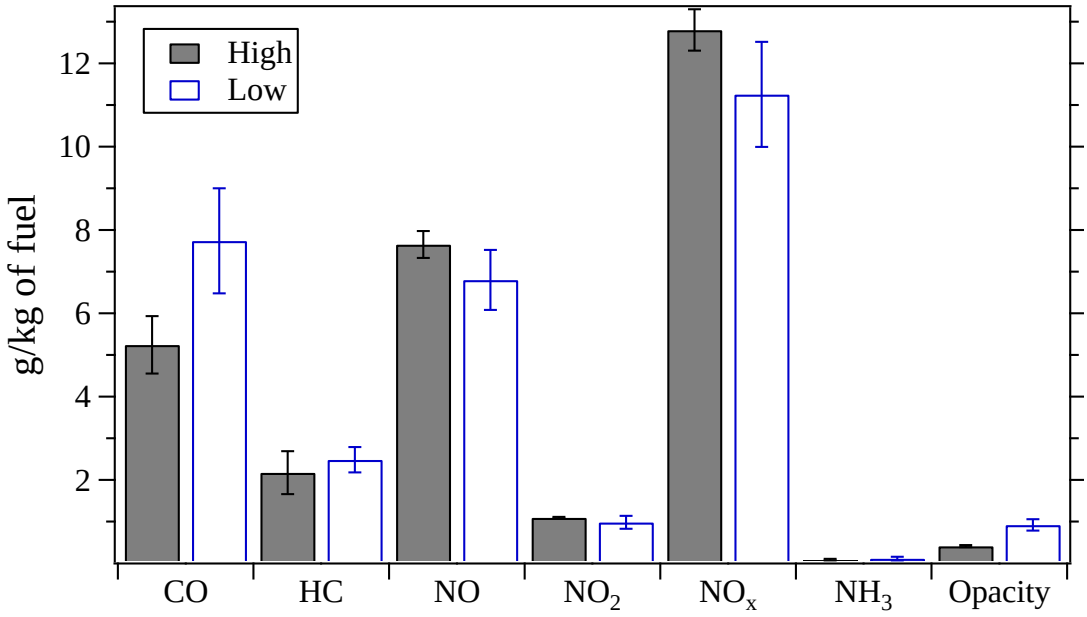

Figure 43. HDV CO, HC, NO, NO_2, NO_x, and NH_3 fuel specific emissions (g/kg of fuel) and IR %Opacity for the High (black, solid) and Low (blue, open) FEAT. Uncertainties are SEM calculated using the daily means.

Table 9. Emissions summary comparison for California registered and out-of-state-plate matched heavy-duty vehicles. Uncertainties are SEM calculated using the daily means.

State	Vehicles	Mean gCO/kg	Mean gHC/kg	Mean gNO/kg	Mean gNO_2/kg	Mean gNO_x/kg	Mean gNH_3/kg	Mean Model Year
CA	1488	5.6 ± 0.9	2.2 ± 0.5	8.2 ± 0.3	1.2 ± 0.04	13.7 ± 0.6	0.07 ± 0.03	2010.4
Other	356	6.9 ± 1.3	2.3 ± 0.4	4.4 ± 0.5	0.5 ± 0.05	7.2 ± 0.8	0.2 ± 0.02	2013.9
Δ		-21%	-0.04%	46%	58%	47%	-186%	-3.5

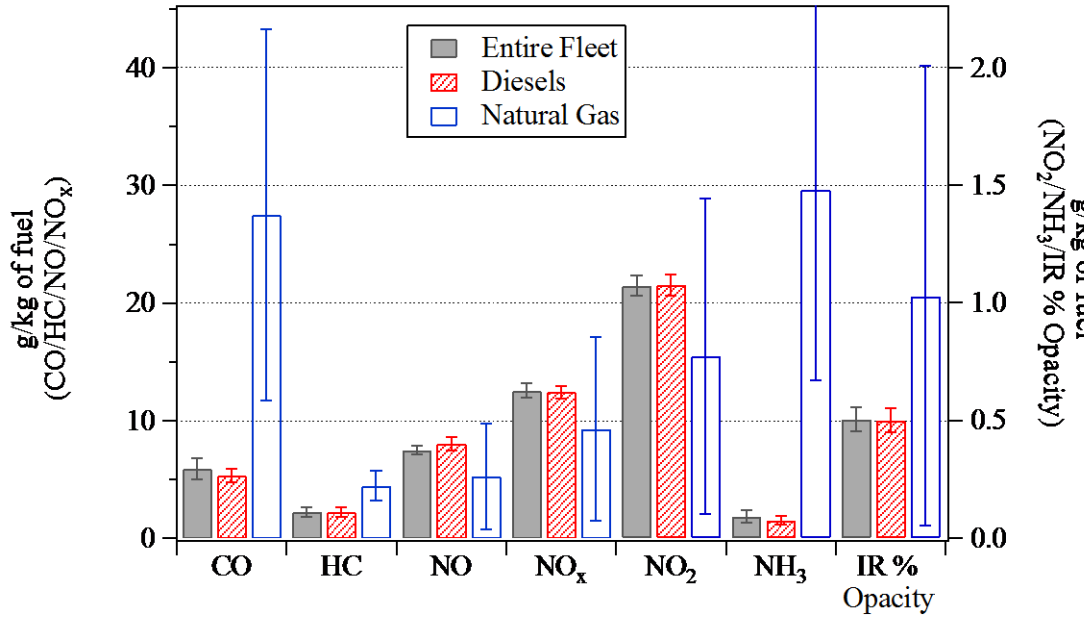

Figure 44. CO, HC, NO, NO_x (all on left axis) NO_2, and NH_3 (right axis) fuel specific emissions (g/kg of fuel) and IR %Opacity (right axis) for the entire Peralta fleet (gray, solid), diesels (red, hatched) and the natural gas portion of the fleet (blue, open). Uncertainties are SEM calculated using the daily means.

3.2 FEAT Heavy-duty Vehicles Historical Trends

A historical look at HDV information for data collected with FEAT is shown in Figure 45 for fleet average gNO_x/kg of fuel (black bars, left axis) and IR %opacity (gray bars, right axis) for all years Peralta has been measured. Uncertainties are SEM calculated using the daily means. NO is plotted as moles of NO_2 with the total bar height equal to total fuel specific NO_x emissions. The fuel specific NO has decreased 61% from 1997 (NO_2 was not measured until the 2008 field work), and a decrease of 37% from 2012 to 2017 has occurred for total NO_x, in part due to the introduction of SCRs. The fleet measured in 2012 had more HDVs with SCRs on-board, which is why there is a reduction in NO_x from 2010 to 2012 measurement years, and with a growing percentage

of HDVs with SCRs in 2017, fleet NO_x continues to decrease.[70] The reductions between 2008 and 2010 likely comes from engine management changes that allowed the manufacturers to have richer air to fuel ratio engines, lowering NO_x, and relying on DPFs to control PM.

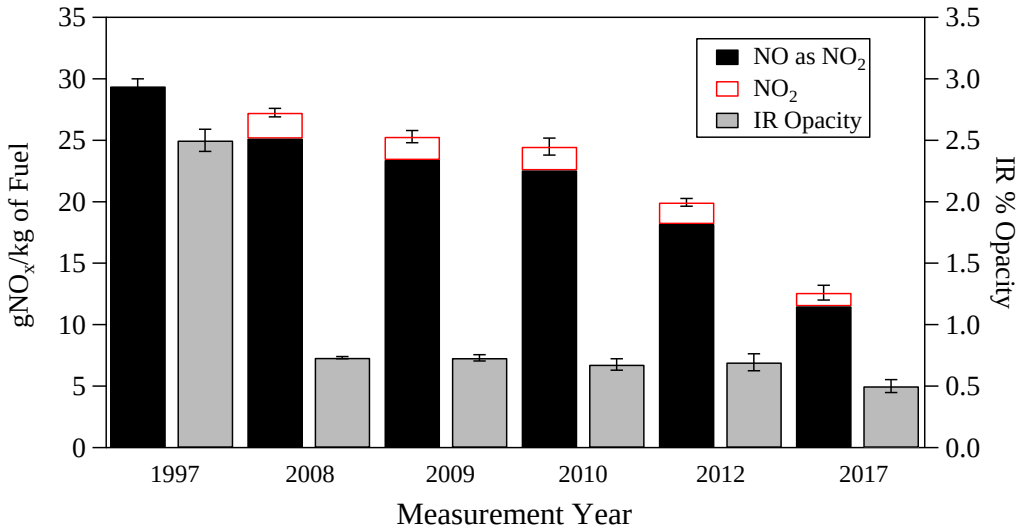

Figure 45. Infrared %opacity (gray bars, right axis) and NO as NO_2 equivalents (black bars, left axis), gNO_2 (open red bars, left axis) and gNO_x/kg of fuel (total bar height, left axis) by measurement year. Uncertainties are SEM calculated using the daily means.

Between 1997 and the 2008 campaign, there was a 70% decrease in IR %opacity. Since 2008, the fleet opacity average did not significantly change until this last campaign, which had a further decrease of 14% from the 2012 fleet mean and is similar to the values observed for the fully DPF equipped Port of Los Angeles fleet in 2012.[37] 2017 data is compared to other measurement years in Figure 45 for all HDVs measured with both High and Low FEAT. Previous studies only used the High FEAT and so for comparison purposes, the %opacity for 2017 High FEAT HDVs was 0.38 and 12.8 gNO_x/kg of fuel. The fleet has incorporated the new lower emissions technology, and regulated species,

such as NO_x and PM, were positively impacted. Table 10 further supports this claim, as the fleet is now mainly comprised of vehicles 2012 and newer (58% of the HDV fleet), which likely have after-treatment systems responsible for decreasing the fleet average opacity and NO_x.

Table 10. Vehicles measured by model year during the 2017 measurement year separated by HDVs and MDVs.

Year	Count	
	HDV	MDV
2007 and Older	321 (17%)	191 (41%)
2008	128 (7%)	23 (5%)
2009	146 (8%)	10 (2%)
2010	93 (5%)	13 (3%)
2011	98 (5%)	15 (3%)
2012	169 (9%)	22 (5%)
2013	173(9%)	32 (7%)
2014	164 (9%)	35 (7%)
2015	175 (9%)	45 (10%)
2016	239 (13%)	52 (11%)
2017	131 (7%)	33 (7%)
2018	7 (<1%)	0 (0%)

These gaseous emissions, and IR %opacity, were analyzed further by model year and compared to the 2012 measurements to show how the 2017 fleet has changed over the course of 5 years. All model years depicted in subsequent figures have more than 10 HDVs. Figure 46 shows gNO/kg of fuel (moles of NO) by model year for 2012 (black squares) and 2017 (blue circles) HDVs with SEM uncertainties calculated using the daily means. The 2017 data shows increases for all model years from the 2012 averages. Both data sets show the reductions in NO emissions with the start of the installation of SCRs between the 2010 to 2011 model years. The continual decrease in NO in subsequent model years is presumably due to the increasing percentage of HDVs having SCRs. However, some of the initial NO emission decreases have been lost as the fleet of HDVs has aged from 2012 to 2017.

2010 (red triangles), 2012 (black squares) and 2017 (blue circles) measurement year data for NO_2 versus chassis model year are shown in Figure 47. Uncertainties are SEM calculated using the daily means. One unintended consequence of first generation DPFs, mentioned previously, was that their catalyzed surfaces, to aid in passive regeneration of the filter, produced elevated levels of NO_2 emissions. Without NO_x after-treatment systems these increased NO_2 emissions are clearly seen in the 2010 and 2012 measurements for the 2008 – 2010 model year HDVs.[71] As these model years age, the catalyst loses its ability to oxidize NO to NO_2 a process known as de-greening, which corresponds to the decrease seen in NO_2 emissions for these model years in the 2017 measurements. HDVs without catalyzed DPFs (model year 2011 and newer), have a rapid

decline in NO_2 benefiting from SCR systems until model year 2014 where tailpipe NO_2 plateaus.

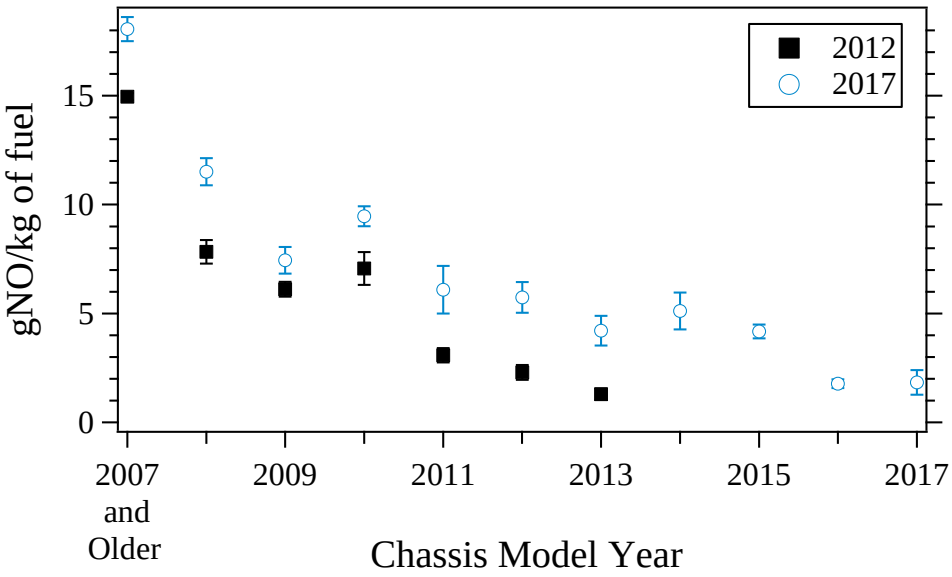

Figure 46. Fuel specific gNO/kg of fuel by chassis model year for 2012 (black squares) and 2017 (blue circles) data. Uncertainties are SEM calculated using the daily means.

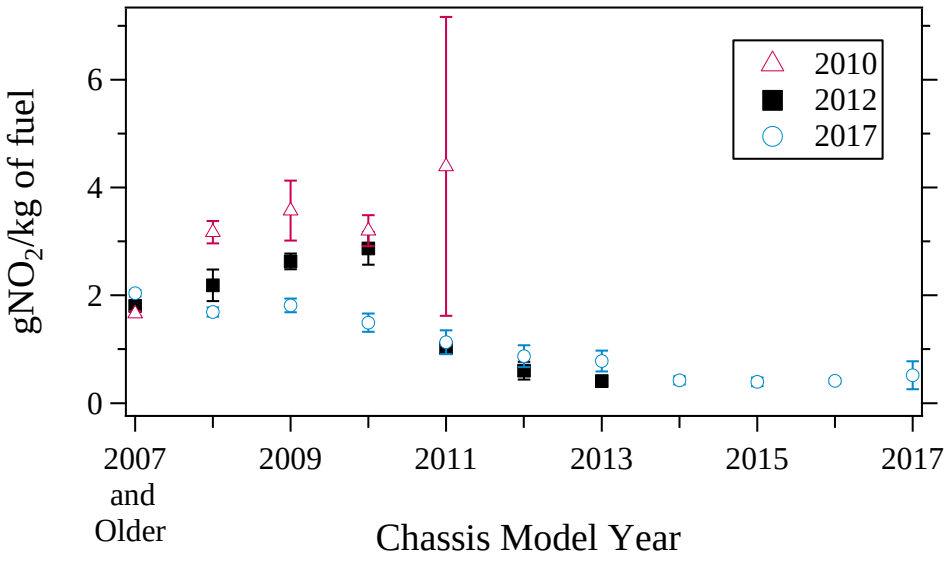

Figure 47. Fuel specific gNO_2/kg of fuel by chassis model year for 2010 (red triangles), 2012 (black squares) and 2017 (blue circles) data. Uncertainties are SEM calculated using the daily means.

Figure 48 shows fuel specific NO_x emissions by model year, where 2012 is represented as black squares and 2017 as blue circles. Uncertainties are SEMs calculated using the daily means. NO_x for model year 2013 in the 2012 data is identical to the average NO_x for model years 2016 and 2017 in the 2017 data. The age of these vehicles are the same, indicating that the measured NO_x emissions start out at the same level for vehicles with new SCR systems. Also, the 2016 and 2017 model year vehicles measured in 2017 show an additional 50% reduction in their average NO_x emissions compared to model year 2015. This suggests additional improvements in the newest SCR systems. The mass ratio of NO_2 to NO_x by model year is shown in Figure 49 comparing 2012 (black squares) and 2017 (blue circles) data. Uncertainties are SEM calculated using the daily means. The ratio plot reflects the mean fuel specific emissions shown for NO and NO_2 in Figures 46 and 47 with an increase in the ratio for the 2008 – 2010 model year vehicles in the 2012 measurements.

Figure 50 is fuel specific NH_3 emissions by model year for 2012 (black squares) and 2017 (blue circles) data. Uncertainties are SEM calculated using the daily means. Here, the influence of ammonia used as the reduction agent in SCR systems is evident. With the increased presence of SCR systems, and therefore increased urea use, the ammonia slip increases from the start of SCR use in model year 2011 until 2015. However, it appears that advancements in SCR technology for the newest model year vehicles has begun to reduce the ammonia slip.[69] These levels are still much lower than currently observed NH_3 emissions in the light-duty gasoline fleet (0.4 to 0.6 gNH_3/kg of fuel).[72] In 2017, the newer model years have consistently low NO_x measurements,

indicating their SCR systems are working as intended with an optimized NH_3 to NO_x ratio and at temperatures that allow this reduction to occur.

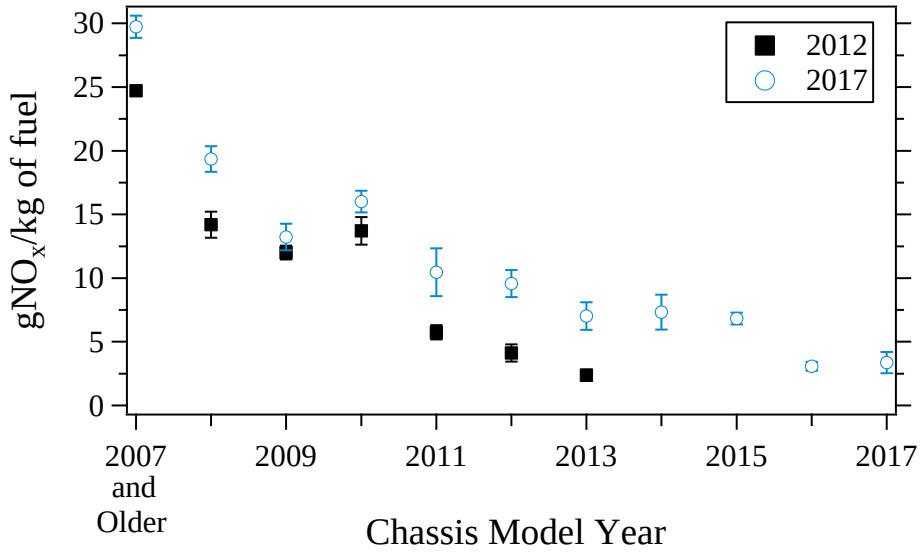

Figure 48. Fuel specific gNO_x/kg of fuel by chassis model year for 2012 (black squares) and 2017 (blue circles) data. Uncertainties are SEM calculated using the daily means.

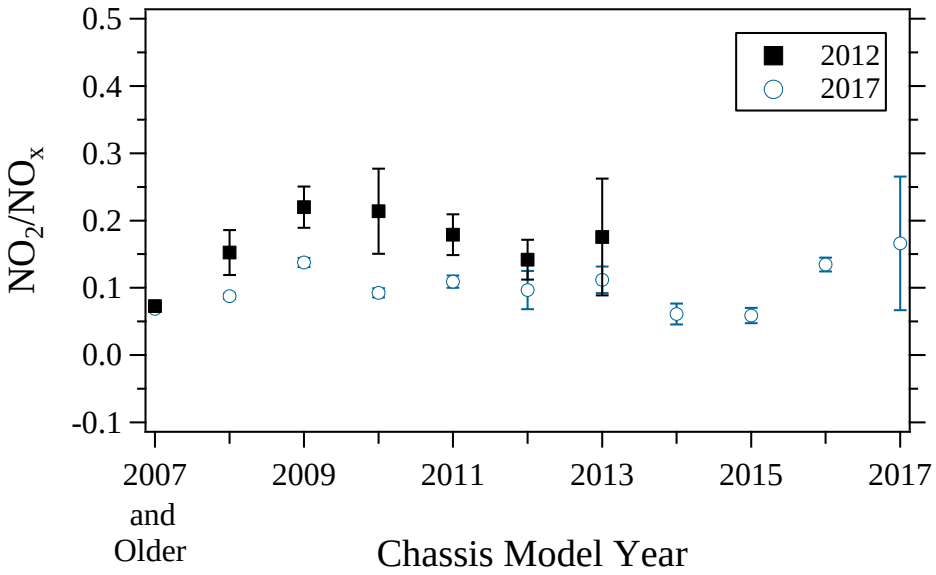

Figure 49. NO_2/NO_x mass ratio for 2012 (black squares) and 2017 (blue circles) data. Uncertainties are SEM calculated using the daily means.

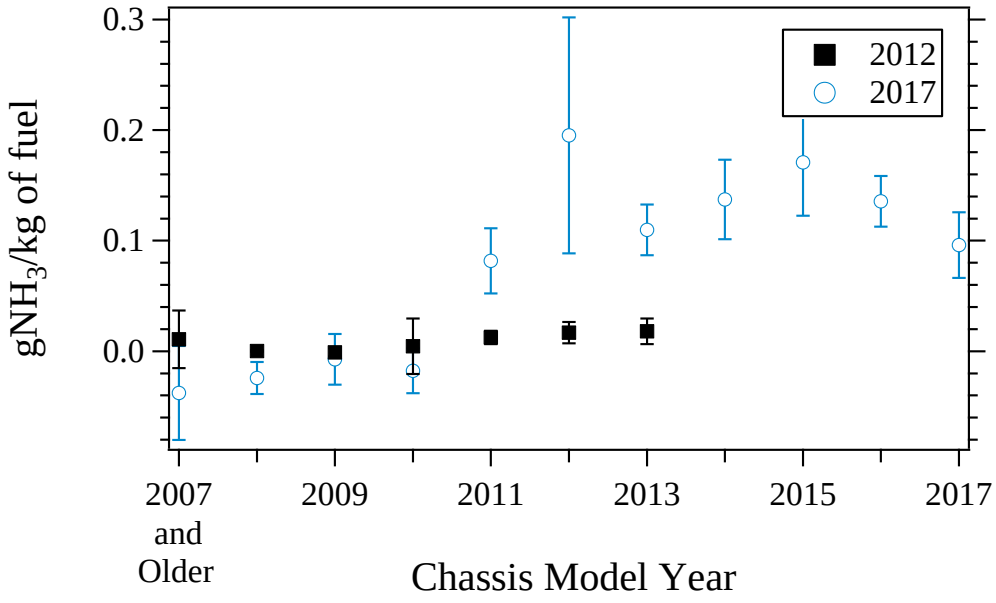

Figure 50. Fuel specific gNH_3/kg of fuel by chassis model year for 2012 (black squares) and 2017 (blue circles) data. Uncertainties are SEM calculated using the daily means.

Changes in certification standards have led to new technologies and combustion management in order for vehicles to achieve these standards. Although vehicles may pass laboratory certification standards, it is important to understand how the standards translate to on-road emission performance. Long-haul HDVs at the Peralta weigh station, shown in Figure 51 for 2012 (black) and 2017 (blue) measurements have been grouped into four model year categories that parallel the certification standards: pre-2004 HDVs that have no, or retrofit, after-treatment technologies, 2004-2007 model year vehicles that have combustion management such as EGR and retrofit activity, model years 2008-2010 that have first generation DPFs and are pre-SCR use, and 2011 and newer model years with DPFs and an increasing fraction of SCR systems.

Figure 51a shows NO_x (black or blue solid bars for the 2012 and 2017 measurements respectively) and IR %opacity (black or blue hatched bars for 2012 and 2017 respectively). Uncertainties are SEM calculated using the daily means. Figure 51b shows the fleet percentage for the corresponding model year groups for the 2012 and 2017 fleets represented by black solid bars and blue open bars respectively. Consistent with the previous graphs, NO_x continually decreases as technologies advance, seen in the newer model year groupings. Similarly, the IR %opacity in the 2012 measurements continually decreases for newer model year vehicles. The IR %opacity in 2017 measurements shows significant reductions in the two oldest model year groupings indicating that the older model year vehicles are likely to have retrofit DPFs installed in compliance with the California Truck and Bus Rule and follows suit with previous findings at Cottonwood, as mentioned previously. Notable in Figure 51b, the fleet in 2012 is dominated by vehicles older than model year 2004 (41%) but in 2017, the percentage of HDVs model year 2004 and older has decreased significantly to 10% which has positively influenced the overall emissions measured at Peralta.

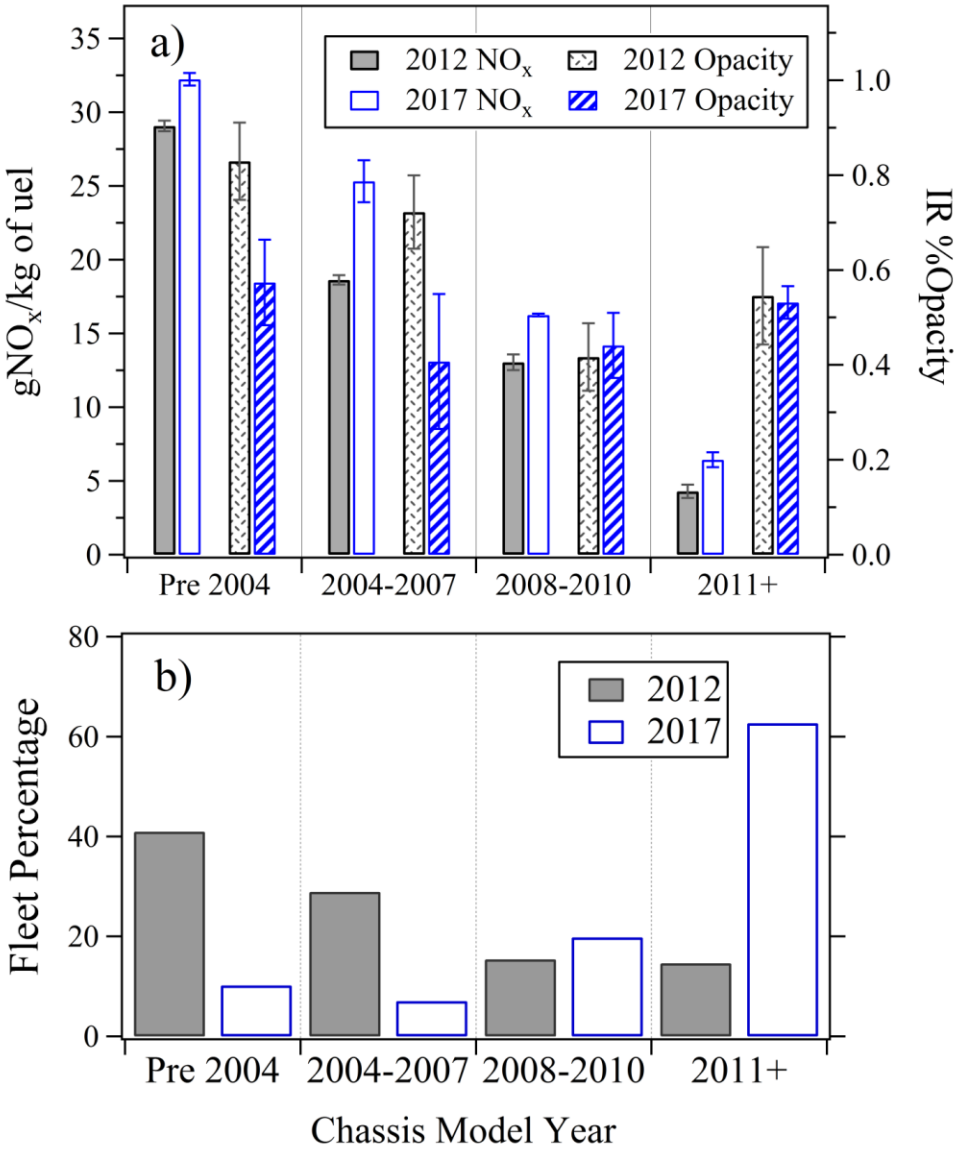

Figure 51. a) IR %Opacity (right axis, hatched bars) and gNO_x/kg of fuel (left axis, filled bars) for 2012 (black) and 2017 (blue) data grouped by model year. Uncertainties are SEM calculated using the daily means. b) Fleet percentage for grouped model years in 2012 (solid black bars) and 2017 (open blue bars) data.

3.3 FEAT Medium-duty Vehicle Comparisons

The assortment of vehicles at Peralta provides an opportunity, for the first time, to gain insights into how MDVs and HDVs compare in their emissions profiles. MDVs were categorized by fuel and compared with the HDVs in Figure 52 with the 2017 HDV diesel fleet (black solid bars) and the MDV gasoline (green striped bars) and diesel (blue open bars) fleets for all species measured. Fuel specific CO, HC, NO and NO_x are on the left-axis and NO_2 and NH_3 are on the right axis. Total fuel specific CO emissions for gas MDV fleet are four times higher than the MDV diesel fleet. Diesel engines are lean burn compression ignition engines and have significantly higher engine temperatures than gasoline engines, and thus have higher engine out NO_x than gasoline vehicles.[73] Therefore, as expected, NO_x (both NO and NO_2) are elevated for the diesel MDVs compared to the gasoline MDVs. The diesel MDVs are slightly higher than diesel HDVs NO_x due to the MDV fleet being older than the HDV fleet, but the difference is not significant for the overall fleet average emissions. For the subsequent figures, diesel MDVs will be used in comparison to the diesel HDVs.

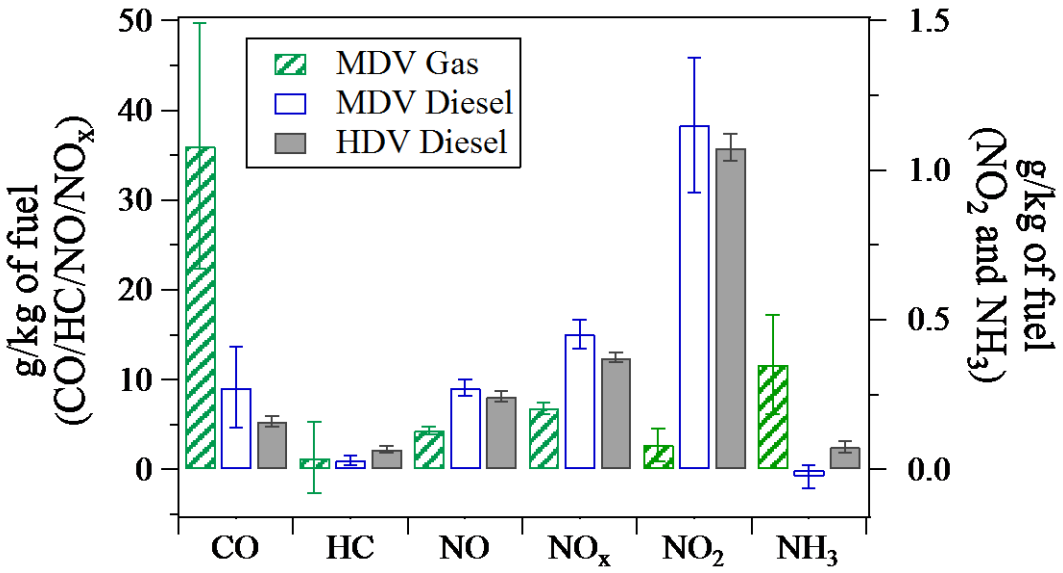

Figure 52. Fuel Specific emissions (g/kg of fuel) for CO, HC, NO and NO_x (left-axis) and NO_2 and NH_3 (right-axis) emissions fuel for gas MDVs (green striped bars, left-axis) and diesel (right-axis) MDVs (blue open bars) and HDVs (black solid bars). Uncertainties are SEM calculated using the daily means.

Fuel specific NO emissions by model year are shown in Figure 53 for medium and heavy-duty vehicles represented by blue diamonds and black triangles, respectively. Uncertainties are SEM calculated using the daily means. From the 2007 and older model year vehicles to model year 2017, there is a 91% and 94% reduction in NO for MDVs (16.5 to 1.5 gNO/kg of fuel) and HDVs (17.8 to 1.8 gNO/kg of fuel), correspondingly. Comparing the diesel MDVs to the diesel HDVs by model year, the NO emissions are statistically equivalent by model year, except for model years 2014-2016, where the decreases in HDVs emissions experience a plateau while the MDVs NO emissions continue to decline. NO_2, however, shown in Figure 54 for MDVs (blue triangles) and HDVs (black triangle), have consistent decreases by model year and no significant differences between medium and heavy-duty vehicles except for model year 2010, which

is unexplained. It should be mentioned that model years 2008 – 2010 have very few measurements for MDVs (46 measurements). Uncertainties in Figure 54 are SEM calculated using the daily means.

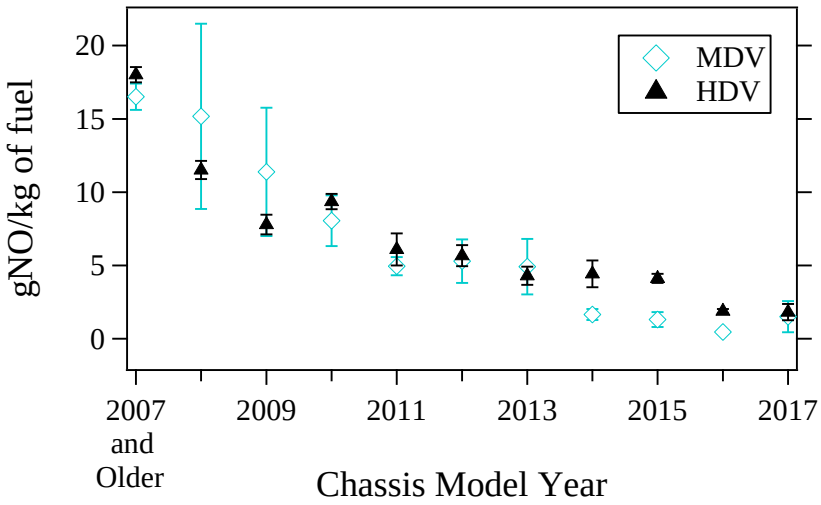

Figure 53. 2017 fuel Specific gNO/kg of fuel by model year for heavy-duty (black triangles) and medium-duty (blue diamonds) vehicles. Uncertainties are SEM calculated using the daily means.

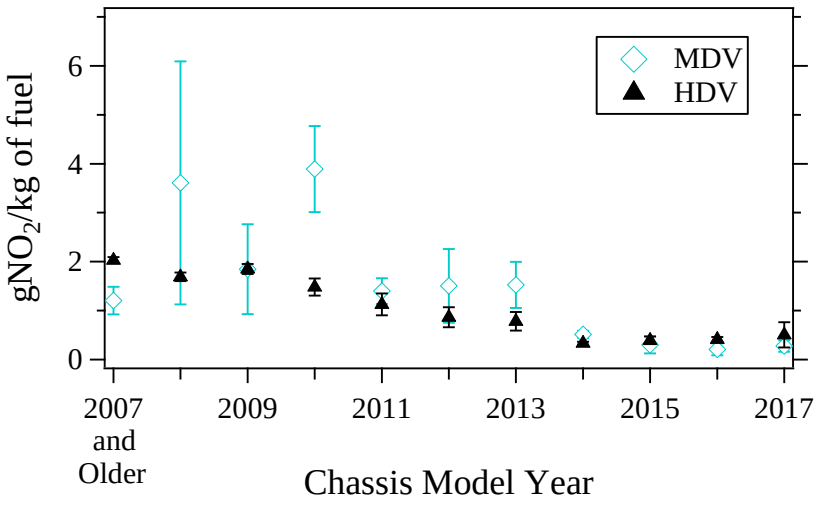

Figure 54. 2017 fuel Specific gNO_2/kg of fuel by model year for heavy-duty (black triangles) and medium-duty (blue diamonds) vehicles. Uncertainties are SEM calculated using the daily means.

Figure 55 shows the apportionment of NO as NO_2 equivalent (open bars), NO_2 (solid and striped bars) and total NO_x (total bar height). Uncertainties are SEM calculated using the daily means by model year for MDVs (blue) and HDVs (black). Noticeably, both MDVs and HDVs have a decrease in NO_x emissions between model years 2010 and 2011, when first generation SCRs became available, and model years 2010-2013 are consistent between these two vehicle classes. However, newer MDVs have lower NO_x emission than their HDV counterparts.

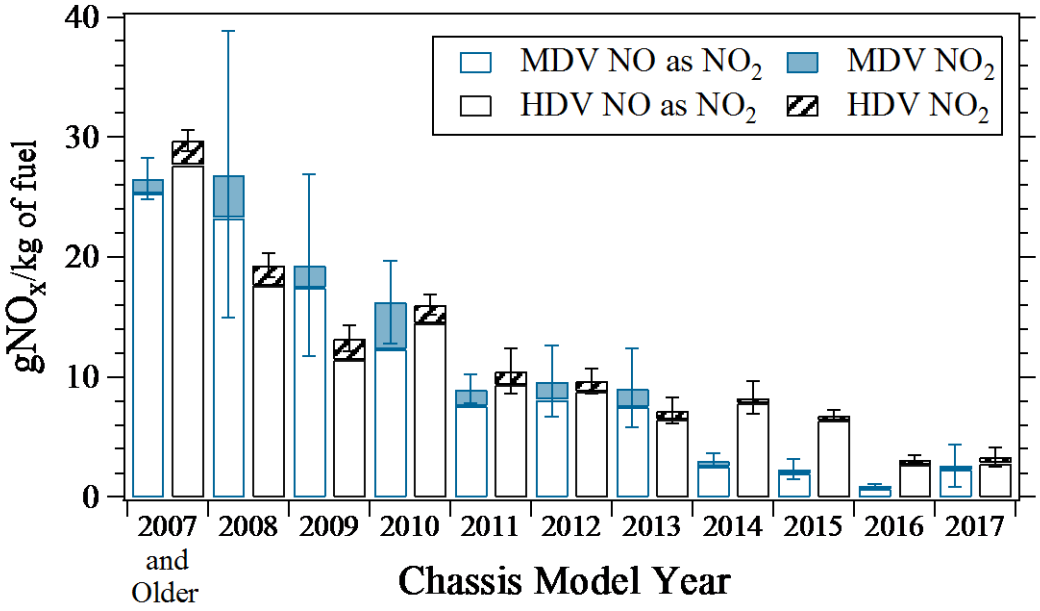

Figure 55. Total gNO_x/kg of fuel (total bar height) for MDVs (blue) and HDVs (black) vehicles. Mean gNO_2/kg of fuel (solid or hatched) and gNO/kg of fuel as gNO_2/kg of fuel (open bars) as graphed by chassis model year. Uncertainties are SEM calculated using the daily means.

MDVs had an overall reduction from 26.5 gNO_x/kg of fuel for vehicles 2007 and older to 2.6 gNO_x/kg of fuel for model year 2017 (90% reduction), and HDVs followed suit with an 88% reduction from 29.4 gNO_x/kg of fuel for 2007 and older model year vehicles to 2017 model year average of 3.4 gNO_x/kg of fuel. HDVs deviate from the

MDVs in model years 2014-2016 for NO_x due to increase NO emissions as previously discussed in Figure 55. The exact reason for this is unknown but it is possible that these HDV model years have a lower fraction of vehicles that fully meet the low NO_x standards due to FEL averaging.[74, 75]

A box and whisker plot, Figure 56, shows gNO_x/kg of fuel by chassis model year for HDVs and MDVs. The horizontal line within the box dictates the median, the box encloses the 25th to the 75th percentiles and the whiskers denote the 10th to 90th percentiles. The measurements beyond the 10th to the 90th percentiles are shown in black triangles (HDVs) and blue diamonds (MDVs) and the model year means are represented by black squares. The 90th percentile for MDVs 2014-2016 are 47, 78 and 72% lower than for the same model year of HDVs, meaning there are fewer high emitting MDVs than HDVs for these model years.

Interestingly, the increase in HDV NO_x for model years 2014-2016 is also accompanied by an increase in NH_3 emissions, shown in Figure 57, where HDVs (black triangles) are elevated from the MDVs (blue squares) of those same model years. Uncertainties are SEM calculated using the daily means. The exact reason for this is unknown, and hard to deduce with the information available. However, these MDVs' emissions have lower NO_x and lower NH_3 than the HDVs, indicating that the ammonia dosing could be more efficient on these MDVs. Figure 58 further analyzes the 2014-2016 model year vehicles. Individual ammonia measurements have been plotted against their NO_x reading for just model year 2014-2016 diesel HDVs. The subcategory of this fleet has been separated by chassis manufacturer: Freightliner (FRHT, blue crosses),

International (INTL, red squares), Kenworth (KW, black triangles), Peterbilt (PTRB, purple diamonds) and Volvo (orange Xs). The highest emitting NO_x vehicles have near zero ammonia levels, similar to older vehicles that do not have an SCR installed, whereas higher NH_3 emitting vehicles have low NO_x measurements, which could represent urea overdosing within the SCR and not fully reducing NO_x leading to increased NH_3 slip.

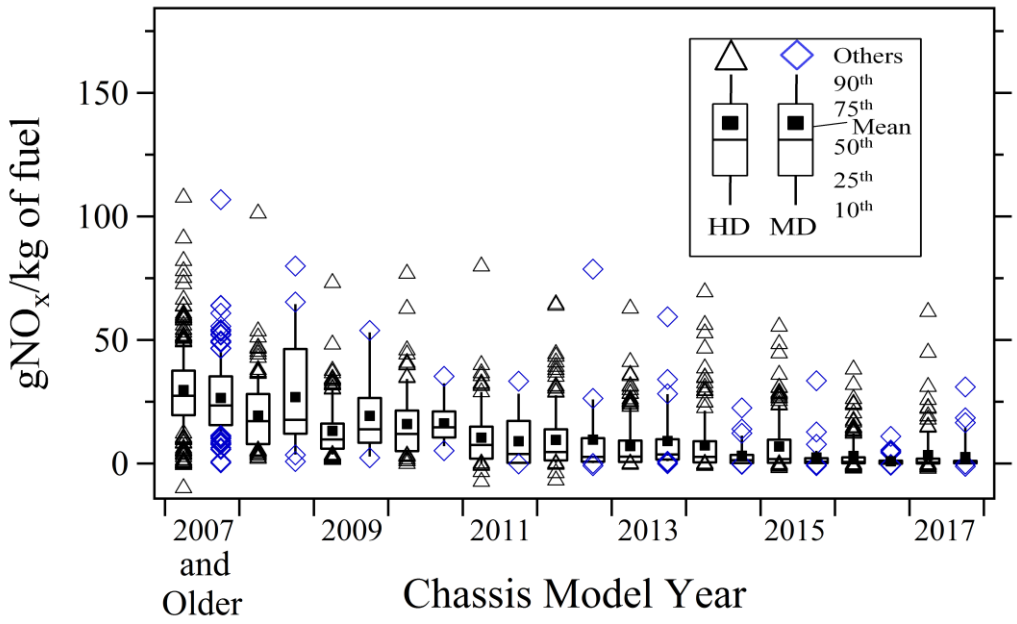

Figure 56. Box and whisker plot for gNO_x/kg of fuel by chassis model year for heavy-duty (HD) and medium-duty (MD) vehicles. The horizontal line dictates the median, the box encloses the 25th to the 75th percentiles and the whiskers denote the 10th to 90th percentiles. The measurements beyond the 10th to the 90th percentiles are shown in black triangles (HDVs) and blue diamonds (MDVs) and the means are represented by filled black squares.

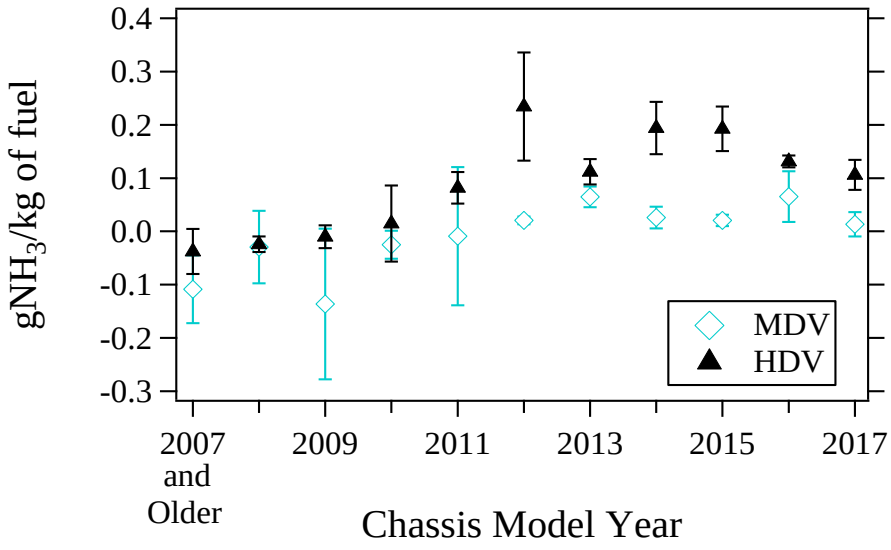

Figure 57. 2017 fuel Specific gNH_3/kg of fuel by model year for heavy-duty (black triangles) and medium-duty (blue diamonds) vehicles. Uncertainties are SEM calculated using the daily means.

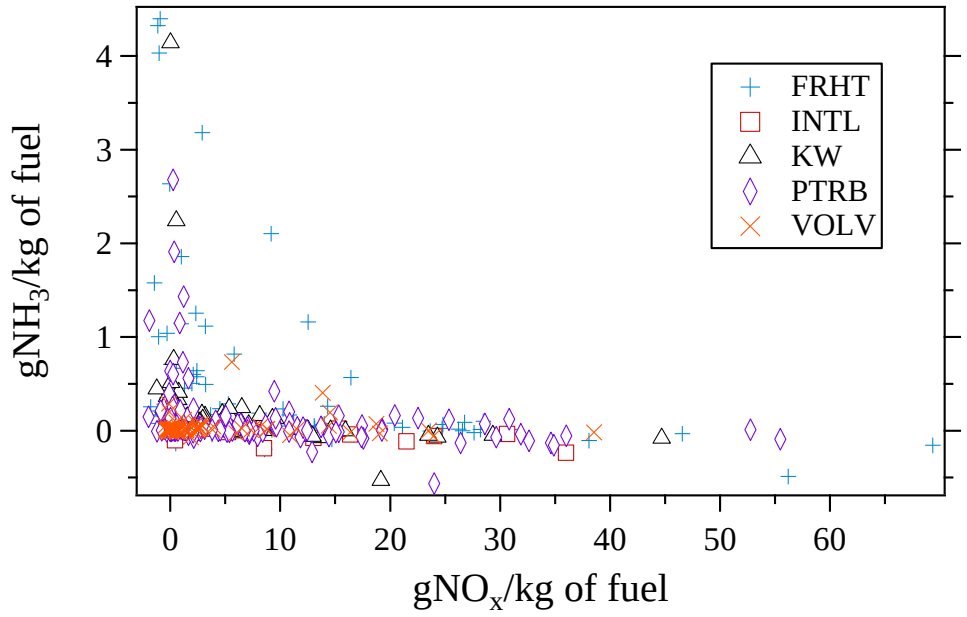

Figure 58. Individual fuel specific NH_3 emissions versus their individual NO_x emissions for diesel HDVs at Peralta for model years 2014-2016. Measurements separated by manufacturer: Freightliner (FRHT, blue crosses), International (INTL, red squares), Kenworth (KW, black triangles), Peterbilt (PTRB, purple diamonds) and Volvo (orange Xs).

To understand the improvements in solely the MDV diesel fleets, the Peralta MDVs were compared to vehicles measured at a site in Chicago, IL using license plate weight codes to extract MDVs from the Chicago fleet measured in 2014 and 2016. Figure 59 shows the fleet average fuel specific NO, NO_2 and NO_x emissions for Chicago's measured fleet in 2014 (green open bars) and 2016 (blue hatched bars), as well as the Peralta 2017 fleet (solid grey bars). Uncertainties are the SEM calculated using the daily means.

The average model year for the measured Chicago fleet went from 2006.1 in 2014 to 2009.2 measured in 2016, and the 2017 Peralta fleet had a model year average of 2009.6. As the fleets incorporate newer vehicles with SCRs, represented by a newer model year average, NO_x emissions decrease, indicating MDVs from both Illinois and California are continually reducing NO_x emissions from their medium-duty fleets, and following similar trends observed with HDV fleets. Interestingly, NO_x emissions by model year for all three fleets, Figure 60, are relatively similar, with a characteristic drop in NO_x (45% at Peralta) for model year 2011 coinciding with the introduction SCR systems, and a 66% further reduction in model year 2014 and newer vehicles measured at Peralta. These reductions are also noticeable in both Chicago fleets. Changes to on-board diagnostic regulations could be an additional factor influencing these continued decreases in the NO_x in later model years.[76]

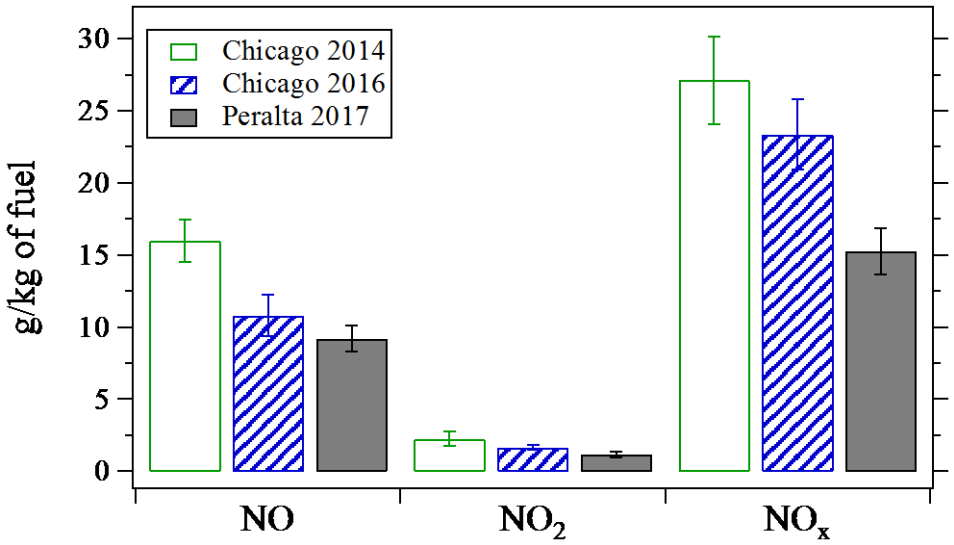

Figure 59. Chicago 2014 (green open bars), Chicago 2016 (blue hatched bars) and Peralta 2017 (grey filled bars) fleet averages for gNO/kg of fuel (moles of NO), gNO_2/kg of fuel and gNO_x/kg of fuel (moles of NO_2). Uncertainties are SEM calculated using the daily means.

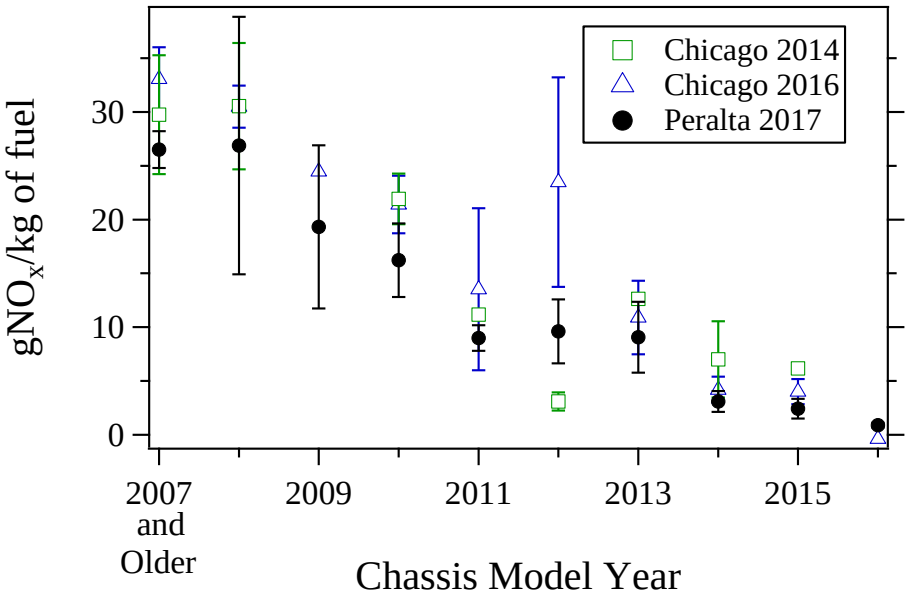

Figure 60. Fuel specific NO_x by chassis model year for Chicago 2014, (green squares) 2016 (blue triangles) data and 2017 Peralta data (black circles). Uncertainties are SEM calculated using the daily mean.

Chapter 4 – OHMS and FEAT

Heavy-duty Vehicle Comparison

One of the criteria pollutants established by the EPA, NO_x, was measured by both FEAT and OHMS in two similar long-haul HDV fleets. PM, although inferred with FEAT through IR %opacity measurements, was only explicitly measured by OHMS and will not be compared to the FEAT data. Therefore, the two weigh stations monitored for this research, Peralta weigh station (red squares) and Cottonwood weigh station (blue circles), have been compared in Figure 61 for only fuel specific NO_x to help understand how generalizable this research is for other fleets within California. Uncertainties are SEM calculated using the daily means. NO_x emissions are similar for the oldest and newest model year vehicles (model year <2004 or >2015). Vehicles without NO_x reduction technologies have similar emissions by model year at these two weigh station sites, and HDV model years that are largely equipped with SCRs perform similarly as well. Because both of these subcategories are similar between measurement methods, the differences observed between the intermediate model years is unlikely from calibration and or measurement technique variances. Peralta's emissions for model years 2011-2014 are slightly below the corresponding averages at Cottonwood, but this could be the result of Peralta having more HDVs with SCRs installed than at Cottonwood for these model years. The difference in model years 2008, 2009 and 2010 are statistically different and

Peralta's model year averages are 40, 52 and 38% lower than those observed at Cottonwood. These specific model years comprise 25 and 20% of their fleets, respectively.

The exact reason for this is unknown, but it does coincide with elevated NO_2 emissions in the Cottonwood fleet. Figure 62 shows gNO_2/kg of fuel for Peralta (red squares) and Cottonwood (blue circles) for model years 2007-2015. Uncertainties are SEM calculated using the daily means. Peralta has consistently low NO_2 emissions; however, there is a model year dependence for the vehicles at Cottonwood. The introduction of SCRs in 2011 model year vehicles saw a 59% reduction in NO_2 and averages continued to decrease as more HDVs have SCRs. The two techniques do measure NO_2 differently, as FEAT measures it directly spectroscopically, while OHMS reports it as the difference between two measurements of total NO_x and NO. The difference method will always have higher uncertainties because two numbers with similar magnitude are being subtracted and that is evident in Figure 62. However, the increased levels of NO_2 found in the Cottonwood fleet are unexplained.

Other possible explanations for higher NO_x emissions for the 2008-2010 HDVs are the difference in elevation (which are small, less than 100m), to differences in temperature and humidity. To account for the difference in humidity and temperature at these two sites, corrected NO_x averages were calculated according to the Code of Federal Regulation's humidity correction factor.[77] With this, it was proven that the humidity and temperature lowered the differences between the two sets (~1-2%) but could not account for the majority of the differences observed.

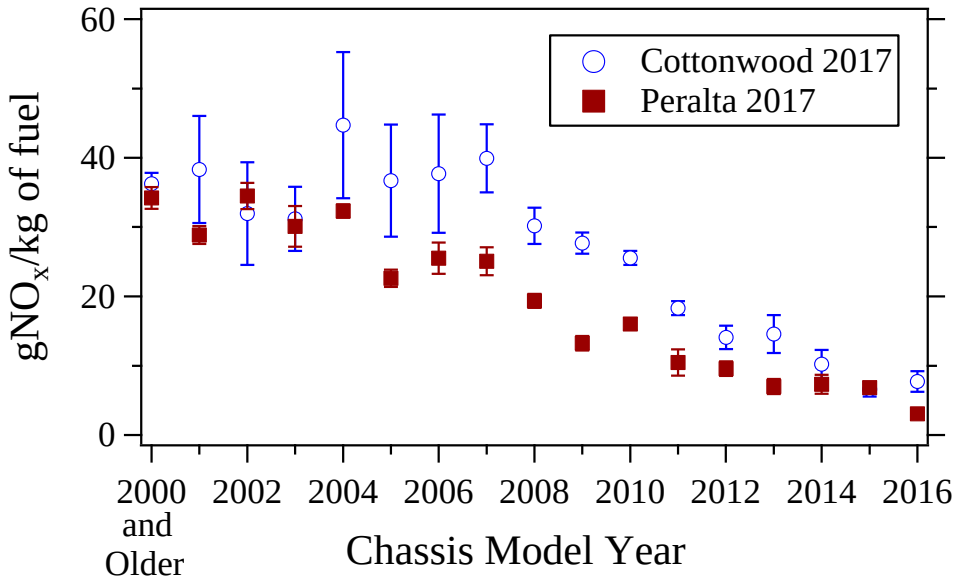

Figure 61. Fuel specific NO_x emissions by chassis model year for Cottonwood (blue circles) and Peralta (red squares), both with 2017 data shown. Uncertainties are SEM calculated using the daily means.

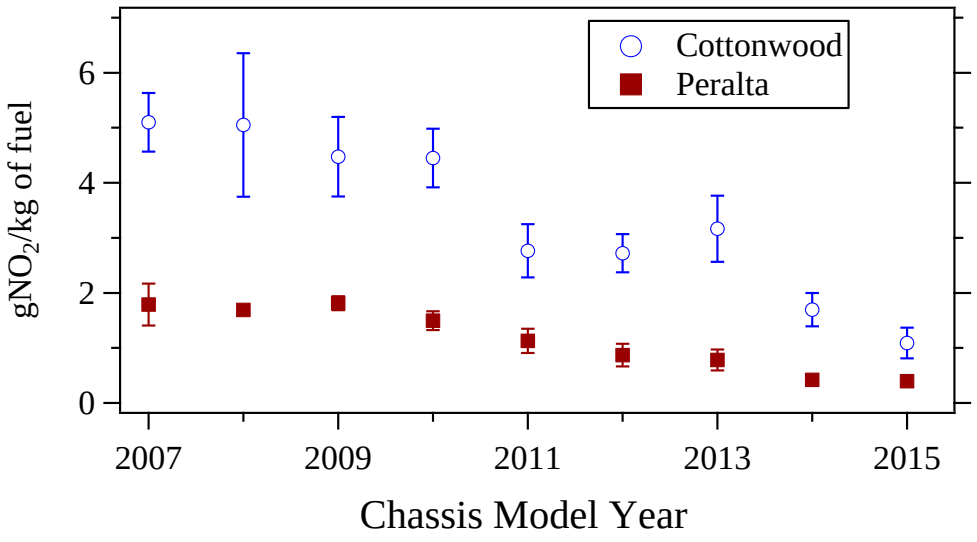

Figure 62. Fuel specific NO_2 emissions by chassis model year for Cottonwood (blue circles) and Peralta (red squares), both with 2017 data shown. Uncertainties are SEM calculated using the daily means.

Chapter 5 – Conclusion

OHMS was used to collect fuel specific emission factors for CO, HC, NO, NO_x, NO_2 by difference (NO_x-NO), PM, PN and BC. With this technology, the University of Denver has successfully conducted three data collection campaigns for HDVs at two California sites in the spring of 2013, 2015 and 2017. The first site was located at the Port of Los Angles and the second was at the California Highway Patrol's Cottonwood scales along I-5 in northern California just south of Redding CA. These sites provided contrasting fleets with the Port location having a short-haul drayage fleet that had only recently been required to retire any HDV which was not equipped with a DPF. The Cottonwood location consisted of an interstate long-haul fleet subject to more traditional fleet turnover changes. The Port fleet provided an opportunity to follow the aging process on emissions from a relatively new vehicle fleet all equipped with DPFs. Cottonwood had observed changes in the fleet emission trends that took place during the introduction of new technology vehicles via fleet turnover.

These three campaigns have resulted in the collection of a total of 7,073 HDV emission measurements and is one of the largest in-use emissions data set collected to date on HDVs. Since the first measurements were collected in 2013, the fleet sampled at the Port of Los Angeles has increased in age by approximately 3.3 years as the fleet's

mean model year only changed from 2009.1 to 2009.8 over the five year period. The fleet's dominant vehicle chassis model years are 2008 and 2009 models that were purchased prior to the 2010 San Pedro Clean Ports Clean Air Action Plan deadline to upgrade to a 2007 PM compliant engine. In 2013 these models made up 70% of the measurements and in 2017 these two models still represented 57% of the measurements. However, 2011 and newer chassis model year vehicles have increased from just 11% of the measurements to 25%. Despite the fleet age increases the 2017 fleet sampled at the Port is still significantly younger than the nonregulated drayage fleet sampled at this location in 2008 (7.2 vs. 12.4 years old). In contrast, the fleet at the Cottonwood weigh station has become steadily newer as the fleet has turned over. In 2013 the mean model year of 2005.6 corresponded to an approximate fleet age of 7.4 years. In 2015 the mean model year observed was 2008.1 (~6.9 years old) and in 2017 that further improved to 2011.3 (~5.7 years old).

At the Port of LA, the only gaseous species that changed significantly over the five year period was the oxide of nitrogen emissions, increasing ~25%. NO_x emissions at the Port are generally higher and less affected by model year than similarly aged vehicles at Cottonwood as the Ports activity cycle and subsequent lower operating temperatures are not conducive to successful SCR operation. For the HDVs measured at Cottonwood, overall all of the gaseous species showed reductions over the five year period, though HC and the oxides of nitrogen did not have consistent trends. The observed increases in oxides of nitrogen emissions in 2015 were the result of unexplained systematic increases for all model years. The 2017 measurements by model year are more consistent with the

2015 measurements and the reductions in the mean are a result of the age decrease of the fleet with newer and lower emitting HDV replacing older and higher emitting HDV. Indirectly indicating that SCR performance at Cottonwood is significantly more efficient than at the Port, which also coincides with higher exhaust pipe temperatures at Cottonwood than vehicles at the Port of Los Angeles.

Particle emissions trends at the two locations have followed different paths with emissions at the Port location increasing from very low levels in 2015 and then decreasing in 2017 while Cottonwood has consistently declined with each successive measurement campaign. After the Port's particle emissions experienced significant increases in emissions in 2015 due to an increase in the number of high emitters in the 2008 to 2010 chassis model year vehicles, the 2017 data saw those high emitter fractions significantly reduced to levels nearer those observed in 2013 with fuel specific PM, BC and PN emissions decreasing 64%, 63% and 20% respectively (0.11 to 0.04 gPM/kg of fuel, 0.08 to 0.03 gBC/kg of fuel and 2.8 x 10^{14} to 2.2 x10^{14} PN/kg of fuel). One potential explanation for fewer high emitting vehicles in 2017 at the Port of Los Angeles is that the Air Resources Board increased roadside compliance testing, which included concurrent information only opacity testing at the Port during the 2015 campaigns and the issuance of statewide citations since 2015 has increased significantly. This may have encouraged corrective maintenance or relocation for some of the high emitting vehicles observed in 2015.

At Cottonwood, the combination of a newer fleet and continued DPF retrofitting of older vehicles sustained a consistent reduction in particle emissions. Reductions of

almost a factor of 3 over the 2015 fuel specific PM (0.22 to 0.08 gPM/kg of fuel) emission levels, a 57% reduction for PN ($1.7x\ 10^{15}$ to $7.7\ x\ 10^{14}$ PN/kg of fuel) emissions and smaller but continued reductions for BC (0.077 to 0.056 gBC/kg of fuel) emission levels were observed. Since 2013 there have been observed decreases of 87%, 76% and 64% for fuel specific PM, BC and PN emissions respectively. These constant reductions have brought the Cottonwood fleets mean particle emissions to levels that are approaching those observed at the Port indicating that the vast majority of HDV operating through the Cottonwood scales are now DPF equipped. Noticeable reductions from the 2007 and older group, that while the range of observed fuel specific PM emissions is similar for each data set, show significant reductions in the number of the higher readings. This has dramatically lowered mean emissions by more than a factor of 2 for this group.

FEAT was used to optically measure pollutants from medium and heavy-duty vehicles at the Peralta weigh station in California in the spring of 2017 resulting in 2315 on-road measurements using an elevated FEAT and a ground-level FEAT. This location has been monitored since 1997, albeit only with High FEAT. The Peralta research gives historical insight into how HDVs' emissions have changed over the course of 20 years, as well as how new technologies are improving as well as their durability.

There was a continued decrease in critical pollutants for HDVs, NO_x and PM (inferred with IR %opacity), since the first measurements at this location in 1997. From 1997, NO has decreased a total of 61% in 2017 and total NO_x, first measured in 2008, was reduced by 54% by 2017. The HDVs at Peralta in 2017 were mainly newer than

2012 (58% of the fleet), which have the potential of having an SCR system onboard, which would aid in the NO_x reduction observed in 2017. With the introduction of SCR systems in model year 2012 and newer, there is also an increase in ammonia, needed to reduce NO_x to N_2. However, as these technologies advance, the ammonia slip has been improved in later model years.

There was a 70% decrease in IR %opacity from 1997 to 2008 and a further reduction of 14% from 2012 to 2017, as the IR %opacity from 2008 to 2012 changed insignificantly. This is a result of vehicles coming into the fleet with DPFs that filter out BC, lowering IR %opacity. Not only are their newer model year vehicles with improved after-treatment technologies in the fleet, but pre-DPF HDVs have installed retrofit DPFs that have also lowered tailpipe opacity.

The early generation DPFs were often catalyzed, and decreases in the NO_2/NO_x ratio are shown from model years 2008 – 2010 as these catalysts lose their ability to oxidize NO to NO_2 to help with soot oxidation. Newer model years from this rely on SCR systems to reduce NO_x, which is why the NO_x emissions are lower for newer model years and the observed NO_x continues to decrease as more HDVs are equipped with SCRs in subsequent model years.

Because FEAT is an optical technique that can capture ground-level exhaust as well, MDVs were able to be analyzed as well, creating the largest on-road dataset in the world for MDVs. The regulations imposed on HDVs are also mandated for MDVs and therefore the observed emissions by model year are nearly identical for these two vehicle groupings. The only deviation detected between diesel MDVs and HDVs measurements

was the 2014 – 2016 model year vehicles for NO and NH_3, where MDVs had lower emitting vehicles for both species than their HDV counterparts. This could be an indication of newer technologies being implemented into MDVs sooner that have more effective ammonia dosing strategies, but cannot be proven with the information available. However, it is encouraging that MDVs continue to reduce criteria pollutant emission as technologies improve.

The comparison of HDVs between the two sites, although the data was collected with different measurement techniques, show similar model year NO_x averages for HDVs not equipped or fully equipped with SCR systems. There is a discrepancy with HDVs' NO_x averages for model year 2008-2010. There are a variety of after-treatment technology variations for these model years and therefore it is hard to pinpoint the crux of these differences. Interestingly, it is not merely NO that is responsible for the increase, but NO_2 as well, which indicates there are likely multiple reasons for these differences. The important message with the FEAT and OHMS NO_x comparison is that these two measurement techniques determine statistically equivalent model year NO_x averages, indicating that both techniques can be used to measure on-road HDV emissions, and that these two distant weigh station fleets show comparable trends for vehicle with matching after-treatment technologies. This helps to prove that the data presented here can be relatively generalized for other weigh stations within California.

Both PM and NO_x ambient concentration reductions depend on the reduction in emissions from diesel vehicles as 24% and 48% of California's South Coast anthropogenic NO_x and PM respectively comes from diesel vehicles.[78, 79] Overall, the

reductions in PM and NO_x observed with this research correspond to the atmospheric reduction trends predicted by California. Figure 63 shows Cottonwood weigh station measurement year averages (blue squares, left axis) compared to the state of California's reported annual average PM for all diesel vehicles in California (green circles, right axis).[20] The fleet at Cottonwood represented a fleet turnover schedule subject to all diesel vehicles throughout California and shows larger reductions in atmospheric PM than state predictions.

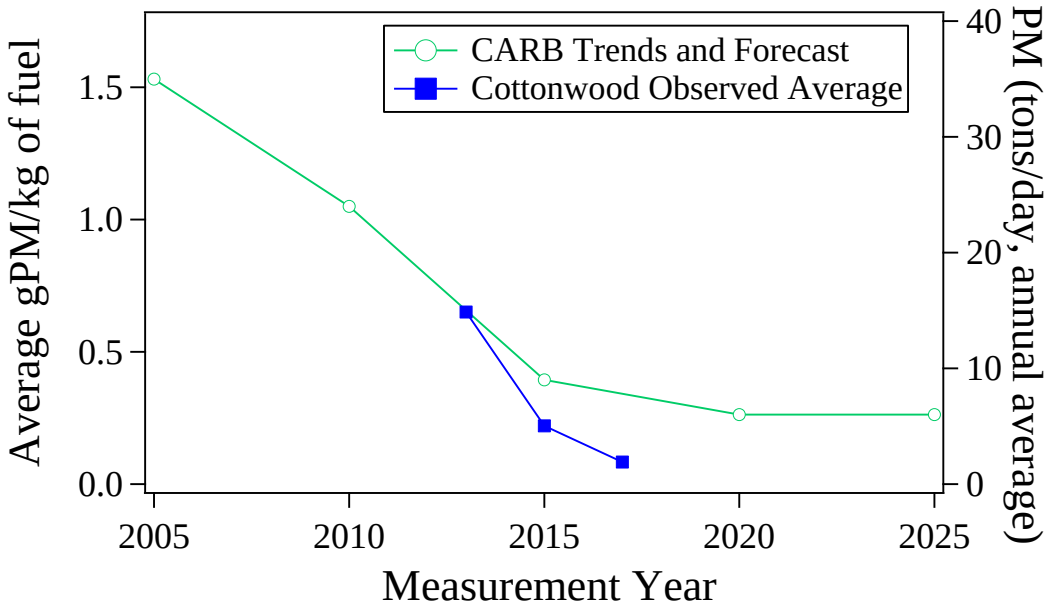

Figure 63. Average PM measured at Cottonwood (blue squares, left axis) using OHMS and the annual PM average (green circles, right axis) by measurement year.

Overall NO_x emissions due to diesel vehicles in California are comparable to the reductions observed at Peralta.[20] Figure 64 shows HDV NO_x monitored at Peralta (purple squares, left axis) since 1997 and provides a comparison for CARB's (green circles, right axis) observed and forecasted NO_x reductions by calendar year. Noticeable, reductions in

NO_x from diesel vehicles parallel the reductions anticipated by CARB, showing the implications of NO_x reduction on ambient concentrations.

California is slightly ahead of their anticipated 85% reduction in PM by 2020, as shown with the Cottonwood PM decreases. As these technologies continue to improve and more on-road vehicles have DPFs on-board, the fleet average will continue to lower and therefore reduce ambient PM. NO_x emissions are approaching the ambient reductions anticipated by California in large part due to diesel vehicle NO_x reductions. The research presented here illustrates that as on-road emissions improve, there is a corresponding reduction in atmospheric NO_x and PM, contributing to dramatic improvements in air quality thus lowering the health effects risk from diesel exhaust.[80, 81] The advancements in diesel exhaust emissions presented here is encouraging that air quality, and thus quality of life, is progressing towards more optimal conditions.

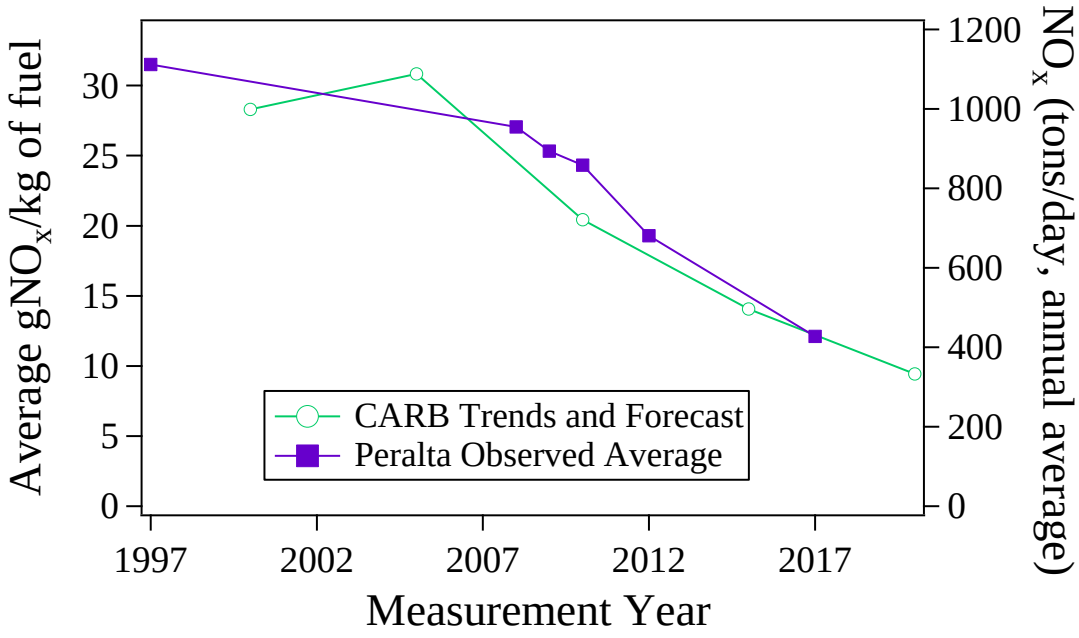

Figure 64. Average NO_x measured at Peralta (purple squares, left axis) using FEAT and the annual NO_x average (green circles, right axis) by measurement year.

References

1. U.S. Energy Information Administration International Energy Outlook 2016. http://www.eia.gov/forecasts/ieo/transportation.cfm

2. Dallmann, T. R.; Harley, R. A. Evaluation of mobile source emission trends in the United States. *Journal of Geophysical Research, [Atmospheres]* **2010,** 115, D14305-D14312.

3. McDonald, B. C.; Dallmann, T. R.; Martin, E. W.; Harley, R. A. Long-term trends in nitrogen oxide emissions from motor vehicles at national, state, and air basin scales. *Journal of Geophysical Research, [Atmospheres]* **2012,** 117, (D18), 1-11.

4. McDonald, B. C.; Goldstein, A. H.; Harley, R. A. Long-Term Trends in California Mobile Source Emissions and Ambient Concentrations of Black Carbon and Organic Aerosol. *Environ. Sci. Technol.* **2015,** 49, (8), 5178-5188.

5. U.S. Environmental Protection Agency *Population and activity of on-road vehicles in MOVES2014*; 2016; pp 27-28.

6. U. S. Environmental Protection Agency Our Nation's Air: Status and trends through 2010. http://www.epa.gov/airtrends/2011/

7. Heywood, J. B., *Internal combustion engine fundamentals*. McGraw Hill: New York, 1988.

8. Bahadur, R.; Feng, Y.; Russell, L. M.; Ramanathan, V. Impact of California's air pollution laws on black carbon and their implications for direct radiative forcing. *Atmos. Environ.* **2011,** 45, 1162-1167.

9. Simon, H.; Reff, A.; Wells, B.; Xing, J.; Frank, N. Ozone trends across the United States over a period of decreasing NO_x and VOC emissions. *Environ. Sci. Technol.* **2015,** 49, 186-195.

10. Gentner, D. R.; Jathar, S. H.; Gordon, T. D.; Bahreini, R.; Day, D. A.; El Haddad, I.; Hayes, P. L.; Pieber, S. M.; Platt, S. M.; de Gouw, J.; Goldstein, A. H.; Harley, R. A.; Jimenez, J. L.; Prévôt, A. S. H.; Robinson, A. L. Review of urban secondary organic aerosol formation from gasoline and diesel motor vehicle emissions. *Environ. Sci. Technol.* **2017,** 51, (3), 1074-1093.

11. U.S. Environmental Protection Agency, The Clean Air Act. In 2004.

12. Office of Environmental Health Hazard Assessment; California Environmental Protection Agency *Part B: Health risk assessment for diesel exhaust*; Sacramento, 1998.

13. U. S. Environmental Protection Agency; Air and Radiation Highway diesel progress review. www.epa.gov/oms/highway-diesel/compliance/420r02016.pdf (accessed Jan. 2015),

14. U.S. Environmental Protection Agency *Heavy-duty highway compression-ignition engines and urban buses: exhaust emission standards*; 2016; pp 18-19.

15. DieselNet Emission standards, United States, cars and light-duty trucks - California. https://www.dieselnet.com/standards/us/ld_ca.php (accessed Jun. 2018),

16. California Air Resources Board Risk reduction plan to reduce particulate matter emissions from diesel-fueled engines and vehicles. https://www.arb.ca.gov/diesel/documents/rrpFinal.pdf

17. Port of Long Beach; Port of Los Angeles San Pedro Bay Ports Clean Air Action Plan: About the Clean Air Action Plan. http://www.cleanairactionplan.org (Dec. 2016),

18. California Code of Regulations, In-use on-road diesel-fueled heavy-duty drayage trucks. In *Title 13*, 2008.

19. California Code of Regulations, Regulation to reduce emissions of diesel particulate matter, oxides of nitrogen and other criteria pollutants, from in-use heavy-duty diesel-fueled vehicles. In *Title 13*, 2008.

20. California Air Resources Board Background material: Almanac of emissions and air quality 2013 Edition- Chapter 3 statewide trends and forecasts. https://www.arb.ca.gov/aqd/almanac/almanac13/chap313.htm (June 2018),

21. Adler, J. Ceramic diesel particulate filters. *International Journal of Applied Ceramic Technology* **2005,** 2, (6), 429-439.

22. California Air Resources Board *Technology assessment: lower NO_x heavy-duty diesel engines*; 2015.

23. May, A. A.; Nguyen, N. T.; Presto, A. A.; Gordon, T. D.; Lipsky, E. M.; Karve, M.; Gutierrez, A.; Robertson, W. H.; Zhang, M.; Brandow, C.; Chang, O.; Chen, S.; Cicero-Fernandez, P.; Dinkins, L.; Fuentes, M.; Huang, S.-M.; Ling, R.; Long, J.; Maddox, C.; Massetti, J.; McCauley, E.; Miguel, A.; Na, K.; Ong, R.; Pang, Y.; Rieger, P.; Sax, T.; Truong, T.; Vo, T.; Chattopadhyay, S.; Maldonado, H.; Maricq, M. M.; Robinson, A. L. Gas- and particle-phase primary emissions from in-use, on-road gasoline and diesel vehicles. *Atmos. Environ.* **2014,** 88, 247-260.

24. Lemaire, J. How to select efficient diesel exhaust emissions control strategies for meeting air quality targets in 2010. *Österreichische Ingenieur-und Architekten-Zeitschrift* **2007,** 152, 1-12.

25. Stedman, D. H. Photochemical ozone formation, simplified. *Environmental Chemistry* **2004,** 1, 65-66.

26. Williams, M. L.; Carslaw, D. C. New directions: Science and policy - Out of step on NO_x and NO_2? *Atmos. Environ.* **2011,** 45, (23), 3911-1912.

27. Carslaw, D. C.; Beevers, S. D.; Tate, J. E.; Westmoreland, E. J.; Williams, M. L. Recent evidence concerning higher NO_x emissions from passenger cars and light duty vehicles. *Atmos. Environ.* **2011,** 45, 7053-7063.

28. California Code of Regulations, Verification procedure, warranty and in-use compliance requirements for in-use strategies to control emissions from diesel engines. In *Title 13*, 2003.

29. Koebel, M.; Elsener, M.; Kleemann, M. Urea-SCR: a promising technique to reduce NO_x emissions from automotive diesel engines. *Catal. Today* **2000,** 59, (3-4), 335-345.

30. Gekas, I.; Vressner, A.; Johansen, K. NOx reduction potential of V-SCR catalyst in SCR/DOC/DPF configuration targeting Euro VI limits from high engine NOx levels. *SAE International* **2009**.

31. Manufacturers of Emission Controls Association, Emission control technologies for diesel-powered vehicles. In 2007; p 28.

32. Smirniotis, P. G.; Peña, D. A.; Uphade, B. S. Low-temperature selective catalytic reduction (SCR) of NO with NH_3 by using Mn, Cr, and Cu oxides supported on Hombikat TiO_2. *Angew. Chem. Int. Ed.* **2001,** 40, (13), 2479-2482.

33. Dixit, P.; Miller, J. W.; III, D. R. C.; Oshinuga, A.; Jiang, Y.; Durbin, T. D.; Johnson, K. C. Differences between emissions measured in urban driving and certification testing of heavy-duty diesel engines. *Atmos. Environ.* **2017,** 166, 276-285.

34. Quiros, D. C.; Thiruvengadam, A.; Pradhan, S.; Besch, M.; Thiruvengadam, P.; Dermirgok, B.; Carder, D.; Oshinuga, A.; Huai, T.; Hu, S. Real-world emissions from modern heavy-duty diesel, natural gas, and hybrid diesel trucks operating along major California freight corridors. *Emiss. Control Sci. Technol.* **2016,** 2, 156-172.

35. Bishop, G. A.; Stedman, D. H. A decade of on-road emissions measurements. *Environ. Sci. Technol.* **2008,** 42, (5), 1651-1656.

36. Bishop, G. A.; Schuchmann, B. G.; Stedman, D. H.; Lawson, D. R. Emission changes resulting from the San Pedro Bay, California Ports Truck Retirement Program. *Environ. Sci. Technol.* **2012,** 46, 551-558.

37. Bishop, G. A.; Schuchmann, B. G.; Stedman, D. H. Heavy-duty truck emissions in the South Coast Air Basin of California. *Environ. Sci. Technol.* **2013,** 47, (16), 9523-9529.

38. Ban-Weiss, G. A.; McLaughlin, J. P.; Harley, R. A.; Lunden, M. M.; Kirchstetter, T. W.; Kean, A. J.; Strawa, A. W.; Stevenson, E. D.; Kendall, G. R. Long-term changes in emissions of nitrogen oxides and particulate matter from on-road gasoline and diesel vehicles. *Atmos. Environ.* **2008,** 42, 220-232.

39. Dallmann, T. R.; Harley, R. A.; Kirchstetter, T. W. Effects of diesel particle filter retrofits and accelerated fleet turnover on drayage truck emissions at the Port of Oakland. *Environ. Sci. Technol.* **2011,** 45, 10773-10779.

40. McDonald, B. C.; Gentner, D. R.; Goldstein, A. H.; Harley, R. A. Long-Term Trends in Motor Vehicle Emissions in U.S. Urban Areas. *Environ. Sci. Technol.* **2013,** 47, (17), 10022-10031.

41. Bishop, G. A.; Hottor-Raguindin, R.; Stedman, D. H.; McClintock, P.; Theobald, E.; Johnson, J. D.; Lee, D.-W.; Zietsman, J.; Misra, C. On-road heavy-duty vehicle emissions monitoring system. *Environ. Sci. Technol.* **2015,** 49, (3), 1639-1645.

42. The Engineering ToolBox Emissivity Coefficients of some common Materials. http://www.engineeringtoolbox.com/emissivity-coefficients-d_447.html (accessed January 2013),

43. Burgard, D. A.; Bishop, G. A.; Stedman, D. H.; Gessner, V. H.; Daeschlein, C. Remote sensing of in-use heavy-duty diesel trucks. *Environ. Sci. Technol.* **2006,** 40, 6938-6942.

44. Bishop, G. A.; Stedman, D. H. Measuring the emissions of passing cars. *Acc. Chem. Res.* **1996,** 29, 489-495.

45. Popp, P. J.; Bishop, G. A.; Stedman, D. H. Development of a high-speed ultraviolet spectrometer for remote sensing of mobile source nitric oxide emissions. *J. Air Waste Manage. Assoc.* **1999,** 49, 1463-1468.

46. Burgard, D. A.; Dalton, T. R.; Bishop, G. A.; Starkey, J. R.; Stedman, D. H. Nitrogen dioxide, sulfur dioxide, and ammonia detector for remote sensing of vehicle emissions. *Rev. Sci. Instrum.* **2006,** 77, (014101), 1-4.

47. Singer, B. C.; Harley, R. A.; Littlejohn, D.; Ho, J.; Vo, T. Scaling of infrared remote sensor hydrocarbon measurements for motor vehicle emission inventory calculations. *Environ. Sci. Technol.* **1998,** 32, 3241-3248.

48. Singer, B. C.; Harley, R. A.; D., L.; Ho, J.; Vo, T. Scaling of infrared remote sensor hydrocarbon measurements for motor vehicle emission inventory calculations. *Environ. Sci. Technol.* **1998,** 32, (21), 3241-3248.

49. Haugen, M. J.; Bishop, G. A. Long-term fuel-specific NO_x and particle emission trends for in-use heavy-duty vehicles in California *Environ. Sci. Technol.* **2018,** 52, 6070-6076.

50. The Port of Los Angeles; Port of Long Beach *2010 Update San Pedro Bay Ports Clean Air Action Plan*; Los Angeles, 2010.

51. Khalek, I. A.; Bougher, T., L.; Merritt, P., M.; Zielinska, B. Regulated and unregulated emissions from highway heavy-duty diesel engines complying with U.S.Environmental Protection Agency 2007 emissions standards. *Journal of Air and Waste Management Association* **2011,** 61, 427-442.

52. Preble, C. V.; Dallmann, T. R.; Kreisberg, N. M.; Hering, S. V.; Harley, R. A.; Kirchstetter, T. W. Effects of particle filters and selective catalytic reduction on heavy-duty diesel drayage truck emissions at the Port of Oakland. *Environ. Sci. Technol.* **2015,** 49, (14), 8864-8871.

53. Johnson, K. C.; Durbin, T. D.; Jung, H.; Cocker, D. R.; Bishnu, D.; Giannelli, R. Quantifying in-use PM measurements for heavy duty diesel vehicles. *Environ. Sci. Technol.* **2011,** 45, (14), 6073-6079.

54. Quiros, D. C.; Thiruvengadam, A.; Pradhan, S.; Besch, M.; Thiruvengadam, P.; Demirgok, B.; Carder, D.; Oshinuga, A.; Huai, T.; Hu, S. Real-World Emissions from Modern Heavy-Duty Diesel, Natural Gas, and Hybrid Diesel Trucks Operating Along

Major California Freight Corridors. *Emission Control Science and Technology* **2016,** 2, (3), 156-172.

55. Society of Automotive Engineers, Snap Acceleration Smoke Test Procedure for Heavy-Duty Powered Vehicles. In Society of Automotive Engineers, Inc.: 1996.

56. California Air Resources Board Heavy-Duty Diesel Information Series. https://www.arb.ca.gov/enf/hdvip/hdvip_pamphlet.pdf (accessed February 2017),

57. Li, X.; Xu, Z.; Guan, C.; Huang, Z. Particle size distributions and OC, EC emissions from a diesel engine with the application of in-cylinder emission control strategies. *Fuel* **2014,** 121, 20-26.

58. Li, X.; Xu, Z.; Guan, C.; Huang, Z. Oxidative reactivity of particles emitted from a diesel engine operating at light load with EGR. *Aerosol Sci. Technol.* **2015,** 49, 1-10.

59. Yang, J.; Stewart, M.; Maupin, G.; Herling, D.; Zelenyuk, A. Single wall diesel particulate filter (DPF) filtration efficiency studies using laboratory generated particles. *Chem. Eng. Sci.* **2009,** 64, 1625-1634.

60. Barone, T. L.; Storey, J. M. E.; Domingo, N. An analysis of field-aged diesel particulate filter performance: particle emissions before, during, and after regeneration. *J. Air & Waste Manage. Assoc.* **2010,** 60, (8), 968-976.

61. Bell, J., *Modern Diesel Technology: Electricity and Electronics*. 2 ed.; Cengage Learning: 2013.

62. Bishop, G. A.; Stedman, D. H.; Ashbaugh, L. Motor vehicle emissions variability. *J. Air Waste Manage. Assoc.* **1996,** 46, 667-675.

63. California Environmental Protection Agency Air Resources Board Truck and Bus Regulation Reporting. http://www.arb.ca.gov/msprog/onrdiesel/reportinginfo.htm (accessed July 2016),

64. Miller, W.; Johnson, K. C.; Durbin, T.; Dixit, P. *In-use emissions testing and demonstration of retrofit technology for control of on-road heavy-duty engines*; University of California CE-CERT: 2013; pp 89-92.

65. Thiruvengadam, A.; Besch, M. C.; Thiruvengadam, P.; Pradhan, S.; Carder, D.; Kappanna, H.; Gautam, M.; Oshinuga, A.; Hogo, H.; Miyasato, M. Emission rates of regulated pollutants from current technology heavy-duty diesel and natural gas goods movement vehicles. *Environ. Sci. Technol.* **2015,** 49, 5236-5244.

66. Herner, J. D.; Hu, S.; Robertson, W. H.; Huai, T.; Collins, J. F.; Dwyer, H.; Ayala, A. Effect of advanced aftertreatment for PM and NO_x control on heavy-duty diesel truck emissions. *Environ. Sci. Technol.* **2009,** 43, 5928-5933.

67. California Air Resources Board Enforcement Reports. https://www.arb.ca.gov/enf/reports/reports.htm (December 5 2017),

68. Haugen, M. J.; Bishop, G. A. Repeat fuel specific emission measurements on two California heavy-duty truck fleets. *Environ. Sci. Technol.* **2017,** 51, 4100-4107.

69. De-La-Torre, U.; Pereda-Ayo, B.; Moliner, M.; González-Velasco, J. R.; Corma, A. Cu-zeolite catalysts for NO_x removal by selective catalytic reduction with NH_3 and coupled to NO storage/reduction monolith in diesel engine exhaust aftertreatment systems. *Applied Catalysis B: Environmental* **2016,** 187, 419-427.

70. Johnson, T. V. Review of diesel emissions and control. *Int. J. Engine Res.* **2009,** 10, (5), 275-285.

71. U.S. Environmental Protection Agency Diesel Particulate Filter General Information. https://www.epa.gov/sites/production/files/2016-03/documents/420f10029.pdf

72. Bishop, G. A.; Stedman, D. H. Reactive Nitrogen Species Emission Trends in Three Light-/Medium-Duty United States Fleets. *Environ. Sci. Technol.* **2015,** 49, (18), 11234-11240.

73. Sawyer, R. F.; Johnson, J. H. *Diesel exhaust: A critical analysis of emissions, exposure, and health effects*; Health Effects Institue: Cambridge, MA, 1995; pp 67-81.

74. Code of Federal Regulations, NO_x and particulate averaging, trading and banking for heavy-duty engines. In *Title 40*, 2001; pp 7, 215-290.

75. Code of Federal Regulations, NO_x plus NMHC and particulate averaging, trading and banking for heavy-duty engines. In *Title 40*, 2000; pp 7-169.

76. California Air Resources Board, On-board diagnostic system requirements--2010 and subsequent model-year heavy-duty engines. In *Title 13*, California Air Resources Board, Ed. 2016.

77. Lindhjem, C.; Chan, L.-M.; Pollack, A.; Kite, C. *Applying humidity and temperature corrections to on and off-road mobile source emissions*; 2004.

78. California Air Resources Board EMFAC2017 SOCAB CY2032 NOX emissions overview. www.arb.ca.gav/app/emsinv/fcemssumcat/fcemssumcat2016.php (July 2018),

79. McDonald, B.; Goldstein, A. H.; Harley, R. A. Long-Term Trends in California Mobile Source Emissions and Ambient Concentrations of Black Carbon and Organic Aerosol. *Environ. Sci. Technol.* **2015,** 49, 5178-5188.

80. Jerrett, M.; Burnett, R. T.; Pope, C. A.; Ito, K.; Thurston, G.; Krewski, D.; Shi, Y.; Calle, E.; Thun, M. Long-Term Ozone Exposure and Mortality. *New England Journal of Medicine* **2009,** 360, (11), 1085-1095.

81. U.S. Environmental Protection Agency Benefits and cots of the Clean Air Act 199-2020, the second prospective study. https://www.epa.gov/clean-air-act-overview/benefits-and-costs-clean-air-act-1990-2020-second-prospective-study (July 2018).

Appendices

Appendix A – Field Calibration of Infra-Red Camera Used in OHMS

The FLIR A320 infrared camera that was used in the OHMS system was initially calibrated in the lab using a single stainless steel exhaust pipe heated on a hot plate. A thermocouple was attached to the pipe and the IR image color was then assigned to the temperature read by the thermocouple. There was concern regarding the representativeness of this calibration and an in-field calibration was conducted.

The contraption that was constructed to make these measurements is shown in Figure A1. The device consisted of a long wooden pole with a thermocouple spring mounted on one end and the IR camera, a color video camera and a volt meter mounted on the other. The pink box highlights the FLIR IR camera and its video monitor, and the visible video camera and its monitor is shown with the green box. Below and between the cameras is the thermocouples voltage reading (blue box) and at the end of the pole is the thermocouple respectively (red box). The camera and thermocouple signals were passed to a computer with dual imaging boards and an analog to digital converter. A trigger in the handle was pulled when the volt meter had reached equalibrium to signal the computer to acquire the IR image, visible image and thermocouple temperature. The FLIR IR cameras color scale's temperature range (Figure A2) was determined by assigning the measured thermocouple temperatures to the IR image color collected. This allowed the camera images to be used to estimate exhaust pipe temperatures without having to physically touch the exhaust pipe with a thermocouple and eliminate any material emissivity differences.

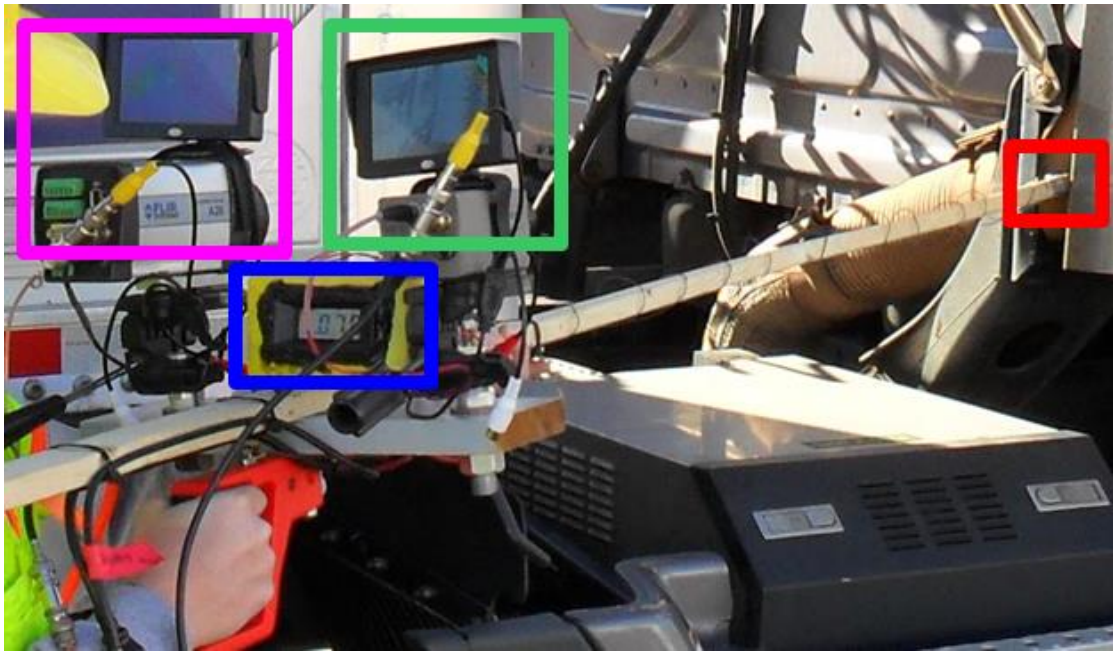

Figure A1. Device used for measuring temperature of exhaust pipes on HDV. In the upper left is the FLIR A320 IR camera and video monitor (pink box), to its right is the color video camera and monitor (green box), below is the thermocouple voltage readout (blue box) and to the far right is the thermocouple (red box) pressed up against the vehicle's exhaust pipe.

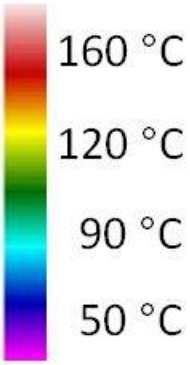

Figure A2. Infrared image color scale with associated temperatures determined from the thermocouple measurements.

Measurements were taken at two locations, the Dumont weigh station on I-70 in the Rocky Mountains, approximately 35 miles West of Denver and at Coors Brewery's distribution plant in Golden, CO. Over the course of four days, December 2, 3, 5 and 8, 2014, 226 exhaust pipes were measured.

The two locations measured are representative of the two locations where we have deployed the OHMS system in California. The brewery location had lower temperature pipes due to the short-haul and stop-and-go nature of the distribution yard operations much like the Port of Los Angeles site. The Dumont weigh station had a fleet comprised of HDV on an interstate highway route where measurements were collected after the vehicles were required to drive up the mountainous road resulting in hotter exhaust pipes more like the Cottonwood weigh station site in northern CA. The histogram showing the temperatures measured at both locations is shown in Figure A3. The HDV at Dumont, as expected were on average warmer and had more vehicles that extended into hotter regions of the color scale than observed in the Coors fleet.

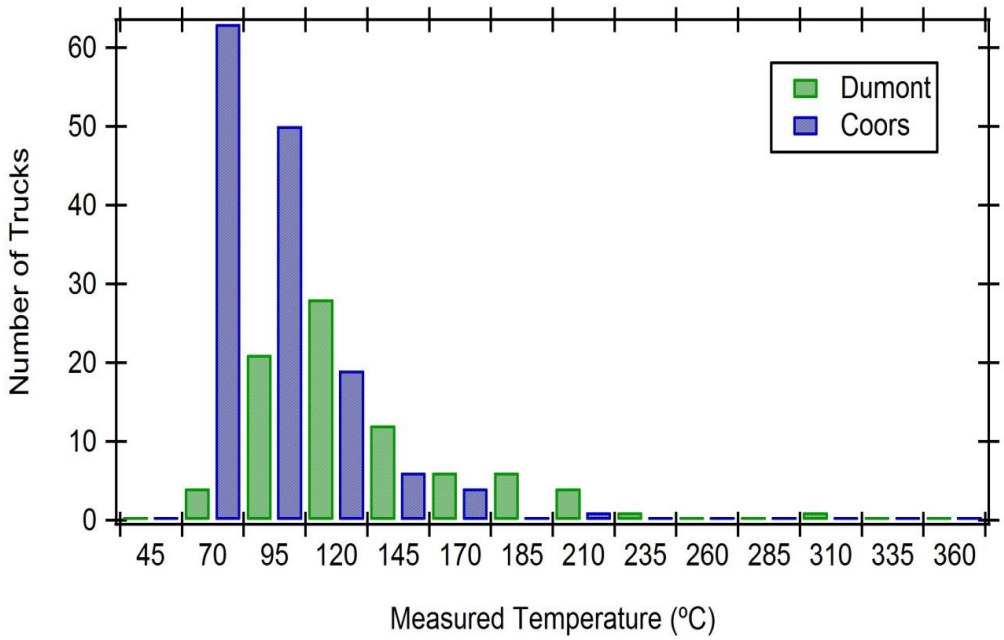

Figure A3. Histogram of exhaust pipe temperatures at Dumont weigh station (green bars) and Coors Brewery (blue bars).

Figure A4 graphs the measured thermocouple temperature against the previously determined IR image temperature calibration. The crosses plot are the individual thermocouple measurements collected from each truck with the solid black line showing the least squares best fit line. The parallel black dashed lines how the 95% prediction bands for the best fit line. The red solid line is the 1:1 line showing the previously determined IR temperature calibration.

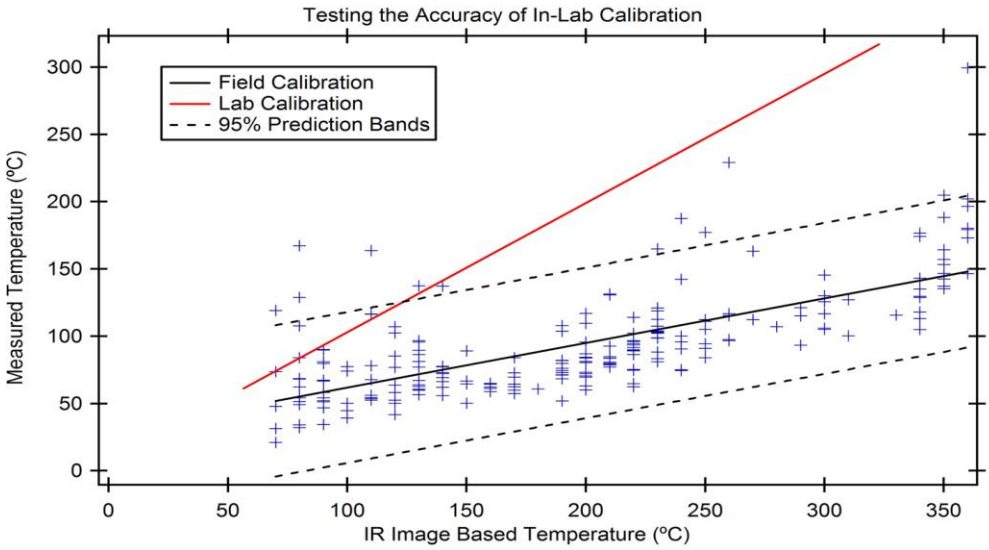

Figure A4. Thermocouple temperature measurements (+) versus the previous in-lab calibrated IR image-based temperature in degrees C. The solid black line is the least squares best fit line to the data with the parallel dashed lines showing the 95% prediction bands for that fit. The red line is the 1:1 line showing the previous in-lab calibration line.

This field calibration has greatly improved the temperature accuracy assigned to the IR images in the OHMS system. We believe that we have sampled enough exhaust pipes to minimize the emissivity variable associated with different metals that exhaust pipes are made out of in order to improve the temperature estimates.

To correct the 2013 IR image temperature data that used the in-lab calibration the equation below was used, where y is the temperature represented by the field calibration and x is the temperature previously assigned using the in-lab calibration.

$$y = 0.331x + 28.8$$

Appendix B – OHMS Measurements Validity Criteria

Not measured:

1) Body sensor blocked and after 15 or 20 seconds of data collection the maximum increase in CO_2 is less than 80ppm over background.

Invalid:

1) gCO/kg < -2;

   gCO/kg <= 6 and error > 1.5;

   gCO/kg > 6 and percent error > 25%

2) gHC/kg < -10;

   gHC/kg <= 10 and error > 2;

   gHC/kg > 10 and percent error > 20%

3) gNO/kg < -10

   gNO/kg <= 10 and error > 2

   gNO/kg > 10 and percent error > 20%

4) gNO_x/kg < -10

   gNO_x/kg <= 10 and error > 2

   gNO_x/kg > 10 and percent error > 20%

5) gNO_2/kg < -10

   gNO_2/kg invalid if either gNO/kg or gNO_x/kg values invalid

6) gPM/kg < -2

   gPM/kg <= 2 and error > 1

   gPM/kg > 2 and percent error > 50%

7) gBC/kg < -2

   gBC/kg <= 2 and error > 1

   gBC/kg > 2 and percent error > 50%

Speed/Acceleration valid only if at least two blocks and two unblocks in the time buffer and all blocks occur before all unblocks on each sensor and the number of blocks and unblocks is equal on each sensor and 100mph>speed>1mph and 14mph/s>accel>-13mph/s.

Appendix C – FEAT Measurements Validity Criteria

Invalid :

1) insufficient plume to rear of vehicle relative to cleanest air observed in front or in the rear; at least five, 10ms >160ppm CO_2 or >400 ppm CO. (0.2 %CO_2 or 0.5% CO in an 8 cm cell. This is equivalent to the units used for CO_2 max.). For HDDV's this often occurs when the vehicle shifts gears at the sampling beam.

2) excessive error on CO/CO_2 slope, equivalent to $\pm$20% for $CO/CO_2 > 0.069$, 0.0134 CO/CO_2 for $CO/CO_2 < 0.069$.

3) reported CO/CO_2 , < -0.063 or > 5. All gases invalid in these cases.

4) excessive error on HC/CO_2 slope, equivalent to $\pm$20% for $HC/CO_2 > 0.0166$ propane, 0.0033 propane for $HC/CO_2 < 0.0166$.

5) reported $HC/CO_2 < -0.0066$ propane or > 0.266. HC/CO_2 is invalid.

6) excessive error on NO/CO_2 slope, equivalent to $\pm$20% for $NO/CO_2 > 0.001$, 0.002 for $NO/CO_2 < 0.001$.

7) reported $NO/CO_2 < -0.00465$ or > 0.0465. NO/CO_2 is invalid.

8) excessive error on SO_2/CO_2 slope, ± 0.0134 SO_2/CO_2.

9) reported SO_2/CO_2 , < -0.00053 or > 0.0465. SO_2/CO_2 is invalid.

10) excessive error on NH_3/CO_2 slope, ± 0.00033 NH_3/CO_2.

11) reported $NH_3/CO_2 < -0.00053$ or > 0.0465. NH_3/CO_2 is invalid.

12) excessive error on NO_2/CO_2 slope, equivalent to $\pm$20% for $NO_2/CO_2 > 0.00133$, 0.000265 for $NO_2/CO_2 < 0.00133$.

13) reported $NO_2/CO_2 < -0.0033$ or > 0.0465. NO_2/CO_2 is invalid.

Speed/Acceleration valid only if at least two blocks and two unblocks in the time buffer and all blocks occur before all unblocks on each sensor and the number of blocks and unblocks is equal on each sensor and 100mph>speed>5mph and 14mph/s>accel>-

13mph/s and there are no restarts, or there is one restart and exactly two blocks and unblocks in the time buffer.

Appendix D – Standard Error of the Mean Calculation Example

Vehicle emissions from US vehicle fleets are not normally distributed, thus the assigning of uncertainties on fleet emission means involves a process that many readers may not be familiar with. Standard statistical methods that were developed for normally distributed populations, when used on a skewed distribution, results in uncertainties that are unrealistically too small due to the large number of samples. The Central Limit Theorem in general indicates that the means of multiple samples, randomly collected, from a larger parent population will be normally distributed, irrespective of the parent populations underlying distribution. Since we almost always collect multiple days of emission measurements from each site, we use these daily measurements as our randomly collected multiple samples from the larger population and report uncertainties based on their distribution. We calculate means, standard deviations and finally standard errors of the mean for this group of daily measurements. We report the means for all of the emission measurements and then calculate a standard error of the mean for the entire sample by applying the same error percentage obtained from the ratio of the standard error of the mean for the daily measurements divided by the daily measurement mean. An example of this process is provided below for the 2015 Port of Los Angeles, CA gNO/kg of fuel and gPM/kg of fuel measurements. While this example is for a fleet mean we also use this technique when we report standard errors of the mean for individual model years or specific fuel or technology types. For example each model year will have its daily mean calculated and then its standard error of the mean for the daily average computed and that percent uncertainty will be applied to that model year's fleet emissions mean.

Cottonwood, CA 2017.

Date	Mean gNO/kg of fuel	Counts	Mean gPM/kg of fuel	Counts
4/10/2017	9.5	318	0.08	325
4/11/2017	12.1	166	0.08	170
4/12/2017	8.2	183	0.09	190
4/13/2017	9.8	215	0.10	223
4/14/2017	8.1	134	0.08	137
Daily Means	9.5		0.09	
Standard Error for the Daily Means	0.7		0.005	
Weighted Fleet Mean	9.6		0.09	
Standard Error for the Fleet Means	0.7		0.005	
As Reported in Table 5	9.6 ± 0.7		0.09 ± 0.005	

Appendix E – Explanation of the Databases (OHMS)

The Cwood13.dbf, LAPort13.dbf, Cwood15.dbf, LAPort15.dbf, Cwood17.dbf, LAPort17.dbf are Microsoft FoxPro database files, and can be opened by any version of MS FoxPro. These files can be read by a number of other database management and spreadsheet programs as well, and is available from www.feat.biochem.du.edu. The grams of pollutant/kilogram of fuel consumed are calculated assuming that diesel fuel has 860 grams of carbon per kilogram of fuel and natural gas has 750 grams of carbon per kilogram of fuel. The following is an explanation of the data fields found in this database:

License Vehicle license plate.

State State license plate issued by.

Date Date of measurement, in standard format.

Time Time of measurement, in standard format.

Co_co2 Measured carbon monoxide / carbon dioxide ratio

Co_err Standard error of the CO/CO_2 measurement.

Hc_co2 Measured hydrocarbon / carbon dioxide ratio (propane equivalents).

Hc_err Standard error of the HC/CO_2 measurement.

No_no2 Measured nitric oxide / carbon dioxide ratio.

No_err Standard error of the NO/CO_2 measurement.

Nox_co2 Measured nitrogen oxides / carbon dioxide ratio.

Nox_err Standard error of the NO_x/CO_2 measurement.

Gpm_kg Calibrated grams of particulate matter per kilogram of fuel.

Gpm_error Standard error of the Gpm_kg measurement.

Gbc_kg Calibrated grams of black carbon per kilogram of fuel.

Gbc_error Standard error of the Gbc_kg measurement.

Co2_max Delta CO_2 plume maximum observed in ppm.

Banr_flag Indicates a single vehicle was measured. "V" = single, "X" = more than one.

Co_flag Indicates a valid carbon monoxide measurement by a "V', invalid by an "X".

Hc_flag Indicates a valid hydrocarbon measurement by a "V", invalid by an "X".

No_flag Indicates a valid nitric oxide measurement by a "V", invalid by an "X".

Nox_flag Indicates a valid nitrogen oxide measurement by a "V", Invalid by an "X".

Pm_flag Indicates a valid total particulate measurement by a "V", Invalid by an "X".

Bc_flag Indicates a valid black carbon measurement by a "V", Invalid by an "X".

File_name File name for a CSV file containing the vehicles second by second data.

Speed1_flg Indicates a valid speed measurement at the tent entrance by a "V", an invalid by an "X".

Speed1 Measured speed of the vehicle at the tent entrance, in mph.

Accel1 Measured acceleration of the vehicle at the tent entrance, in mph/s.

Speed2_flg Indicates a valid speed measurement at the tent exit by a "V", an invalid by an "X".

Speed2 Measured speed of the vehicle at the tent exit, in mph.

Accel2 Measured acceleration of the vehicle at the tent exit, in mph/s.

Tag_name File name for digital image file of the front of the vehicle measured.

Exh_temp Estimated temperature in Celsius of the vehicles elevated exhaust pipe.

Scr_cap Indicates the presence of an observable urea tank by a "Y".

Gco_kg Calibrated grams of carbon monoxide per kilogram of fuel.

Gco_error Standard error of the Gco_kg measurement.

Ghc_kg Calibrated grams of total hydrocarbons per kilogram of fuel.

Ghc_error Standard error of the Ghc_kg measurement.

Gno_kg Calibrated grams of nitric oxide per kilogram of fuel.

Gno_error Standard error of the Gno_kg measurement.

Gno2_kg Calibrated grams of nitrogen dioxide per kilogram of fuel.

Gnox_kg Calibrated grams of nitrogen oxides per kilogram of fuel.

Gnox_error Standard error of the Gnox_kg measurement.

Body_type DMV designation of vehicle body type. (not all states provided this)

Year	Model year of the vehicles chassis.
Vin	Vehicle identification number.
Model	DMV designation of vehicle model.
Make	Manufacturer of the vehicle.
Fuel	DMV fuel type designation.
City	City where vehicle is registered. (not all states provided this)
Zipcode	Zipcode where vehicle is registered. (not all states provided this)
County	County code where vehicle is registered. (not all states provided this)
Gvw	Vehicle gross vehicle weight. (not all states provided this)

Appendix F – Explanation of the Database (FEAT)

The Peralt12.dbf and LAPort12.dbf are Microsoft FoxPro database files, and can be opened by any version of MS FoxPro. These files can be read by a number of other database management and spreadsheet programs as well, and is available from www.feat.biochem.du.edu. The grams of pollutant/kilogram of fuel consumed are calculated assuming that diesel fuel has 860 grams of carbon per kilogram of fuel and natural gas has 750 grams of carbon per kilogram of fuel. The following is an explanation of the data fields found in this database:

License Vehicle license plate.

State State license plate issued by.

Date Date of measurement, in standard format.

Time Time of measurement, in standard format.

Co_co2 Measured carbon monoxide / carbon dioxide ratio

Co_err Standard error of the CO/CO_2 measurement.

Hc_co2 Measured hydrocarbon / carbon dioxide ratio (propane equivalents).

Hc_err Standard error of the HC/CO_2 measurement.

No_no2 Measured nitric oxide / carbon dioxide ratio.

No_err Standard error of the NO/CO_2 measurement.

So2_co2 Measured sulfur dioxide / carbon dioxide ratio.

So2_err Standard error of the SO_2/CO_2 measurement.

Nh3_co2 Measured ammonia / carbon dioxide ratio.

Nh3_err Standard error of the NH_3/CO_2 measurement.

No2_co2 Measured nitrogen dioxide / carbon dioxide ratio.

No2_err Standard error of the NO_2/CO_2 measurement.

Opacity IR Opacity measurement, in percent.

Opac_err Standard error of the opacity measurement.

Restart Number of times data collection is interrupted and restarted by a close-following vehicle, or the rear wheels of tractor trailer.

Hc_flag Indicates a valid hydrocarbon measurement by a "V", invalid by an "X".

No_flag Indicates a valid nitric oxide measurement by a "V", invalid by an "X".

So2_flag Indicates a valid sulfur dioxide measurement by a "V", Invalid by an "X".

Nh3_flag Indicates a valid ammonia measurement by a "V", Invalid by an "X".

No2_flag Indicates a valid Nitrogen dioxide measurement by a "V", Invalid by an "X".

Opac_flag Indicates a valid opacity measurement by a "V", invalid by an "X".

Max_co2 Reports the highest absolute concentration of carbon dioxide measured by the remote sensor over an 8 cm path; indicates plume strength.

Speed_flag	Indicates a valid speed measurement by a “V”, an invalid by an “X”, and slow speed (excluded from the data analysis) by an “S”.
Speed	Measured speed of the vehicle, in mph.
Accel	Measured acceleration of the vehicle, in mph/s.
Feat	Indicates High FEAT “H” or Low FEAT “L” measurement
Gco_kg	Calibrated grams of carbon monoxide per kilogram of fuel.
Gco_error	Standard error of the Gco_kg measurement.
Ghc_kg	Calibrated grams of total hydrocarbons per kilogram of fuel.
Ghc_error	Standard error of the Ghc_kg measurement.
Gno_kg	Calibrated grams of nitric oxide per kilogram of fuel.
Gno_error	Standard error of the Gno_kg measurement.
Gno2_kg	Calibrated grams of nitrogen dioxide per kilogram of fuel.
Gnox_kg	Calibrated grams of nitrogen oxides per kilogram of fuel.
Gnox_error	Standard error of the Gnox_kg measurement.
Gnh3_kg	Calibrated grams of ammonia per kilogram of fuel.
Gnh3_kgerr	Standard error of the Gnh3_kg measurement.
Year	Model year of the vehicles chassis.
Make	Manufacturer of the vehicle.

Series	Vehicle make body style.
Model	DMV designation of vehicle model.
Gvw_code	Gross vehicle weight code classification.
Fuel	Type of fuel used.
Vin	Vehicle identification number.
Exh_temp	Estimated exhaust pipe temperature using calibrated IR camera.
VSP	Vehicle specific power in kw/tonne.
Weight	Classification for MDVs “M” and HDVs “H”